Award Number: W81XWH-12-1-0377

TITLE: The Role of Peripheral Nerve Function in Age-Related Bone Loss and Changes in Bone Adaptation

PRINCIPAL INVESTIGATOR: Blaine A. Christiansen

CONTRACTING ORGANIZATION: Regents of the University of California
Davis, CA 95618

REPORT DATE: December 2015

TYPE OF REPORT: Final

PREPARED FOR: U.S. Army Medical Research and Materiel Command
Fort Detrick, Maryland 21702-5012

REPORT DOCUMENTATION PAGE

Form Approved
OMB No. 0704-0188

1. REPORT DATE	2. REPORT TYPE	3. DATES COVERED
December 2015	Final	30 Sep 2012 – 29 Sep 2015

4. TITLE AND SUBTITLE
The Role of Peripheral Nerve Function in Age-Related Bone Loss and Changes in Bone Adaptation

5a. CONTRACT NUMBER
PR110178

5b. GRANT NUMBER
10914228

5c. PROGRAM ELEMENT NUMBER

6. AUTHOR(S)
Blaine A. Christiansen

E-Mail: bchristiansen@ucdavis.edu

5d. PROJECT NUMBER

5e. TASK NUMBER

5f. WORK UNIT NUMBER

7. PERFORMING ORGANIZATION NAME(S) AND ADDRESS(ES)

University of California Davis Medical Center
Department of Orthopaedic Surgery
4635 2nd Avenue, Suite 2000
Sacramento, CA 95817-2000

8. PERFORMING ORGANIZATION REPORT NUMBER

9. SPONSORING / MONITORING AGENCY NAME(S) AND ADDRESS(ES)
U.S. Army Medical Research and Materiel Command
Fort Detrick, Maryland 21702-5012

10. SPONSOR/MONITOR'S ACRONYM(S)

11. SPONSOR/MONITOR'S REPORT NUMBER(S)

12. DISTRIBUTION / AVAILABILITY STATEMENT
Approved for Public Release; Distribution Unlimited

13. SUPPLEMENTARY NOTES

14. ABSTRACT

Current osteoporosis therapies are able to treat the symptoms of osteoporosis, however little progress has been made toward understanding and addressing the underlying mechanisms contributing to age-related bone loss, or the ability to adapt to mechanical loading (exercise). Degeneration in peripheral nerve function with age may be one of these mechanisms, as neuropeptides affect the function of osteoblasts and osteoclasts in vitro, and nerve deactivation causes bone loss in vivo. This research investigates mechanisms by which peripheral sensory nerves influence bone maintenance and mechanotransduction using capsaicin-injected mice as a model of decreased peripheral sensory nerve function. We hypothesize that decreased sensory nerve function will result in increased functional adaptation of bone. In Aim 1 we investigated the relationship between peripheral sensory nerve function and bone structure. We found that capsaicin treatment resulted in a small but statistically significant decrease in trabecular and cortical bone structure. In Aim 2 we will determine the bone adaptation response of capsaicin- and vehicle-treated mice to increased mechanical loading. We hypothesize that capsaicin-treated mice will have an increased bone adaptation response to mechanical loading. The proposed research will establish the role of peripheral sensory nerves in age-related decreases in bone's ability to adapt to exercise. These studies may lead to novel therapies aimed at preserving healthy bone turnover with age. This research will be the basis for future studies investigating the interaction of peripheral nerves and bone, and peripheral nerve function as a potential mechanism of age-related bone loss.

15. SUBJECT TERMS
Peripheral sensory nerves, osteoporosis, bone structure, trabecular, cortical, mechanical loading, bone adaptation

16. SECURITY CLASSIFICATION OF:			17. LIMITATION OF ABSTRACT	18. NUMBER OF PAGES	19a. NAME OF RESPONSIBLE PERSON
a. REPORT	b. ABSTRACT	c. THIS PAGE			USAMRMC
U	U	U	UU	142	19b. TELEPHONE NUMBER *(include area code)*

Table of Contents

INTRODUCTION: Osteoporosis is a major public health concern for an ever-growing aging population, affecting over 44 million Americans [1]. Osteoporotic fractures are associated with morbidity, increased mortality, and a general decrease in quality of life. While current pharmacological therapies are useful for treating symptoms of osteoporosis, little progress has been made toward understanding and addressing the *underlying mechanisms leading to age-related bone loss*. Diminished innervation of bone with age may be one of these mechanisms, as peripheral nerve function has been shown to affect bone metabolism both *in vitro* [2-7] and *in vivo* [8, 9]. The proposed research investigates the role of peripheral sensory nerve function on bone maintenance and mechanotransduction using capsaicin-treated mice as a model of decreased peripheral nerve function. We hypothesized that decreased peripheral nerve function will result in an *increased* functional adaptation response of bone, due to decreased negative feedback on osteoblast and osteoclast function. To test this hypothesis, we proposed two specific aims. The first aim determined the effects of neonatal capsaicin treatment on bone structure and metabolism compared to vehicle-injected mice. The second aim determined the bone adaptation and peripheral nerve response of capsaicin- and vehicle-injected mice to increased mechanical loading. This research will establish the role of peripheral nerves in bone metabolism and mechanotransduction, and may lead to novel therapies aimed at preserving healthy bone turnover with age.

BODY:

Approved Statement of Work:
Aim 1. *Determine the effects of neonatal capsaicin treatment on bone structure and metabolism, and neuropeptide concentrations in bone compared to vehicle-injected mice* (months 1-12):

1a. Institutional approval of animal use protocols (*this will be done before the funding period begins)
1b. Capsaicin or vehicle treatment of neonatal mice (months 1-3)
1c. Micro-computed tomography of mouse bones (months 2-6)
1d. ELISA analysis of neuropeptides in bone (months 2-10)
1e. Multiplex analysis of bone biomarkers (months 2-10)
1f. Embedding/cutting/imaging/analysis of bones for dynamic histomorphometry (months 4-12)

Aim 2. *Determine the bone adaptation and peripheral nerve response of capsaicin- and vehicle-injected mice to increased mechanical loading* (months 6-18):

2a. Strain gage analysis of bone strain during tibial compression (months 6-7)
2b. Capsaicin or vehicle treatment of neonatal mice (months 6-8)
2c. Tibial compression of capsaicin- and vehicle-injected mice (months 8-10)
2d. Micro-computed tomography of mouse bones
2e. ELISA analysis of neuropeptides in bone
2f. Multiplex analysis of bone biomarkers
2g. Embedding/cutting/imaging/analysis of bones for dynamic histomorphometry

As of the date of this report (7 April 2016), all items for Aim 1 have been accomplished, and this work has been published in the Journal of Musculoskeletal and Neuronal Interaction (attached). All items for Aim 2 have been accomplished, and a manuscript describing this work has been submitted to the journal Bone, and is in revision.

PROGRESS REPORT

Aim 1. *Determine the effects of neonatal capsaicin treatment on bone structure and metabolism, and neuropeptide concentrations in bone compared to vehicle-injected mice*:

1a. Institutional approval of animal use protocols
An institutional IACUC protocol was submitted and approved prior to the beginning of the funding period. This protocol (#15972: Interdependence of neurotransmitters and functional adaptation of bone to mechanical loading") was originally approved on 4 June 2011. Approval by ACURO was obtained within the first six months of the funding period.

1b. Capsaicin or vehicle treatment of neonatal mice

A total of 42 male and female C57BL/6 neonatal mice were used in this study, from 7 timed pregnant females (Harlan Laboratories, Indianapolis, IN). Neonatal capsaicin treatment was performed as previously described [10]. Briefly, neonatal mice were given subcutaneous injections of capsaicin (50 mg/kg) or vehicle (10% ethanol, 10% Tween 80 in isotonic saline) on day 2 and 5 after birth (n = 21 vehicle, 21 capsaicin). Following capsaicin or vehicle treatment, neonatal mice were returned to normal cage activity until weaning (28 days). Mice were sacrificed 4, 8, or 12 weeks after birth, with a total of 7 vehicle- and 7 capsaicin-treated mice per time point (2-5 mice per age/sex/treatment group). We selected these time points to observe developmental changes from weaning until skeletal maturity, and to account for any possible recovery from sensory nerve inactivation by adulthood. Mice were weighed 1-2 times per week from birth until sacrifice.

Capsaicin- and vehicle-treated mice were subjected to hot-plate analgesia testing at 4, 8, and 12 weeks of age to determine response time to a constant thermal stimulus of 55 °C as previously described [11]. Mice were placed on a hot-plate (LE 7406, Coulborn Instruments, Whitehall, PA) and removed after indication of discomfort, determined as twitching or licking of a hind limb or jumping, or after a maximum of 30 seconds, and the latency time of the response was recorded. Each mouse was tested twice at each time point, and the latency times were averaged for each mouse/time point.

Neonatal capsaicin treatment did not have a statistically significant effect on body weights of male mice; there was no difference in body weight between capsaicin- and vehicle-treated male mice for any time point from weaning through 12 weeks (**Fig. 1**). However, capsaicin treatment significantly affected body weights of female mice at early time points. Female mice treated with capsaicin had 8-13% lower body weights than vehicle-treated female mice from weaning until 47 days of age (Fig. 1; $p < 0.05$ for both time points). There were no significant differences in body weights for capsaicin- and vehicle-treated female mice from 8 to 12 weeks of age.

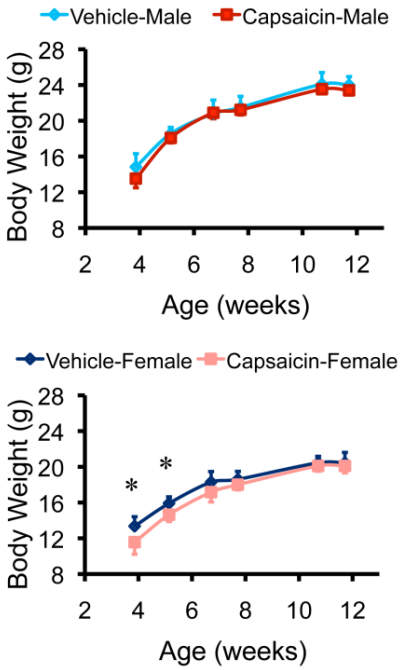

Figure 1: Body weights of treated and untreated mice were recorded from weaning until 12 weeks of age. Female mice treated with capsaicin had lower body weight than vehicle-treated female mice from weaning until day 47. Body weights of male mice were unaffected at all time points. * Capsaicin vs. vehicle; $p < 0.05$.

Mice treated with capsaicin had significantly longer latency times when exposed to the constant thermal stimulus than vehicle-treated mice at all time points examined (**Fig. 2**; $p < 0.0001$). For example, at 8 weeks of age, the average latency time of capsaicin-treated mice was 63% longer than that of vehicle-treated mice ($p = 0.0002$), while at 12 weeks of age the latency time was 67% longer for capsaicin-treated mice ($p = 0.0007$). This confirms that mice treated with capsaicin had decreased peripheral sensory nerve function, which persisted until at least 12 weeks of age. Age was also a main effect for latency time ($p = 0.0052$); latency times for both capsaicin- and vehicle-treated mice at 12 weeks of age were significantly shorter than at 4 or 8 weeks.

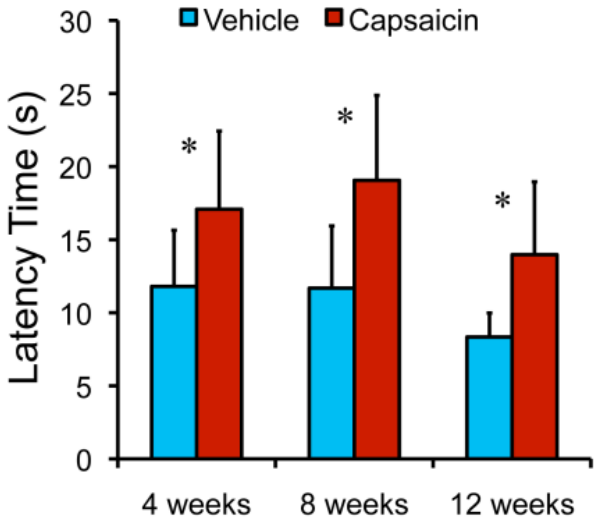

Figure 2: Hot-plate analgesia testing of treated and untreated mice was performed to verify decreased peripheral sensory nerve function. Treatment and age were main effects for latency time ($p < 0.0001$, $p = 0.0052$). Capsaicin-treated mice had significantly longer latency times than vehicle-treated mice at all time points when exposed to a constant 55° C thermal stimulus. * Capsaicin vs. vehicle; $p < 0.05$.

1c. Micro-computed tomography of mouse bones

Right tibias, right femurs, and L5 vertebrae were removed post mortem and preserved in 70% ethanol. Bones were scanned using micro-computed tomography (SCANCO, µCT 35, Bassersdorf, Switzerland); images were acquired at 6 µm nominal voxel size (energy=55 kVp, intensity=114 µA, integration time = 900 ms). Trabecular bone was analyzed at the metaphysis and epiphysis of the distal femur and at the L5 vertebral body using manually drawn contours inside the cortical shell on two-dimensional slices. The metaphysis was defined by a 900 µm thick volume of interest beginning below the middle break of the growth plate. Trabecular bone volume per total volume (BV/TV), trabecular number, trabecular thickness (Tb.Th), trabecular separation (Tb.Sp), and bone mineral density (BMR) were determined using the manufacturer's 3-D analysis tools. Cortical bone was analyzed at the mid-diaphysis of the tibia and femur, using a 240 µm thick volume of interest centered at the measured midpoint of each bone. Bone area (B.Ar), medullary area (M.Ar), total cross-sectional area (Tt.Ar), cortical thickness (Ct.Th), and bone mineral density (BMR) were determined using the manufacturer's 3-D analysis tools.

Capsaicin treatment resulted in small but significant decreases in bone structure parameters in trabecular bone of mice relative to vehicle-treated controls (**Fig. 3**). For example, we observed a significant main effect of capsaicin treatment on Tb.Th at the femoral metaphysis and L5 vertebral body ($p = 0.0002$ and 0.0024, respectively). Female capsaicin-treated mice had 5.2-9.5% lower Tb.Th than vehicle-treated female mice at these sites at each time point ($p = 0.0056$-0.049). However, we did not observe a significant effect of capsaicin treatment on BV/TV or Tb.Sp at the femoral metaphysis. At the femoral epiphysis, we observed a significant treatment*sex interaction for Tb.Th. ($p = 0.026$), with female mice being more severely affected by capsaicin treatment than male mice. We also found a significant treatment*sex*age interaction for BV/TV at the femoral epiphysis. For example, female capsaicin-treated mice had 8.7% lower BV/TV at the femoral epiphysis than vehicle-treated female mice at 8 weeks ($p = 0.015$), whereas male mice had similar BV/TV at this time point.

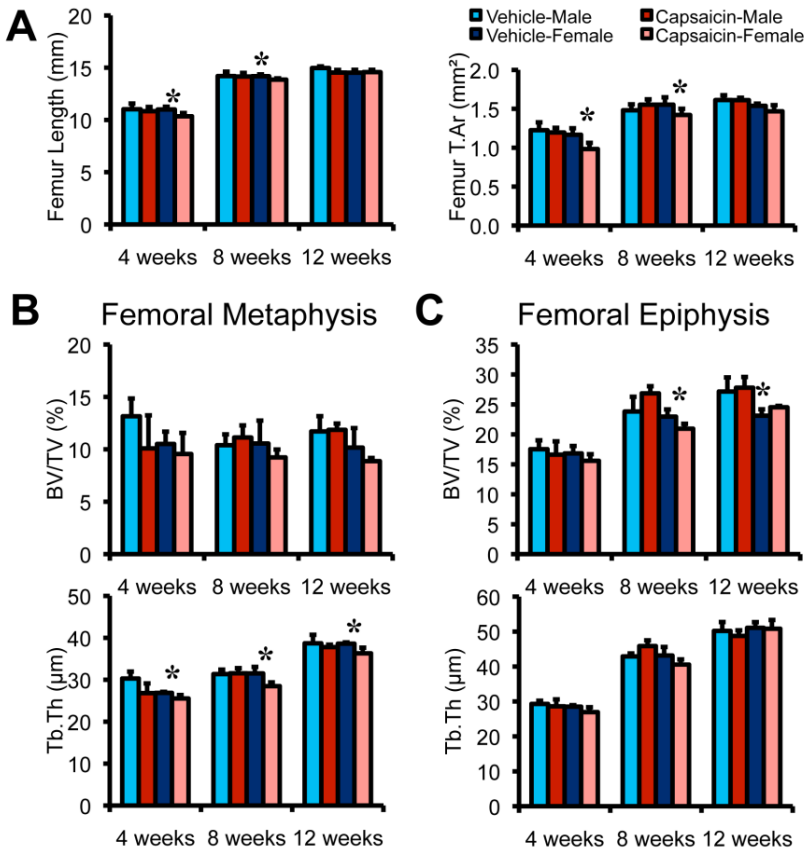

Figure 3: Micro-computed tomography of femoral cortical and trabecular bone. (A) Femur length and total cross-sectional area (Tt.Ar) of the femoral diaphysis were significantly affected in capsaicin-treated female mice. (B) Capsaicin treatment did not significantly affect trabecular bone volume fraction (BV/TV) at the femoral metaphysis but reduced trabecular thickness (Tb.Th) at this location in female mice. (C) Capsaicin treatment significantly affected BV/TV at the femoral epiphysis in female mice, but did not alter Tb.Th at this location. * Capsaicin vs. vehicle; $p < 0.05$.

We also observed significant effects of capsaicin treatment on cortical bone structure, with significant main effects of capsaicin treatment on femur length, M.Ar, and Tt.Ar ($p = 0.0094$, 0.026, and 0.026, respectively). For example, femurs from female mice treated with capsaicin were 6.0% and 2.3% shorter than femurs from female vehicle-treated mice at 4 and 8 weeks, respectively ($p = 0.034$, 0.0097). At 4 weeks, femurs from female capsaicin-treated mice had 15% smaller M.Ar and 16% smaller Tt.Ar compared with vehicle-treated mice ($p = 0.042$, 0.031). Capsaicin treatment also affected cortical bone of the tibia. There were significant treatment*sex interactions for tibia M.Ar and Tt.Ar ($p = 0.025$, 0.0032). At 4 weeks, the tibias from female capsaicin-treated mice had 16% smaller M.Ar and 15% smaller Tt.Ar compared with vehicle-treated mice ($p = 0.022$, 0.029). We did not observe any significant effects of capsaicin treatment on bone mineral density of either trabecular or cortical bone. As expected, sex and age had significant effects for several measured bone structure parameters.

1d. ELISA analysis of neuropeptides in bone

Femora, tibiae, muscle, and skin samples were collected from capsaicin- and vehicle-treated mice at the time of sacrifice, and were analyzed for neuropeptide concentrations using ELISA (**Fig. 4**). Bones were analyzed for calcitonin-gene related peptide (CGRP) and substance P (SP). Tissue samples were flash frozen with liquid nitrogen immediately following dissection, and were then crushed into small fragments, boiled in 2 M acetic acid in 4% EDTA (pH 3.5), and centrifuged at 3000 *g* for 15 min. Supernatants were freeze-dried and dissolved in ELISA buffer. Neuropeptide concentrations were determined using commercial mouse-specific ELISA assays (USCN Life Sciences, Inc., Wuhan, China), and data was normalized to the wet weight of the tibia to account for variation in bone size. Using this technique we were unable detect any effects of capsaicin treatment on concentrations of CGRP or SP in bone.

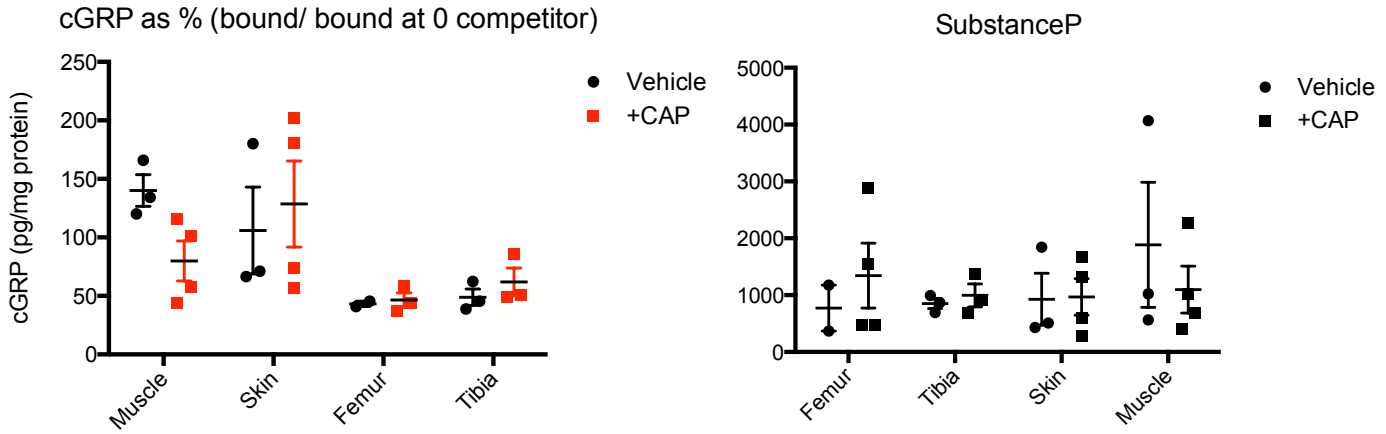

Figure 4: Concentrations of calcitonin gene-related peptide (CGRP) and substance P (SP) in bone, skin, and muscle of capsaicin- and vehicle-treated mice. No significant differences in neuropeptide concentrations were observed for any of the tissues, and a large amount of variance was present in the experimental groups. We are currently considering alternative

1e. Multiplex analysis of bone biomarkers

Blood was collected from capsaicin- and vehicle-treated mice immediately prior to sacrifice for quantification of systemic biomarkers of bone metabolism. Mice were anesthetized with isoflurane and approximately 100-200 µL of blood was collected retro-orbitally. Samples were allowed to clot for 2-4 hours in an ice bath and then centrifuged at 1000 g for 5 minutes. The supernatants were collected and frozen rapidly to -80 °C until analyzed. Serum was analyzed in duplicate to determine the concentrations of carboxy-terminal collagen crosslinks I (CTX-I) and procollagen type 1 amino-terminal propeptide (P1NP) using commercial mouse-specific ELISAs (Cusabio, Wuhan, China) per the manufacturer's instructions. CTX-I is a common biomarker for bone resorption, while P1NP is a biomarker for bone formation [12].

We did not detect any significant main effects of capsaicin treatment on serum concentrations of CTX-I or P1NP (**Fig. 5**), although male capsaicin-treated mice at 8 weeks of age had 37% lower CTX-I concentrations than vehicle-treated male mice of the same age ($p = 0.046$). We also observed a significant effect of sex on concentrations of CTX-I ($p = 0.043$), with female mice exhibiting lower concentrations of CTX-I than male mice. P1NP serum concentrations did not vary significantly by treatment, sex, or age.

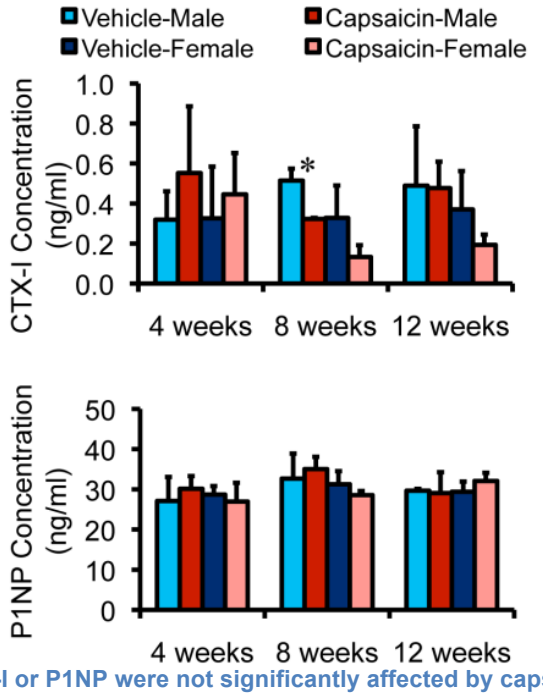

Figure 5: Serum concentrations of CTX-I or P1NP were not significantly affected by capsaicin treatment, as measured using ELISAs. Sex was a main effect for serum concentrations of CTX-I, while P1NP concentrations did not vary significantly by sex or age. * Capsaicin vs. vehicle; $p < 0.05$.

1f. Embedding/cutting/imaging/analysis of bones for dynamic histomorphometry
Mice received injections of calcein green (10 mg/kg; Sigma-Aldrich, St. Louis, MO) and Alizarin-3-methlimino-diacetic acid (30 mg/kg; Sigma-Aldrich, St. Louis, MO) 10 days and 3 days prior to sacrifice, respectively. After scanning with μCT, the right tibias were embedded in Technovit (Kulzer, Wehrheim, Germany) using standard techniques for undecalcified bone [13]. Two sections were cut from each bone on a bandsaw (Model 310, Exakt Technologies, Norderstedt, Germany) in the transverse plane at 40% of the length from the proximal end. Sections were ground to an approximate thickness of 40 μm. Two color fluorescent images were obtained at 10x magnification (Nikon Eclipse TE2000-E, Tokyo, Japan). Dynamic histomorphometric analysis was performed using commercial software (Bioquant, Nashville, TN) and the results were averaged for the replicate slides from each bone. Mineral apposition rate (MAR), percent mineralizing surface (MS/BS), and bone formation rate (BFR/BS) were quantified for the endosteal and periosteal surfaces.

Capsaicin treatment significantly altered bone formation parameters in the tibiae of treated mice (**Fig. 6**). We observed significant treatment*sex*age interactions for MAR and BFR at the endosteal surface (p = 0.023, 0.020) and for MAR and MS/BS at the periosteal surface (p = 0.035, 0.042). For example, at 4 weeks, female capsaicin-treated mice had 39% higher MAR than female vehicle-treated mice at the endosteal surface of the tibia. At 12 weeks, female mice treated with capsaicin had 23.4% lower MS/BS (p = 0.012) and 22.4% lower BFR (p = 0.061) at the periosteal surface than female vehicle-treated mice. Age was a significant main effect for MAR, MS/BS and BFR at the endosteal and periosteal surfaces.

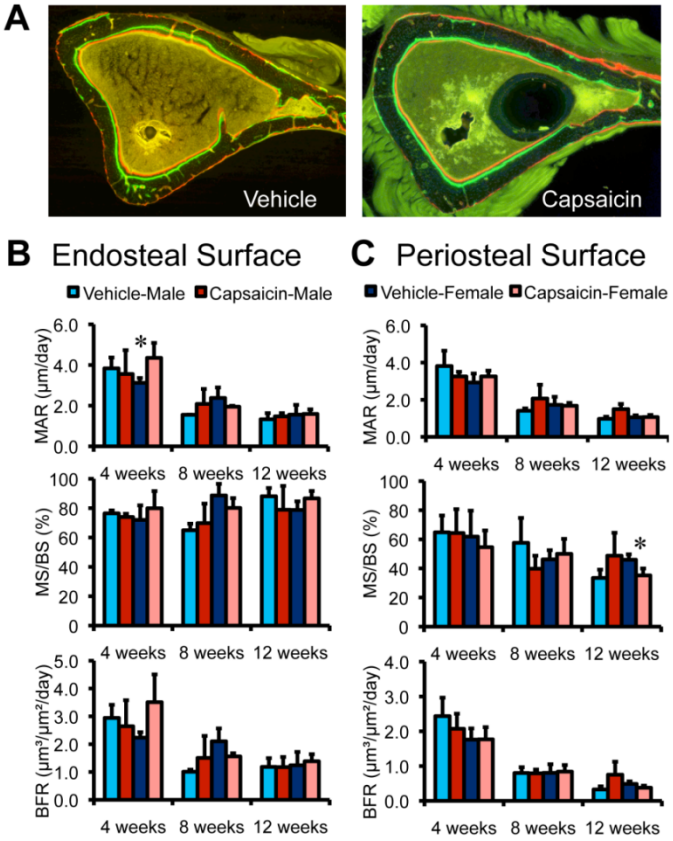

Figure 6: Dynamic histomorphometry was used to identify changes in bone formation rates in capsaicin- and vehicle-treated mice. Fluorescent images (A) show cortical bone from the tibias of 8 week old female vehicle- and capsaicin-treated mice. Mineral apposition rate (MAR), percent mineralizing surface (MS/BS), and bone formation rate (BFR/BS) were quantified for the endosteal (B) and periosteal surfaces (C). Age was a significant main effect for MAR, MS/BS and BFR at the endosteal and periosteal surfaces. * Capsaicin vs. vehicle; p < 0.05.

Aim 1 Discussion and Conclusions
In this study, we investigated the role of peripheral sensory nerves in bone metabolism during development in mice. We found that neonatal capsaicin treatment in mice led to modest and significant decreases in bone structure parameters, but this effect was inconsistent for mechanical properties and bone turnover rate. Capsaicin treatment had the greatest impact on trabecular bone, with treated mice exhibiting lower trabecular

thickness at the femoral metaphysis and L5 vertebral body. However, contrary to our initial hypothesis, mice treated with capsaicin did not exhibit reduced mechanical properties or resistance to fracture. Yield stress and elastic modulus were similar between treated and untreated mice, suggesting that gross geometrical changes in the radii caused the lower yield force of capsaicin-treated mice. Also in opposition to our hypothesis, capsaicin treatment did not lead to substantial reductions in bone turnover rate, measured by dynamic histomorphometry and serum concentrations of CTX-I and P1NP. Altogether, these data indicate that decreased activity of peripheral sensory nerves has a small effect on the trabecular and cortical bone of mice, but that these changes do not result in a meaningful reduction in mechanical properties of whole bones.

In this study we observed only modest differences in bone parameters in capsaicin-treated mice, despite a considerable and sustained decrease in sensory nerve activity. Physiological adaptations during development may allow mice to compensate for the loss of peripheral nerve function, leading to similar development between treated and untreated mice at 12 weeks of age. It is possible that while bone structure and basal metabolic rates are conserved in capsaicin-treated mice as adults, adaptation of bone in response to mechanical loading or injury may be altered, as observed in other mouse models. For example, in a study of adult female mice lacking estrogen receptor–α, the ulnae were only 4% shorter yet demonstrated a three-fold lower osteogenic response to mechanical loading than the ulnae of wild-type littermates [14]. This is further supported by a previous study using neonatal capsaicin treatment in rats, in which capsaicin treatment did not alter normal bone growth and maintenance, but decreased the local bone remodeling response following molar extraction [9]. Future studies using this model will investigate the bone adaptation of capsaicin-treated mice to conditions such as increased mechanical loading or injury.

The effect of neonatal capsaicin treatment on bone properties had a differential effect on female mice versus male mice, although the power of this study was not sufficient to fully determine sex-based differences. At 4 and 8 weeks, female capsaicin-treated mice demonstrated the largest differences in bone structure, with shorter femurs with smaller cross-sectional area and trabecular thickness. Male capsaicin-treated mice had significantly lower trabecular thickness at the L5 vertebral body for the first time at 12 weeks of age, and lower moment of inertia and yield force of the radii compared to vehicle-treated mice at this time point. These potential sex-based differences may be related to hormonal fluctuations, as mice reach sexual maturity at 8 weeks of age.

The mouse model used in this study overcomes critical limitations of previous models investigating decreased peripheral nerve function in bone. Capsaicin treatment isolates the effects of decreased sensory nerve function without requiring surgical procedures or impairing motor function. Other studies utilizing capsaicin treatment in adult rats found that capsaicin-sensitive neurons contribute to the maintenance of trabecular bone [15]. However, capsaicin directly interacts with bone cells [16, 17], making it difficult to separate the primary effect on bone cells from the secondary effect of decreased peripheral nerve function, as both osteoclasts and osteoblasts express receptors for capsaicin [18, 19]. Treating mice as neonates instead of at maturity allows time for recovery of normal bone metabolism, and therefore isolates the effects of sensory nerve inactivation without the complication of direct action on bone cells inherent in adult treatment.

In this study we were able to detect small but significant differences in trabecular and cortical bone structure, but were unable to detect differences in bone mineral density or bone mechanical properties. This suggests that peripheral nerve inactivation may influence bone quantity, but not bone quality. If this is the case, differences in bone formation or resorption would be expected. However, imprecise methods for detecting bone turnover rates may have limited our observation of changes in capsaicin-treated mice. We were able to detect small changes in bone structure because of the high precision of micro-computed tomography. However, we were unable to detect small differences using lower resolution methods such as dynamic histomorphometry and quantification of serum biomarkers. Both of these techniques were further limited by scope: our histomorphometric analysis was limited to cortical bone, and biomarker concentrations were measured from the serum of developing mice. Similarly, three-point bending of radii may not have had adequate sensitivity to fully capture changes in bone mechanical properties.

This study is limited because it did not directly investigate the effects of capsaicin treatment on sensory neurons in bone. While we verified decreased peripheral sensory nerve function using response to a thermal

stimulus, we did not perform a direct quantification in bone, such as counting neurons remaining after treatment or quantification of neuropeptides in bone. It is well established that capsaicin treatment does not affect motor neurons, however it is possible that the reduction in peripheral sensory nerve function could alter spontaneous motor activity in mice. Quantification of activity levels in vehicle- and capsaicin-treated mice could further establish that differences in bone structure are due to decreased sensory nerve function rather than decreased mechanical loading of bone. This study also did not investigate the response of bone to differing levels of sensory nerve inactivation. A more thorough disruption of peripheral sensory nerve function could have a more dramatic effect on bone metabolism than was observed in this study. Further, in this study we used neonatal capsaicin treatment as a surrogate for age-related degeneration of peripheral nerves, but did not directly make comparisons with aged animals. It is possible that aged mice demonstrate a different pattern of neural degeneration than mice treated with capsaicin as neonates. However, we were able to study the isolated effects of decreased peripheral sensory nerve function in mice up to skeletal maturity.

This study further supports a role for peripheral sensory nerves in bone metabolism. Using neonatal capsaicin treatment, we established a mouse model of decreased peripheral sensory nerve function and observed resulting changes in bone structure. We observed only small changes in bone structure with sensory nerve inactivation, with no notable changes in bone metabolism or bone quality. Therefore age-related changes in sensory innervation may not be clinically meaningful with respect to bone strength under normal loading conditions. It is possible that capsaicin-sensitive neurons may become important for bone under stress conditions such as increased mechanical loading or injury. Future studies will investigate this potential role of peripheral sensory nerves in bone adaptation.

Aim 2. *Determine the bone adaptation and peripheral nerve response of capsaicin- and vehicle-injected mice to increased mechanical loading*:

2a. Strain gage analysis of bone strain during tibial compression

A preliminary study was performed to quantify tibial strain in capsaicin- (n = 3) and vehicle-treated mice (n = 4) during axial compression. Immediately after sacrifice, a single element strain gauge (UFLK-1-11-1L, Tokyo Sokki Kenkyujo Co., Ltd., Japan) was bonded to the anteromedial surface of the tibia in alignment with the long axis of the bone. The center of the gauge was located approximately 5 mm distal to the tibial plateau (**Fig. 7A**). This location is commonly used for measuring bone strain during tibial compression in mice [20-22] since positioning of the strain gauge is limited by tibia size and morphology. The strain gauge was wired to amplification circuitry and the data acquired in LabView. The lower leg of each mouse was compressed in intervals of 1 N from 1 N to 7 N at a loading rate of 5.5 mm/sec.

Bone strain measured on the anteromedial surface of the tibia was not different for capsaicin- and vehicle-treated mice for compressive forces of 1-7 N (**Fig. 7B**). Therefore, all mice were loaded to the same target force of 3 N or 7 N for the investigation of bone adaptation.

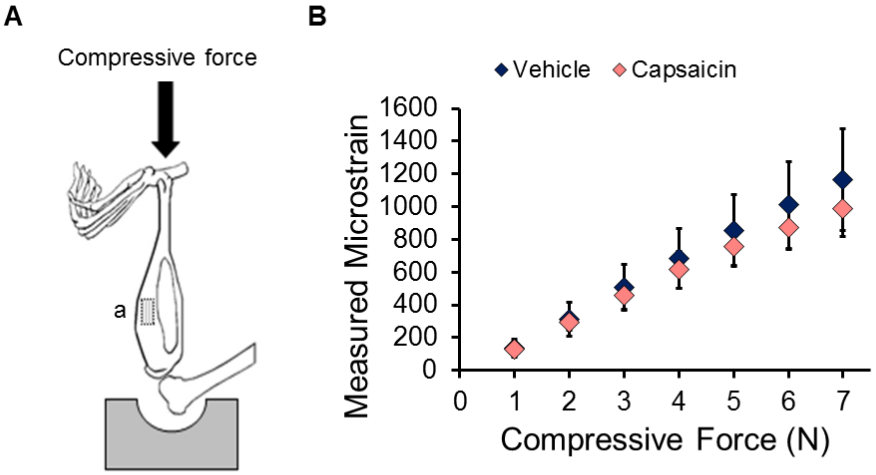

Figure 7: Maximum bone strain during tibial compression was measured at the anteromedial surface of tibias. (A) A diagrammatic representation shows the approximate location of the strain gauge (a). (B) Maximum bone strain measured during tibial compression at compressive magnitudes from 1-7 N. There was not a significant difference in measured strain between capsaicin- and vehicle-treated mice at any of the compressive forces tested.

2b. Capsaicin or vehicle treatment of neonatal mice

A total of 35 female C57BL/6 neonatal mice were used in this study, from 13 timed pregnant females (Harlan Laboratories, Indianapolis, IN). Neonatal capsaicin treatment was performed as previously described [10]. Briefly, neonatal mice were given subcutaneous injections of capsaicin (50 mg/kg) or vehicle (10% ethanol, 10% Tween 80 in isotonic saline) on day 2 and 5 after birth (n = 18 vehicle, 17 capsaicin). Previous studies have shown that this treatment protocol decreases peripheral sensory nerve function for the lifetime of the animal, but motor function is not affected [23]. Following capsaicin or vehicle treatment, neonatal mice were returned to normal cage activity until weaning (28 days). Mice were subjected to tibial compression starting at 12 weeks of age with magnitudes of either 3 N or 7 N, with a total of 7-10 mice/treatment group/compressive force.

Capsaicin- and vehicle-treated mice were subjected to hot-plate analgesia testing at 12 weeks of age before the start of tibial compression to determine response time to a constant thermal stimulus of 55 °C as previously described [11]. Mice were placed on a hot-plate (LE 7406, Coulborn Instruments, Whitehall, PA) and removed after indication of discomfort, determined as twitching or licking of a hind limb or jumping, or after a maximum of 30 seconds, and the latency time of the response was recorded. Each mouse was tested twice and the latency times were averaged for each mouse.

Tibial compression was well tolerated by all animals. Both capsaicin- and vehicle-treated mice had similar body weight on loading day 1, and changes in body weight were similar between treatment groups. Average weight loss between loading days 1 and 10 was 5.6% of body weight for each compressive force.

At 12 weeks of age, capsaicin-treated mice took 55% longer to respond to the thermal stimulus than vehicle-treated mice, consistent with reduced peripheral sensory nerve function resulting from neonatal capsaicin treatment. Mice treated with capsaicin had comparable latency times before 3 N or 7 N tibial compression (**Fig. 8**). Similarly, there was not a significant difference between the latency times of vehicle-treated mice subjected to the different compressive forces.

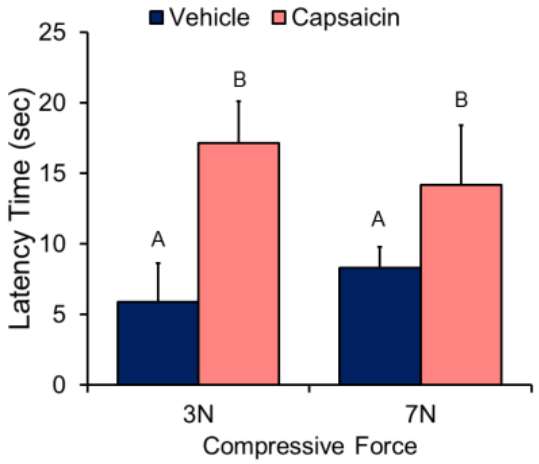

Figure 8: Hot-plate analgesia testing of vehicle- and capsaicin-treated mice was performed at 12 weeks of age to verify decreased peripheral sensory nerve function prior to tibial compression. Capsaicin-treated mice exhibited significantly longer latency times than vehicle-treated mice in both compressive force groups when exposed to a constant 55° C thermal stimulus, indicating decreased thermal sensitivity. Groups not connected by the same letter are significantly different ($p < 0.05$).

2c. Tibial compression of capsaicin- and vehicle-injected mice

The tibial compression loading protocol was similar to that used by others in studies of bone adaptation [20, 24]. The tibial compression system consisted of two custom-built loading platens, positioned vertically within an electromagnetic materials testing machine (Bose ElectroForce 3200, Eden Prairie, MN, USA). The bottom platen held the flexed knee and the top platen positioned the foot. A slight preload (<0.5N) maintained the

position of the limb. Mice were anesthetized with isoflurane inhalation while the right lower leg of each mouse was subjected to cyclic axial compressive loading for 1200 cycles per day for a total of 10 days (M-F) over two weeks. For 18 of the mice, the top platen was driven at 5.5 mm/sec until a target compressive load of 3 N was reached. The remaining 17 mice were loaded at 8.5 mm/sec to a target compressive load of 7 N. Both loading rates resulted in an applied load frequency of approximately 4 cycles/second. Left tibias were used as internal controls. Mice were weighed on days 1, 5 and 10 of loading. Mice were sacrificed the third day after completion of two weeks of tibial compression.

2d. Micro-computed tomography of mouse bones

Bilateral tibias were removed post mortem and preserved in 70% ethanol. Bones were scanned using micro-computed tomography (SCANCO, µCT 35, Brüttisellen, Switzerland); images were acquired at 6 µm nominal voxel size (energy=55 kVp, intensity=114 µA, integration time = 900 ms). Trabecular bone was analyzed at the metaphysis of the tibias using manually drawn contours inside the cortical shell on two-dimensional slices. The metaphysis was defined by a 900 µm thick volume of interest beginning below the middle break of the growth plate. Trabecular bone volume per total volume (BV/TV), trabecular thickness (Tb.Th), and trabecular number (Tb.N) were determined using the manufacturer's 3-D analysis tools. Cortical bone was analyzed at 10, 20, 30, 40 and 50% of the tibia lengths (a region encompassing peak compressive strain [25] and known cortical bone response [26]; **Fig. 9**), using 600 µm thick volumes of interest centered at the measured locations. Total cross-sectional area (Tt.Ar), bone area (B.Ar), medullary area (M.Ar), cortical thickness (Ct.Th), and bone mineral content (BMC) were determined using the manufacturer's 3-D analysis tools.

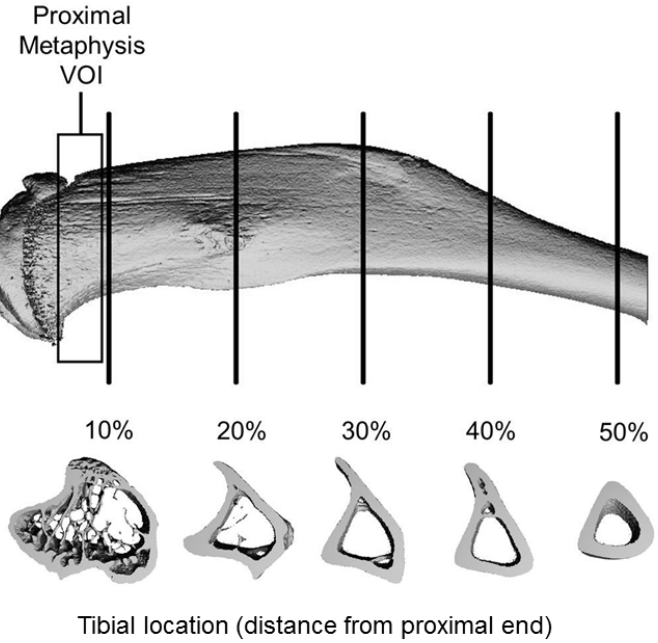

Figure 9: MicroCT analysis of trabecular bone was performed at the proximal tibial metaphysis. Cortical bone analysis was performed using µCT and dynamic histomorphometry at 5 locations along the length of the tibias.

MicroCT analysis revealed that mechanical loading did not affect trabecular bone volume fraction (BV/TV) of the tibial metaphysis, although the microstructure of trabecular bone was slightly altered. For example, loaded and contralateral tibias displayed a similar BV/TV at each compressive force (**Table 1**). However, loaded tibias had greater trabecular thickness and reduced trabecular number relative to contralateral tibias, although these trends were not statistically significant.

Table 1: Trabecular bone parameters assessed at the tibial metaphysis using microCT

Treatment	BV/TV		Tb.Th		Tb.N	
Group	Control	Loaded	Control	Loaded	Control	Loaded
3N compressive force						
Vehicle	0.107±0.013	0.110±0.011	0.0440±0.0016	0.0451±0.0022	4.28±0.244	4.25±0.164
Capsaicin	0.105±0.007	0.108±0.003	0.0421±0.0017	0.0422±0.0020	4.35±0.163	4.40±0.135
7N compressive force						
Vehicle	0.119±0.011	0.112±0.014	0.0449±0.0028	0.0503±0.0029	4.20±0.242	3.89±0.223
Capsaicin	0.127±0.008	0.129±0.017	0.0430±0.0014	0.0471±0.0031	4.51±0.280	4.30±0.351

Data reported as mean±SD.

Tibial compression significantly affected cortical bone of loaded tibias, with adaptation dependent on compressive force and location along the tibia (**Fig. 10, Table 2**). Compression at 7 N generated a larger cortical bone response than 3 N compression. For example, at 10% of the tibia length, Tt.Ar increased 16% at 7 N compared to 3.3% at the lower compressive force. In addition, BMC increased only 1.5% in tibias loaded at 3 N, while the increase was six times higher in tibias loaded at 7 N. Location along the tibia also significantly affected the adaptive response of cortical bone. The largest changes were observed at 10% of the tibia length, whereas bone at 30% often displayed insignificant changes. The increase in Tt.Ar at 10% was accompanied by a 14% increase in M.Ar at the 7 N force. At 20%, the increase in M.Ar was reduced to 8.2%. Changes in Ct.Th also varied by location, with loaded tibias becoming thinner at 10% and thicker at 50% of their length. Often, capsaicin- and vehicle-treated mice displayed similar trends in adaptation to increased loading. However, tibias of capsaicin-treated mice demonstrated greater changes at some locations. For example, at 20%, capsaicin-treated mice had an 8.8% increase in Tt.Ar, while vehicle-treated mice showed no significant change. Furthermore, the increase in BMC at 10% was almost two fold higher for capsaicin-treated mice compared to vehicle-treated mice.

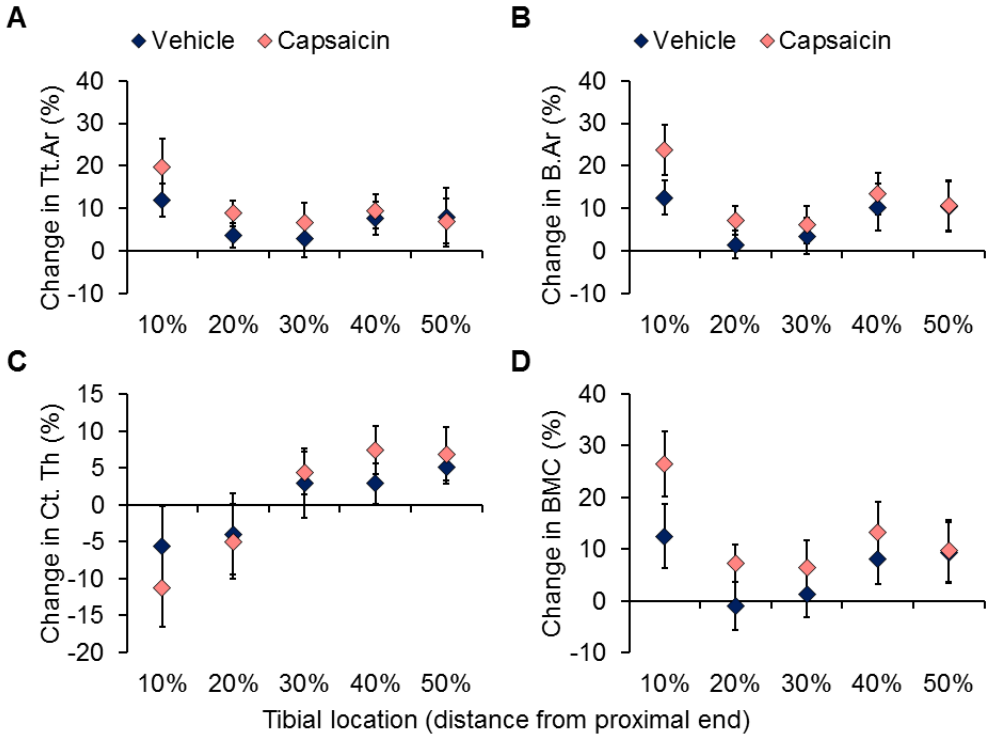

Figure 10: Micro-computed tomography identified changes in cortical bone along the length of the tibias after two weeks of 7 N tibial compression. Diamonds represent the average change of loaded compared to control tibias with error bars indicating standard deviation. (A) Total cross-sectional area (Tt.Ar) was significantly increased in loaded tibias at all locations except 30%. (B) Changes in bone area (B.Ar) mirrored changes in Tt.Ar. (C) Cortical thickness (Ct.Th) decreased at more proximal locations along the tibia. (D) Bone mineral content (BMC) was significantly altered by tibial compression and varied by location on the tibia.

Table 2: Cortical bone parameters assessed along control and loaded tibias using microCT

Tibial Location	Treatment Group	Total area[a,b,c] (mm²)		Medullary area[a] (mm²)		Bone mineral content[a,b] (mgHA)	
		Control	Loaded	Control	Loaded	Control	Loaded
3N compressive force							
10%	Vehicle	2.82±0.18	2.97±0.28	1.91±0.17	2.02±0.24	0.60±0.03	0.63±0.04
	Capsaicin	2.65±0.15	2.67±0.16	1.79±0.13	1.80±0.11	0.60±0.04	0.57±0.05
20%	Vehicle	1.67±0.14	1.70±0.11	0.84±0.12	0.85±0.02	0.53±0.02	0.55±0.03
	Capsaicin	1.57±0.06	1.56±0.05	0.78±0.05	0.77±0.04	0.50±0.02	0.51±0.02
30%	Vehicle	1.40±0.09	1.39±0.06	0.66±0.06	0.65±0.05	0.49±0.03	0.49±0.02
	Capsaicin	1.31±0.04	1.30±0.05	0.61±0.02	0.61±0.03	0.46±0.02	0.46±0.02
40%	Vehicle	1.22±0.08	1.22±0.06	0.54±0.04	0.54±0.03	0.45±0.03	0.46±0.02
	Capsaicin	1.15±0.06	1.15±0.05	0.51±0.03	0.50±0.02	0.43±0.02	0.43±0.02
50%	Vehicle	0.94±0.05	0.92±0.06	0.37±0.03	0.36±0.04	0.40±0.02	0.39±0.02
	Capsaicin	0.89±0.06	0.87±0.04	0.35±0.03	0.34±0.03	0.37±0.02	0.37±0.02
7N compressive force							
10%	Vehicle	3.04±0.10	3.41±0.14*	2.03±0.09	2.27±0.12	0.65±0.03	0.73±0.04*
	Capsaicin	2.79±0.18	3.33±0.12*	1.85±0.13	2.17±0.10	0.60±0.04	0.75±0.04**
20%	Vehicle	1.81±0.07	1.87±0.08	0.90±0.07	0.96±0.06	0.58±0.03	0.57±0.02
	Capsaicin	1.67±0.06	1.82±0.06*	0.81±0.04	0.90±0.06	0.54±0.03	0.58±0.02
30%	Vehicle	1.52±0.04	1.57±0.06	0.72±0.04	0.74±0.04	0.53±0.02	0.54±0.02
	Capsaicin	1.42±0.09	1.51±0.05	0.64±0.05	0.68±0.04	0.51±0.03	0.54±0.01
40%	Vehicle	1.30±0.04	1.40±0.05	0.58±0.03	0.61±0.03	0.49±0.02	0.53±0.03*
	Capsaicin	1.22±0.06	1.33±0.06	0.52±0.03	0.54±0.03	0.47±0.03	0.53±0.03*
50%	Vehicle	1.00±0.03	1.08±0.06	0.39±0.02	0.41±0.03	0.43±0.01	0.47±0.03*
	Capsaicin	0.95±0.06	1.01±0.05	0.36±0.03	0.37±0.03	0.41±0.02	0.45±0.02

Data reported as mean±SD.
[a]: significant leg*VOI interaction, 7N compressive force
[b]: significant treatment*leg*VOI interaction, 7N compressive force
[c]: significant leg*VOI interaction, 3N compressive force
*: significant difference between control and loaded, $p<0.05$
**:significant difference between capsaicin and vehicle response, $p<0.05$

2e. ELISA analysis of neuropeptides in bone

In order to investigate whether neuropeptide concentrations alter in response to the mechanical environment of their target tissue, we used two different loading protocols. A well-established model of non-invasive loading [27], we used tibial compression to model increased mechanical loading of the limb. To simulate decreased mechanical stimulation, we subjected mice to tail suspension. For both loading protocols, we examined two different time points to determine the constancy of modified neuropeptide levels in bone. We hypothesized that both neuropeptides would be elevated after tibial compression because of their expected anabolic effect on bone and likewise diminished by hindlimb unloading.

Methods

Animals

A total of 32 female C57BL/6 mice were used in this study (Harlan Laboratories, Indianapolis, IN). Mice were allowed to acclimate to the housing facility for two weeks prior to the beginning of the experimental protocol. Mice were housed 4 to a cage and allowed food and water ad libitum. Mice were subjected to a mechanical stimulus of tibial compression or hindlimb unloading starting at 12 weeks of age for 1 or 5 days, with a total of 8 mice/stimulus/stimulus duration.

Mechanical loading protocol

The tibial compression loading protocol was similar to that used by others in studies of bone adaptation [20, 24]. The tibial compression system consisted of two custom-built loading platens, positioned vertically within an electromagnetic materials testing machine (Bose ElectroForce 3200, Eden Prairie, MN, USA). The bottom platen held the flexed knee and the top platen positioned the foot. A slight preload (<0.5N) maintained the position of the limb. Mice were anesthetized with isoflurane inhalation while the right lower leg of each mouse was subjected to cyclic axial compressive loading for 1200 cycles per day for a total of 1 day (mice were sacrificed within an hour of the second bout of loading) or 5 days (mice were sacrificed within an hour of the fifth bout of loading). The top platen was driven at 5.5 mm/sec until a target compressive load of 5 N was

reached. The loading rate resulted in an applied load frequency of approximately 4 cycles per second. Left tibias were used as controls. Mice were weighed on each day of loading and sacrificed within an hour after 1 or 5 days of tibial compression.

Hindlimb unloading protocol

To model decreased mechanical loading, mice were tail-suspended as previously described [28]. Mice were housed individually and suspended at a head-down angle of 30° so that the hindlimbs were not able to touch the cage floor. The tail was secured to a metal apparatus hung from a bar on the ceiling of the cage, permitting movement throughout the cage and rotation of 360°. Metal grid flooring was used to facilitate mouse movement. Mice were provided with Enviro-dri and/or Nestlets for environmental enrichment. Water and food were available throughout the experimental period. Mice were monitored daily for signs of distress resulting from the tail suspension protocol. Mice were suspended for either 1 day (24 hours) or 5 days (120 hours).

ELISAs of bone neuropeptides

Tibias were collected from mice immediately after sacrifice for quantification of whole bone concentrations of sensory neuropeptides. Mice were sacrificed and their tibias removed for analysis. Left tibias were transferred to vials of paraformaldehyde for later histological analysis. Right tibias were flash frozen in liquid nitrogen, and transferred to a -80 °C freezer until protein isolation. Frozen whole bones were cut in half and homogenized in Trizol for isolation. Protein was analyzed in duplicate to determine the concentrations of calcitonin gene related peptide and substance P using commercial mouse-specific ELISAs (Cusabio, Wuhan, China) per the manufacturer's instructions. Data were normalized to total protein concentration to account for variation in extraction efficiency.

Results

Mouse body weights

Most mice tolerated the different mechanical loading conditions reasonably well. There was a significant effect of stimulus day ($p = 0.03$), type of stimulus ($p = 0.009$), and the interaction ($p = 0.0003$) on body weight. There was not a difference in body weight between mice assigned to the different loading protocols on the first day of the experiment (**Fig. 11**). Overall, there was a decrease in body weight from the first day of the loading stimulus when mice were 12 weeks of age, to the fifth day at sacrifice. The average 3% increase in body weight of mice subjected to tibial compression was overshadowed by weight loss in the hindlimb unloaded mice. Aside from licking the junction between the suspension apparatus and their tail, mice showed no obvious signs of obvious distress during daily monitoring. However, mice lost an average of 9% of body weight from tail suspension, with one mouse losing 4.9 g during the experimental period.

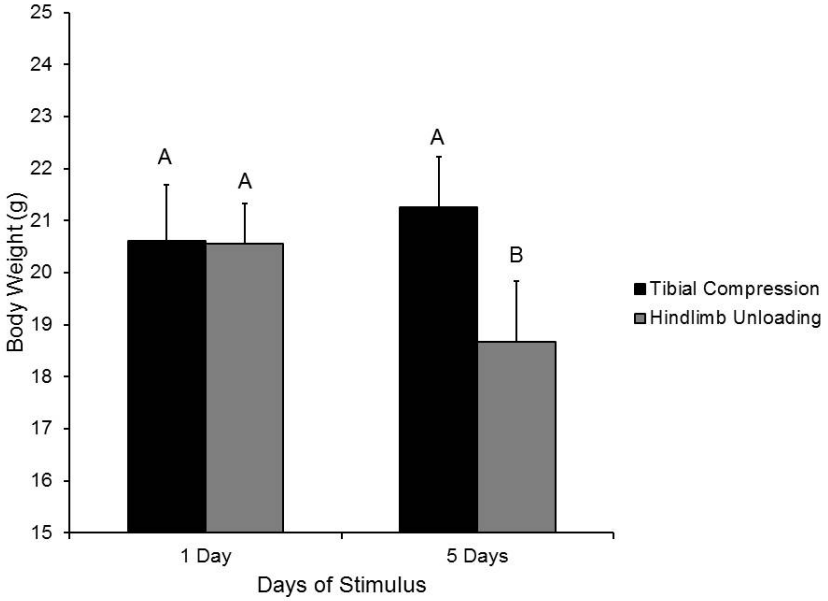

Figure 11: Body weights of mice subjected to 5 days of either tibial compression or hindlimb unloading.

ELISAs of bone neuropeptides

Concentrations of CGRP in bone were altered by the different mechanical environments (**Fig. 12**). The concentration of CGRP in the tibias was significantly lower after 5 days of stimulus than after a single day ($p = 0.0005$). Including both tibial compression and hindlimb unloading, the CGRP concentration was 35% lower after 5 days than after 1 day of stimulus. The type of loading stimulus also significantly affected CGRP concentration ($p = 0.0038$). While unloaded limbs were not significantly different from control ones, tibial compression caused a significant increase in CGRP concentration. Tibial compression raised CGRP concentration 66% compared to controls. After one day of tibial compression, the average CGRP concentration was 128 pg/mg protein compared to 71.5 pg/mg protein in controls. When applied for the longer duration of 5 days, CGRP concentration did not differ significantly from control tibias.

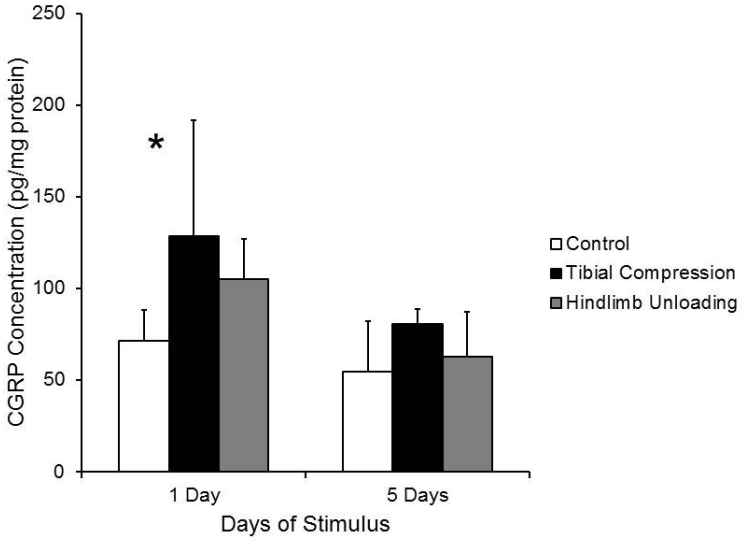

Figure 12: CGRP concentration in the bones of mice subjected to tibial compression or hindlimb unloading to model altered mechanical conditions.

Concentrations of substance P were over 8 times lower than CGRP levels in the tibias. The effects of the altered mechanical conditions also changed trends in neuropeptide concentration. Although tibial compression increased CGRP concentration, average substance P levels decreased in response to this mechanical stimulus. The duration of altered loading did not significantly affect substance P concentration, and the different experimental groups had similar levels between stimulus days (**Fig. 13**). However, the type of stimulus had a significant effect on substance P bone concentration ($p = 0.047$). Irrespective of duration of stimulus, substance P concentration in hindlimb unloaded tibias was 37% higher than tibias subjected to the increased mechanical loading.

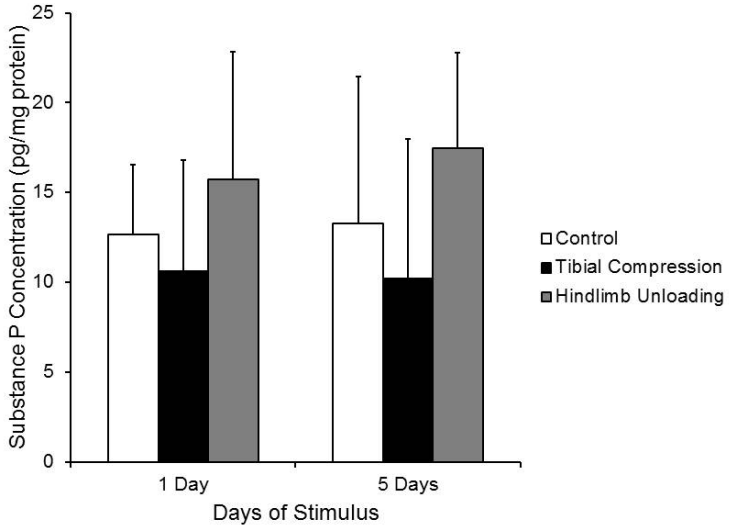

Figure 13: Substance P concentration in the bones of mice subjected to tibial compression or hindlimb unloading to model altered mechanical conditions.

2f. Multiplex analysis of bone biomarkers

For Aim 2, we did not perform Multiplex analysis of biomarkers of bone turnover as originally proposed. This is primarily due to the fact that we did not obtain positive results in Aim 1 for our study of bone turnover biomarkers. Instead, this aim relied on direct quantification of bone formation rates using dynamic histomorphometry (described below). Additionally, we performed a much more thorough analysis of neuropeptide concentrations in bone, including models of increased and decreased mechanical loading. This more thorough analysis provided much more rigorous data concerning the interaction between peripheral sensory nerves and bone in the context of an altered mechanical loading environment.

2g. Embedding/cutting/imaging/analysis of bones for dynamic histomorphometry

Mice received injections of calcein green (10 mg/kg; Sigma-Aldrich, St. Louis, MO) and Alizarin-3-methlimino-diacetic acid (30 mg/kg; Sigma-Aldrich, St. Louis, MO) 10 days and 3 days prior to sacrifice, respectively. After scanning with μCT, tibias were embedded in Technovit (Kulzer, Wehrheim, Germany) using standard techniques for undecalcified bone [13]. Sections were cut from each bone on a bandsaw (Model 310, Exakt Technologies, Norderstedt, Germany) in the transverse plane at 10, 20, 30, 40 and 50% of the tibia length (Fig. 10). Sections were ground to an approximate thickness of 100 μm. Fluorescent images were obtained at 10x magnification (Nikon Eclipse TE2000-E, Tokyo, Japan). Dynamic histomorphometric analysis was performed using commercial software (Bioquant, Nashville, TN). Mineral apposition rate (MAR), percent mineralizing surface (MS/BS), and bone formation rate (BFR/BS) were quantified for the endosteal and periosteal surfaces of cortical bone.

Dynamic histomorphometric analysis revealed that 7 N tibial compression altered bone formation parameters on the endosteal and periosteal surfaces of loaded tibias (**Table 3**). In general, bone formation increased on the periosteal surface of the tibias and decreased on the endosteal surface at locations closest to the proximal metaphysis. There was a significant effect of treatment on the response of MAR to increased loading, with capsaicin-treated mice displaying a larger response compared to vehicle-treated mice at many tibial locations (**Fig. 14**). For example, at 20% of the tibia length, the loaded tibias of capsaicin-treated mice had an average decrease in MAR of 37% compared to a 24% decrease in MAR in vehicle-treated mice. While MAR was lower in loaded tibias compared to controls at 10, 20 and 30% of the tibia length on the endosteal surface, MAR was increased at all measured locations on the periosteal surface. At 20%, capsaicin-treated mice again demonstrated a larger response to increased loading with an approximately 2.5 times larger increase in MAR than vehicle-treated mice on the periosteal surface. There was a significant effect of loading on MS/BS that varied with location along the tibia. However, treatment was not a factor in the response of MS/BS on the periosteal surface. Loading also caused a significant increase in BFR at all locations on the periosteal surface, with a significantly greater response in capsaicin-treated mice at 20% of the tibia length. Tibial compression at 3 N caused a significant decrease in MAR on the endosteal surface at 10 and 20%, but the effect did not differ between treatment groups. Furthermore, the lower magnitude compression did not significantly affect MS/BS or BFR on either surface of the loaded tibias.

Table 3: Bone formation parameters for 7 N compression assessed using dynamic histomorphometry

Tibial Location	Treatment Group	MAR[a,b] (μm/day) Control	MAR[a,b] (μm/day) Loaded	MS/BS[a,b] (%) Control	MS/BS[a,b] (%) Loaded	BFR[a,b] (μm³/μm²/day) Control	BFR[a,b] (μm³/μm²/day) Loaded
Endosteal Surface							
10%	Vehicle	2.05±0.03	1.62±0.01*	62±1	53±5*	1.28±0.03	0.85±0.08*
	Capsaicin	1.96±0.04	1.71±0.02**	65±2	50±3*	1.27±0.05	0.85±0.05*
20%	Vehicle	1.30±0.01	0.98±0.03*	51±3	30±3*	0.66±0.03	0.30±0.03*
	Capsaicin	1.59±0.05	0.99±0.03**	49±5	26±3*	0.77±0.07	0.25±0.03*
30%	Vehicle	1.11±0.01	0.97±0.02*	53±8	40±2*	0.59±0.09	0.39±0.03*
	Capsaicin	1.25±0.02	0.85±0.03**	51±4	36±2*	0.64±0.05	0.31±0.03*
40%	Vehicle	1.07±0.02	1.07±0.02	49±6	39±1*	0.53±0.07	0.41±0.02*
	Capsaicin	0.79±0.03	0.98±0.03*	38±2	33±4	0.30±0.02	0.33±0.04
50%	Vehicle	1.01±0.03	1.11±0.02*	36±6	37±4	0.37±0.06	0.41±0.04
	Capsaicin	0.66±0.02	0.90±0.09**	26±2	37±6*	0.17±0.01	0.33±0.08*

		MAR[a,b] (μm/day)		MS/BS[a] (%)		BFR[a,b] (μm³/μm²/day)	
		Control	Loaded	Control	Loaded	Control	Loaded
Periosteal Surface							
10%	Vehicle	0.91±0.01	1.82±0.02*	10±1	29±3	0.09±0.01	0.52±0.05*
	Capsaicin	1.02±0.02	2.09±0.03*	12±0	33±2	0.13±0.01	0.70±0.05**
20%	Vehicle	1.53±0.02	1.95±0.02*	19±2	43±4	0.29±0.03	0.85±0.08*
	Capsaicin	1.06±0.02	1.77±0.02**	15±1	47±3	0.16±0.01	0.82±0.05**
30%	Vehicle	0.75±0.03	1.11±0.02*	10±1	41±2	0.07±0.01	0.46±0.02*
	Capsaicin	0.82±0.03	1.29±0.03*	10±1	44±7	0.09±0.01	0.56±0.09*
40%	Vehicle	0.87±0.02	1.49±0.02*	11±1	52±5	0.10±0.01	0.77±0.08*
	Capsaicin	0.82±0.04	1.39±0.10*	14±1	53±8	0.11±0.01	0.74±0.14*
50%	Vehicle	0.77±0.02	1.11±0.04*	14±4	52±5	0.11±0.03	0.58±0.07*
	Capsaicin	0.55±0.03	1.14±0.03**	17±1	60±11	0.09±0.01	0.69±0.13*

Data reported as mean±SD.
[a]: significant leg*VOI interaction, 7N compressive force
[b]: significant treatment*leg*VOI interaction, 7N compressive force
*: significant difference between control and loaded, $p<0.05$
**:significant difference between capsaicin and vehicle response, $p<0.05$

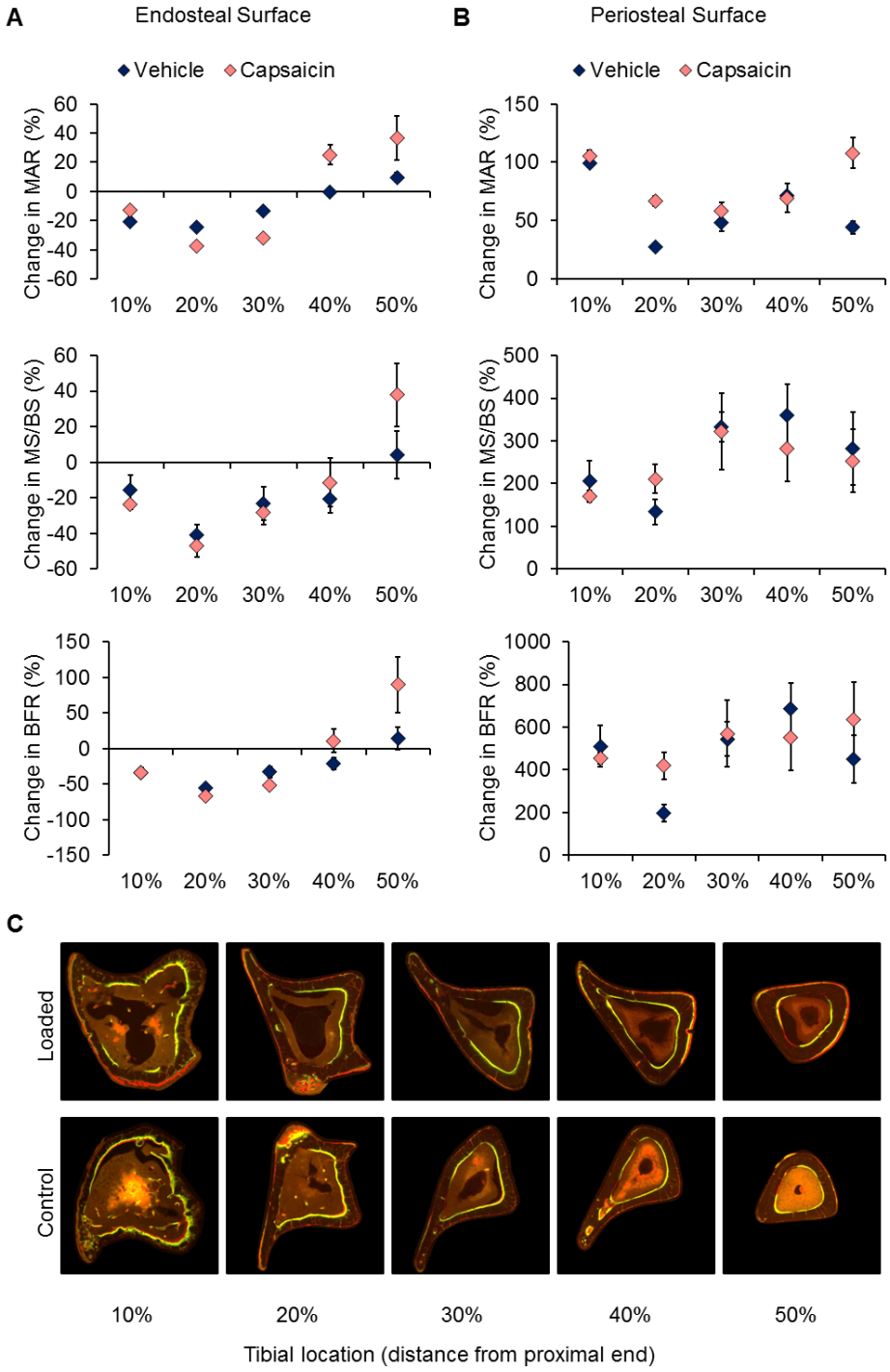

Figure 14: Dynamic histomorphometry was used to identify changes in bone formation rate after 7 N tibial compression in capsaicin- and vehicle-treated mice. Mineral apposition rate (MAR), percent mineralizing surface (MS/BS) and bone formation rate (BFR) were quantified for the endosteal (A) and periosteal surfaces (B). Fluorescent images (C) show cortical bone from the control and loaded tibias of a vehicle-treated mouse.

Aim 2 Discussion and Conclusions:

The purpose of this study was to investigate the role of sensory nerves in adaptation of bone to increased mechanical loading. Tibial compression, particularly at 7 N magnitude, caused an increase in cortical bone area in the loaded tibia, accompanied by changes in bone formation parameters. This adaptive response was dependent on location along the tibia, and was generally greater in capsaicin-treated mice than in vehicle-treated mice. The increased response in capsaicin-treated mice conflicts with our initial hypothesis that reduced sensory nerve function would impair the adaptation of bone to increased loading.

This study was performed at two different compressive loads, producing two different strain magnitudes on loaded tibias. Two weeks of 3 N tibial compression generated only a modest response in cortical bone assessed with μCT, and no significant changes in bone formation measured by dynamic histomorphometry. Similarly, Fritton et al. observed a 1.4% increase in whole bone mineralized tissue volume when using this compressive force, which increased to 3.4% when the loading was conducted for an additional 4 weeks [24]. Although these researchers were able to detect an increase in BMC at 10% of the tibia, we were only able to observe changes at the 7 N compressive force. Tibial compression at 7 N (approximately 28x body weight) caused a greater change in cortical bone than the lower compressive force. Interestingly, we did not observe significant changes in trabecular bone that others have reported in studies of bone adaptation [20, 24, 29]. The small magnitude of the changes in bone structure may be a result of differences in tibial compression systems. For example, we have found that higher compressive forces using our configuration may lead to knee injury and subsequent trabecular bone loss [27]. A group using a similar configuration observed a 20% loss in BV/TV at the proximal metaphysis in tibias loaded to 8 N [29]. Another group using a different configuration for tibial compression found an increase of 44.5% in BV/TV in tibias loaded to a target compressive force of 13.5 N [26].

Location on the tibia influenced the bone adaptive response, consistent with the morphology of the mouse tibia resulting in different strain patterns along its length [22, 25]. We observed the largest changes in Tt.Ar and BMC at 10% of the tibia length, where others have reported the largest compressive magnitude [25]. The shift we observed in bone formation parameters at 30% could be a result of a shift in strain from compression to tension. Tibia surface also factored into the adaptation results, with the endosteal surface of loaded tibias displaying a decrease in BFR at 10-30% compared to control tibias. This is consistent with the observation of increased Tt.Ar and M.Ar from μCT. Tibial compression caused outward expansion of the cortex, with increased bone formation on the periosteal surface and decreased bone formation on the endosteal surface, which may help the tibia adapt to the demands of greater compression [30].

The changes we observed in cortical bone assessed with μCT are consistent with changes in bone formation parameters assessed with dynamic histomorphometry. The increase in Tt.Ar and BMC at 10% of the tibia length were attended by a large increase in MAR and BFR on the periosteal surface. A similar trend occurred at 50% of the tibia length. Although the percent changes in BFR on the periosteal surface appear large, the control values are some of the lowest of either surface. Therefore a 500% increase in BFR on the periosteal surface results in a value less than the reduced BFR on the endosteal surface. Also, the increase in BFR on the periosteal surface and decrease on the endosteal surface could account for the modest increase in Tt.Ar at 10% of the tibia length.

Contrary to our initial hypothesis, capsaicin treatment caused greater changes in parameters such as Tt.Ar, BMC and MAR in response to increased loading. A possible explanation for this observation is that neuropeptide concentrations are antagonistic to the actions of bone cells during adaptation in vivo. In a study of ulnar compression in rats, researchers found that increases in bone area were accompanied by decreases in bone concentrations of CGRP [31]. As CGRP has an anabolic effect on osteoblasts, the reduction from baseline in response to loading appears to work against the bone forming action of osteoblasts. Similarly, another study found that hindlimb casting in rats caused elevated CGRP concentrations in the sciatic nerve [32]. The bone loss associated with immobilization may be antagonized by increased concentrations of this neuropeptide. By reducing nerve function with capsaicin treatment, we may be limiting the antagonistic role of neuropeptides in bone adaptation, allowing a greater response to loading.

The results of our investigation into bone neuropeptide concentration mostly agree with previous findings from other labs. Our observed increase in bone CGRP concentration following tibial compression provides the notable exception. However, there were several differences between this work and the experiments showing a decrease in bone CGRP in response to cyclic compression. The most obvious difference was in the limb subjected to compression, with the use of an ulna rather than tibia. Also dissimilarly, we did not use an analgesic and used a lower compressive force. However, both studies found a decrease in substance P within an hour of increased loading. A possible explanation for the increase is that the osteoclastic stimulating function of substance P outweighs its anabolic function. We would expect increased loading to increase bone mass, and suppression of the resorbing effect of this neuropeptide would contribute to that end. Likewise, we

would expect hindlimb unloading to decrease bone mass in the tibia and in agreement with other groups, substance P concentration was increased in the unloaded bone.

The minimal use of animals in this study presents a limitation to the interpretation of our findings. Especially with respect to substance P, bone concentrations of these neuropeptides were small. Detection of a minor change in concentration resulting from the different mechanical stimuli would have required the use of much higher animal numbers to achieve statistical significance. For example, detecting a significant 15% difference in substance P concentration between control tibias and 1 day compressed tibias would require 162 mice. Another limitation is that while we measured bone concentration, we do not know the origin of these neuropeptides. Osteoblasts themselves express CGRP and might alter their expression as an adaptive mechanism to the new loading environment. Such action would suggest an autocrine or paracrine response rather than a neural one. A final limitation is that we did not have a separate group of mice subjected to normal cage activity to serve as a universal control. Instead we used the left tibias of the compression mice, which are likely more similar within an animal than to the tibias of the hindlimb unloaded mice. An effect of compression on the contralateral limb could also clarified by an additional control group.

Investigation of the neuropeptide concentrations in bone revealed that they change in response to altered mechanical environments. Traditionally classified as transmitters of sensory stimuli, neuropeptides may have an additional role in bone, where they have the potential to regulate the bone cell response necessary for adaptation.

Pending tasks:
None

KEY RESEARCH ACCOMPLISHMENTS:
- Used the naturally occurring compound, capsaicin, to reduce sensory nerve function and observe resulting gross changes in bone quantity and quality
- Quantified reduced sensory function using hot plate analgesia testing, as receptors for capsaicin are also transducers of noxious heat
- Found that mice treated with capsaicin had shorter femurs with thinner trabeculae, but few changes in bone quality
- Found that female mice demonstrated greater consistency in response to capsaicin treatment
- Used tibial compression to model increased loading and investigated effects of denervation on consequent responses in bone structure and formation rate
- Found that reduced sensory nerve function did not impair the adaptive response of bone to increased mechanical demands, but that capsaicin-treated mice showed ***greater*** changes in cortical bone area at proximal tibia locations, associated with higher mineral apposition rates
- Verified that neuropeptide concentrations in bone change in response to both increased and decreased mechanical loading

REPORTABLE OUTCOMES:
- Presented research in poster form at the 2014 International Bone and Mineral Society (IBMS) Sun Valley Workshop and the 2014 American Society for Bone and Mineral Research (ASBMR) Annual Meeting
- Podium presentation at the 2013 Annual Meeting of the Orthopaedic Research Society
- Manuscript encompassing Aim 1 published in the Journal of Musculoskeletal and Neuronal Interaction (attached)
- Manuscript encompassing Aim 2 submitted to Bone, currently in revision
- Doctoral Thesis of Mollie A. Heffner, describing the entirety of this work (attached)

CONCLUSION: This research investigated mechanisms by which peripheral sensory nerves influence bone maintenance and mechanotransduction using capsaicin-injected mice as a model of decreased peripheral sensory nerve function. In **Aim 1** we quantified the relationship between reduced peripheral sensory nerve function and bone structure and mechanical properties. We hypothesized a negative correlation between

reduced sensory nerve function and structure and mechanical properties of bone. Consistent with this hypothesis, we observed a small but statistically significant decrease in trabecular and cortical bone structure due to capsaicin treatment. In **Aim 2** we determined the bone adaptation response of capsaicin- and vehicle-treated mice to increased mechanical loading (tibial compression) at two different magnitudes of compression (3N and 7N). We hypothesized that capsaicin-treated mice will have an *increased bone adaptation response* to mechanical loading due to decreased negative feedback by peripheral sensory nerves. We found that tibial compression loading at 3N magnitude caused a significant bone adaptation response in female vehicle-treated mice, but no significant response in capsaicin-treated mice. In contrast to this finding, 7N tibial compression loading resulted in bone adaptation in all experimental groups, however capsaicin-treated mice exhibited the greatest adaptation response to loading. This differential dose response may be due to a higher threshold for adaptation in capsaicin-treated mice, or may be linked to a lamellar vs. injury response engendered by 3N vs. 7N loading, respectively. We also used tibial compression loading and hindlimb unloading via tail suspension to quantify the change in neuropeptide concentration in bone in response to the mechanical loading environment. We found that both increased and decreased mechanical loading alter the concentration of neuropeptides in bone, further supporting the role of peripheral sensory nerves in bone adaptation.

Altogether, this research helped establish the role of peripheral nerves in bone's ability to adapt to exercise. These studies may lead to novel therapies aimed at preserving healthy bone turnover with age. This research will be the basis for future studies investigating the interaction of peripheral nerves and bone, and peripheral nerve function as a potential mechanism of age-related bone loss. The findings of our research support a role for sensory neuropeptides in bone metabolism. Neurons themselves might be more important to bone development, whereas neuropeptide actions on bone cells might play a more dramatic role in bone adaptation to the mechanical environment. Future research should investigate the origins of these neuropeptides in bone and take advantage of advancements in knockout mice. The actions of neuropeptides on bone cells present a target mechanism in the treatment of bone diseases characterized by abnormal bone formation.

PERSONNEL RECEIVING SALARY FROM THIS AWARD:

Blaine A. Christiansen, Ph.D., Principal Investigator, (Effort: 10%): Dr. Christiansen was principally in charge of microCT imaging, histological analysis, and mechanical loading/unloading, and coordinated experiments conducted by other members of the investigative team. Dr. Christiansen was also primarily responsible for writing manuscripts encompassing this research, and for communicating with the funding body.

Dominik R. Haudenschild, Ph.D., Co-Investigator, (Effort: 5%): Dr. Haudenschild primarily contributed to histological analysis, and ELISA analysis of serum and bone samples.

Damian C. Genetos, Ph.D.: Co-Investigator, (Effort: 5%): Dr. Genetos primarily contributed to histological analysis, and ELISA analysis of serum and bone samples. Dr. Genetos also helped with study design and advising of the graduate student researcher.

Mollie A. Heffner, Graduate Student Researcher, (Effort: 50%): Ms. Heffner was primarily in charge of conducting all experimental procedures, animal handling, microCT, histology, ELISA analysis, and was the primary author on all publications for these projects. This research encompasses her doctoral thesis.

References:

1. *National Osteoporosis Foundation, "Bone Health Basics: Get the Facts". Retrieved March 15, 2013, from National Osteoporosis Foundation Web site:* http://www.nof.org/learn/basics.
2. Spencer GJ, Hitchcock IS, and Genever PG, *Emerging neuroskeletal signalling pathways: a review.* FEBS Lett, 2004. **559**(1-3): p. 6-12.
3. D'Souza SM, MacIntyre I, Girgis SI, and Mundy GR, *Human synthetic calcitonin gene-related peptide inhibits bone resorption in vitro.* Endocrinology, 1986. **119**(1): p. 58-61.
4. Yamamoto I, Kitamura N, Aoki J, et al., *Human Calcitonin Gene-Related Peptide Possesses Weak Inhibitory Potency of Bone-Resorption Invitro.* Calcified Tissue International, 1986. **38**(6): p. 339-341.
5. Bernard GW and Shih C, *The Osteogenic Stimulating Effect of Neuroactive Calcitonin Gene-Related Peptide.* Peptides, 1990. **11**(4): p. 625-632.
6. Akopian A, Demulder A, Ouriaghli F, et al., *Effects of CGRP on human osteoclast-like cell formation: a possible connection with the bone loss in neurological disorders?* Peptides, 2000. **21**(4): p. 559-64.
7. Wang L, Zhao R, Shi X, et al., *Substance P stimulates bone marrow stromal cell osteogenic activity, osteoclast differentiation, and resorption activity in vitro.* Bone, 2009. **45**(2): p. 309-20.
8. Schinke T, Liese S, Priemel M, et al., *Decreased bone formation and osteopenia in mice lacking alpha-calcitonin gene-related peptide.* J Bone Miner Res, 2004. **19**(12): p. 2049-56.
9. Hill EL, Turner R, and Elde R, *Effects of neonatal sympathectomy and capsaicin treatment on bone remodeling in rats.* Neuroscience, 1991. **44**(3): p. 747-55.
10. Jancso G, Kiraly E, and Jancso-Gabor A, *Pharmacologically induced selective degeneration of chemosensitive primary sensory neurones.* Nature, 1977. **270**(5639): p. 741-3.
11. Karl T, Pabst R, and von Horsten S, *Behavioral phenotyping of mice in pharmacological and toxicological research.* Exp Toxicol Pathol, 2003. **55**(1): p. 69-83.
12. Hale LV, Galvin RJ, Risteli J, et al., *PINP: a serum biomarker of bone formation in the rat.* Bone, 2007. **40**(4): p. 1103-9.
13. Baron R, Vignery A, Neff L, et al., *Processing of undecalcified bone specimens for bone histomorphometry*, in *Bone histomorphometry: techniques and interpretations*, R. Recker, Editor. 1983. p. 13-19.
14. Lee KC, Jessop H, Suswillo R, et al., *The adaptive response of bone to mechanical loading in female transgenic mice is deficient in the absence of oestrogen receptor-alpha and -beta.* J Endocrinol, 2004. **182**(2): p. 193-201.
15. Offley SC, Guo TZ, Wei T, et al., *Capsaicin-sensitive sensory neurons contribute to the maintenance of trabecular bone integrity.* J Bone Miner Res, 2005. **20**(2): p. 257-67.
16. Kobayashi M, Watanabe K, Yokoyama S, et al., *Capsaicin, a TRPV1 Ligand, Suppresses Bone Resorption by Inhibiting the Prostaglandin E Production of Osteoblasts, and Attenuates the Inflammatory Bone Loss Induced by Lipopolysaccharide.* ISRN Pharmacol, 2012. **2012**: p. 439860.
17. Lieben L and Carmeliet G, *The Involvement of TRP Channels in Bone Homeostasis.* Front Endocrinol (Lausanne), 2012. **3**: p. 99.
18. Abed E, Labelle D, Martineau C, et al., *Expression of transient receptor potential (TRP) channels in human and murine osteoblast-like cells.* Mol Membr Biol, 2009. **26**(3): p. 146-58.
19. Rossi F, Siniscalco D, Luongo L, et al., *The endovanilloid/endocannabinoid system in human osteoclasts: possible involvement in bone formation and resorption.* Bone, 2009. **44**(3): p. 476-84.
20. De Souza RL, Matsuura M, Eckstein F, et al., *Non-invasive axial loading of mouse tibiae increases cortical bone formation and modifies trabecular organization: a new model to study cortical and cancellous compartments in a single loaded element.* Bone, 2005. **37**(6): p. 810-8.
21. Main RP, Lynch ME, and van der Meulen MC, *In vivo tibial stiffness is maintained by whole bone morphology and cross-sectional geometry in growing female mice.* J Biomech, 2010. **43**(14): p. 2689-94.
22. Willie BM, Birkhold AI, Razi H, et al., *Diminished response to in vivo mechanical loading in trabecular and not cortical bone in adulthood of female C57Bl/6 mice coincides with a reduction in deformation to load.* Bone, 2013. **55**(2): p. 335-46.
23. Holzer P, *Capsaicin: cellular targets, mechanisms of action, and selectivity for thin sensory neurons.* Pharmacol Rev, 1991. **43**(2): p. 143-201.

24. Fritton JC, Myers ER, Wright TM, and van der Meulen MC, *Loading induces site-specific increases in mineral content assessed by microcomputed tomography of the mouse tibia.* Bone, 2005. **36**(6): p. 1030-8.
25. Patel TK, Brodt MD, and Silva MJ, *Experimental and finite element analysis of strains induced by axial tibial compression in young-adult and old female C57Bl/6 mice.* J Biomech, 2014. **47**(2): p. 451-7.
26. Sugiyama T, Price JS, and Lanyon LE, *Functional adaptation to mechanical loading in both cortical and cancellous bone is controlled locally and is confined to the loaded bones.* Bone, 2010. **46**(2): p. 314-21.
27. Christiansen BA, Anderson MJ, Lee CA, et al., *Musculoskeletal changes following non-invasive knee injury using a novel mouse model of post-traumatic osteoarthritis.* Osteoarthritis Cartilage, 2012. **20**(7): p. 773-82.
28. Morey-Holton ER and Globus RK, *Hindlimb unloading rodent model: technical aspects.* J Appl Physiol (1985), 2002. **92**(4): p. 1367-77.
29. Brodt MD and Silva MJ, *Aged mice have enhanced endocortical response and normal periosteal response compared to young-adult mice following 1 week of axial tibial compression.* J Bone Miner Res, 2010.
30. Robling AG, Castillo AB, and Turner CH, *Biomechanical and molecular regulation of bone remodeling.* Annu Rev Biomed Eng, 2006. **8**: p. 455-98.
31. Sample SJ, Behan M, Smith L, et al., *Functional adaptation to loading of a single bone is neuronally regulated and involves multiple bones.* J Bone Miner Res, 2008. **23**(9): p. 1372-81.
32. Guo TZ, Wei T, Li WW, et al., *Immobilization contributes to exaggerated neuropeptide signaling, inflammatory changes, and nociceptive sensitization after fracture in rats.* J Pain, 2014. **15**(10): p. 1033-45.

J Musculoskelet Neuronal Interact 2014; 14(1):1-9

Original Article

Hylonome

Altered bone development in a mouse model of peripheral sensory nerve inactivation

M.A. Heffner[1,2], M.J. Anderson[1], G.C. Yeh[1], D.C. Genetos[3], B.A. Christiansen[1,2]

[1]University of California-Davis Medical Center, Department of Orthopaedic Surgery; [2]University of California-Davis, Biomedical Engineering Graduate Group; [3]University of California-Davis Veterinary School, Department of Anatomy, Physiology, & Cell Biology, USA

Abstract

Objectives: The present study sought to determine the effects of decreased peripheral sensory nerve function on skeletal development and bone metabolism in mice. **Methods:** C57BL/6 neonatal mice were treated with capsaicin to induce peripheral sensory nerve degeneration, and compared to vehicle-treated controls at 4, 8 and 12 weeks of age. Changes in bone structure were assessed using micro-computed tomography, mechanical properties and fracture resistance were assessed using three-point bending of radii, and bone turnover was assessed using dynamic histomorphometry and serum biomarkers. **Results:** Capsaicin treatment resulted in small but significant decreases in bone structure, particularly affecting trabecular bone. Capsaicin-treated mice exhibited lower trabecular thickness at the femoral metaphysis and L5 vertebral body compared with vehicle-treated mice. However, capsaicin- and vehicle-treated mice had similar mechanical properties and bone turnover rates. **Conclusion:** Neonatal capsaicin treatment affected trabecular bone during development; however these small changes may not be meaningful with respect to bone strength under normal loading conditions. It is possible that capsaicin-sensitive neurons may be more important for bone under stress conditions such as increased mechanical loading or injury. Future studies will investigate this potential role of peripheral sensory nerves in bone adaptation.

Keywords: Capsaicin, Sensory Nerves, Bone Turnover, Skeletal Development, Mechanical Testing

Introduction

Osteoporosis is characterized by decreased bone mass and increased risk of fracture[1]. Common treatments for osteoporosis manipulate bone turnover primarily by inhibiting osteoclastic bone resorption[2,3] but can also target osteoblastic bone formation[4]. However, the mechanisms underlying age-related bone loss remain elusive. Degeneration of peripheral nerves may be a contributing factor for age-related bone loss, as substantial changes in peripheral nerve structure and function occur with aging[5-9]. The reductions in axon number and fiber size in aged subjects are associated with decreased peripheral nerve function, with cutaneous thermal and tactile thresholds significantly increased[10]. Further, there is now a well-established link between peripheral nerve function and bone metabolism *in vitro*[11-21]. In addition, denervation has been shown to cause bone loss *in vivo*[22-25], and peripheral neuropathy has been identified as an independent predictor of low bone mass in the affected limb of diabetic subjects[26]. Despite strong evidence of a link between the function of peripheral nerves and bone metabolism, the potential role of decreased peripheral nerve function in age-related bone loss has not been investigated.

Capsaicin treatment is a useful method for isolating the effects of decreased peripheral sensory nerve function in animal models. Capsaicin treatment activates the TrpV1 receptor, which is expressed by unmyelinated and small diameter myelinated sensory neurons, but not by motor neurons, large diameter sensory neurons or sympathetic neurons[27,28]. In this way, capsaicin treatment is able to isolate the effects of peripheral sensory neurons without disrupting normal mechanical loading, which is a confounding consequence of complete denervation. Subcutaneous injection of capsaicin in neonatal animals destroys unmyelinated and small-diameter myelinated sensory neurons for the lifetime of the animal[29]. Neonatal cap-

The authors have no conflict of interest.

Corresponding author: Blaine A. Christiansen, Ph.D., UC Davis Medical Center, Department of Orthopaedic Surgery, 4635 2nd Ave, Suite 2000, Sacramento, CA 95817, USA
E-mail: bchristiansen@ucdavis.edu

Edited by: F. Rauch
Accepted 22 January 2014

saicin treatment is a well-established model that has been used previously to investigate pain in rats[30] and itch in mice[31,32]. We are aware of only one study that used neonatal capsaicin treatment for a study of bone metabolism in rats[22]. This study found that neonatal capsaicin treatment in rats did not appear to alter normal bone growth and maintenance, but that decreased sensory nerve function may decrease local bone remodeling following molar extraction. However, this study did not investigate developmental changes resulting from capsaicin treatment. Importantly, this previous study also did not quantify trabecular bone structure, and did not investigate bone mechanical properties. We are unaware of any studies that have used neonatal capsaicin treatment to investigate bone metabolism in mice.

In this study, we used neonatal capsaicin treatment in mice to investigate the effects of decreased peripheral sensory nerve function on skeletal development and bone metabolism in mice, and to establish a mouse model of decreased peripheral sensory nerve function *in vivo* for future studies in bone. Using vehicle- and capsaicin-treated mice at multiple stages of development (4, 8, and 12 weeks of age) we assessed bone structure using micro-computed tomography, mechanical properties and fracture resistance using three-point bending, and bone turnover rate using dynamic histomorphometry and serum biomarkers. We hypothesized that decreased peripheral nerve function in capsaicin-treated mice would result in decreased bone structure, decreased resistance to fracture, and decreased bone turnover rate.

Material and methods

Neonatal capsaicin treatment

A total of 42 male and female C57BL/6 neonatal mice were used in this study, from 7 timed pregnant females (Harlan Laboratories, Indianapolis, IN). Neonatal capsaicin treatment was performed as previously described[33]. Briefly, neonatal mice were given subcutaneous injections of capsaicin (50 mg/kg) or vehicle (10% ethanol, 10% Tween 80 in isotonic saline) on day 2 and 5 after birth (n=21 vehicle, 21 capsaicin). Following capsaicin or vehicle treatment, neonatal mice were returned to normal cage activity until weaning (28 days). Mice were sacrificed 4, 8, or 12 weeks after birth, with a total of 7 vehicle- and 7 capsaicin-treated mice per time point (2-5 mice per age/sex/treatment group). We selected these time points to observe developmental changes from weaning until skeletal maturity, and to account for any possible recovery from sensory nerve inactivation by adulthood. Mice were weighed 1-2 times per week from birth until sacrifice.

Hot-plate analgesia testing

Capsaicin- and vehicle-treated mice were subjected to hot-plate analgesia testing at 4, 8, and 12 weeks of age to determine response time to a constant thermal stimulus of 55°C as previously described[34]. Mice were placed on a hot-plate (LE 7406, Coulborn Instruments, Whitehall, PA) and removed after indication of discomfort, determined as twitching or licking of a hind limb or jumping, or after a maximum of 30 seconds, and the latency time of the response was recorded. Each mouse was tested twice at each time point, and the latency times were averaged for each mouse/time point.

Micro-computed tomography analysis of bone structure

Right tibias, right femurs, and L5 vertebrae were removed post mortem and preserved in 70% ethanol. Bones were scanned using micro-computed tomography (SCANCO, μCT 35, Bassersdorf, Switzerland); images were acquired at 6 μm nominal voxel size (energy=55 kVp, intensity=114 μA, integration time= 900 ms). Trabecular bone was analyzed at the metaphysis and epiphysis of the distal femur and at the L5 vertebral body using manually drawn contours inside the cortical shell on two-dimensional slices. The metaphysis was defined by a 900 μm thick volume of interest beginning below the middle break of the growth plate. Trabecular bone volume per total volume (BV/TV), trabecular number, trabecular thickness (Tb.Th), trabecular separation (Tb.Sp), and bone mineral density (BMR) were determined using the manufacturer's 3-D analysis tools. Cortical bone was analyzed at the mid-diaphysis of the tibia and femur, using a 240 μm thick volume of interest centered at the measured midpoint of each bone. Bone area (B.Ar), medullary area (M.Ar), total cross-sectional area (Tt.Ar), cortical thickness (Ct.Th), and bone mineral density (BMR) were determined using the manufacturer's 3-D analysis tools.

Three-point bending

Bilateral radii were removed post mortem and preserved in 70% ethanol. Bones were scanned using micro-computed tomography as described above, with a volume of interest that included the entire bone. Average bending moment of inertia for the central 1.0 mm (100 slices) was determined using BoneJ analysis of the microCT images[35]. Following μCT scanning, radii were rehydrated for 25 minutes in phosphate buffered saline (PBS), then mechanically tested in three-point bending to determine cortical bone material properties. The lower supports had a span of 5.02 mm for 4 week samples, and a span of 7.45 mm for 8 and 12 week samples (Figure 4A), and the center loading platen was driven at 0.2 mm/sec until failure. Resulting force and displacement data were analyzed to determine stiffness and yield force. Modulus of elasticity and yield stress were determined using Euler-Bernoulli beam theory.

Dynamic histomorphometry

Mice received injections of calcein green (10 mg/kg; Sigma-Aldrich, St. Louis, MO) and Alizarin-3-methliminodiacetic acid (30 mg/kg; Sigma-Aldrich, St. Louis, MO) 10 days and 3 days prior to sacrifice, respectively. After scanning with μCT, the right tibias were embedded in Technovit (Kulzer, Wehrheim, Germany) using standard techniques for undecalcified bone[36]. Two sections were cut from each bone on a bandsaw (Model 310, Exakt Technologies, Norderstedt, Germany) in the transverse plane at 40% of the length from the proximal end. Sections were ground to an approximate thickness of 40 μm. Two color fluorescent images were obtained at 10x mag-

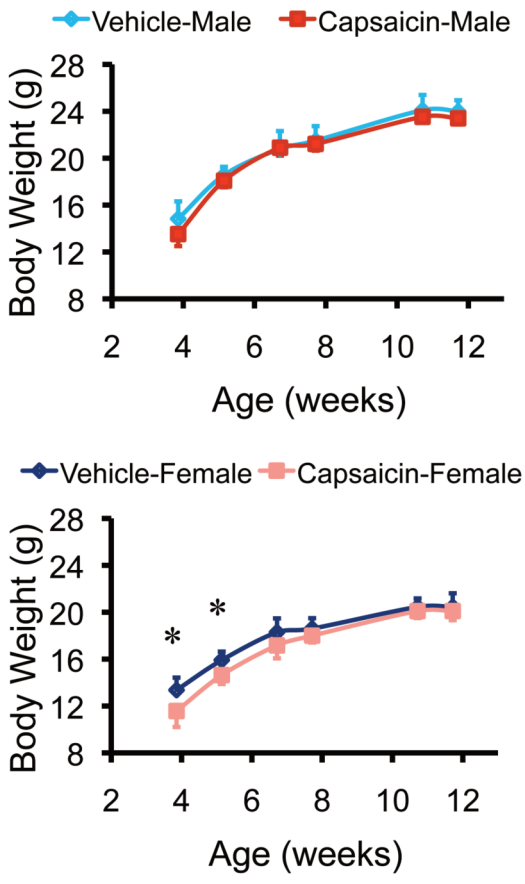

Figure 1. Body weights of treated and untreated mice were recorded from weaning until 12 weeks of age. Female mice treated with capsaicin had lower body weight than vehicle-treated female mice from weaning until day 47. Body weights of male mice were unaffected at all time points. *Capsaicin vs. vehicle; p<0.05.

nification (Nikon Eclipse TE2000-E, Tokyo, Japan). Dynamic histomorphometric analysis was performed using commercial software (Bioquant, Nashville, TN) and the results were averaged for the replicate slides from each bone. Mineral apposition rate (MAR), percent mineralizing surface (MS/BS), and bone formation rate (BFR/BS) were quantified for the endosteal and periosteal surfaces.

Serum biomarkers

Blood was collected from capsaicin- and vehicle-treated mice immediately prior to sacrifice for quantification of systemic biomarkers of bone metabolism. Mice were anesthetized with isoflurane and approximately 100-200 µL of blood was collected retro-orbitally. Samples were allowed to clot for 2-4 hours in an ice bath and then centrifuged at 1000 g for 5 minutes. The supernatants were collected and frozen rapidly to -80°C until analyzed. Serum was analyzed in duplicate to determine the concentrations of carboxy-terminal collagen crosslinks I (CTX-I) and procollagen type 1 amino-terminal propeptide (P1NP) using commercial mouse-specific ELISAs

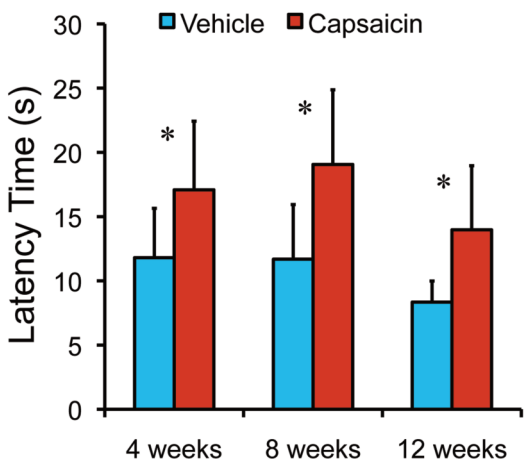

Figure 2. Hot-plate analgesia testing of treated and untreated mice was performed to verify decreased peripheral sensory nerve function. Treatment and age were main effects for latency time (p<0.0001, p=0.0052). Capsaicin-treated mice had significantly longer latency times than vehicle-treated mice at all time points when exposed to a constant 55°C thermal stimulus. *Capsaicin vs. vehicle; p<0.05.

(Cusabio, Wuhan, China) per the manufacturer's instructions. CTX-I is a common biomarker for bone resorption, while P1NP is a biomarker for bone formation[37].

Statistics

Hot-plate, µCT, three-point bending, histomorphometry and biomarker data were analyzed using three-way ANOVA stratified by age, sex, and treatment (JMP, SAS Institute Inc., Cary, NC). Between-group differences were analyzed using an unpaired Student's t-test of capsaicin- vs. vehicle-treated mice at each time point. Data are reported as mean±SD. Significance was defined as p<0.05.

Results

Mouse body weights

Neonatal capsaicin treatment did not have a statistically significant effect on body weights of male mice; there was no difference in body weight between capsaicin- and vehicle-treated male mice for any time point from weaning through 12 weeks (Figure 1). However, capsaicin treatment significantly affected body weights of female mice at early time points. Female mice treated with capsaicin had 8-13% lower body weights than vehicle-treated female mice from weaning until 47 days of age (Figure 1; p<0.05 for both time points). There were no significant differences in body weights for capsaicin- and vehicle-treated female mice from 8 to 12 weeks of age.

Hot-plate analgesia testing

Mice treated with capsaicin had significantly longer latency times when exposed to the constant thermal stimulus than vehicle-treated mice at all time points examined (Figure 2;

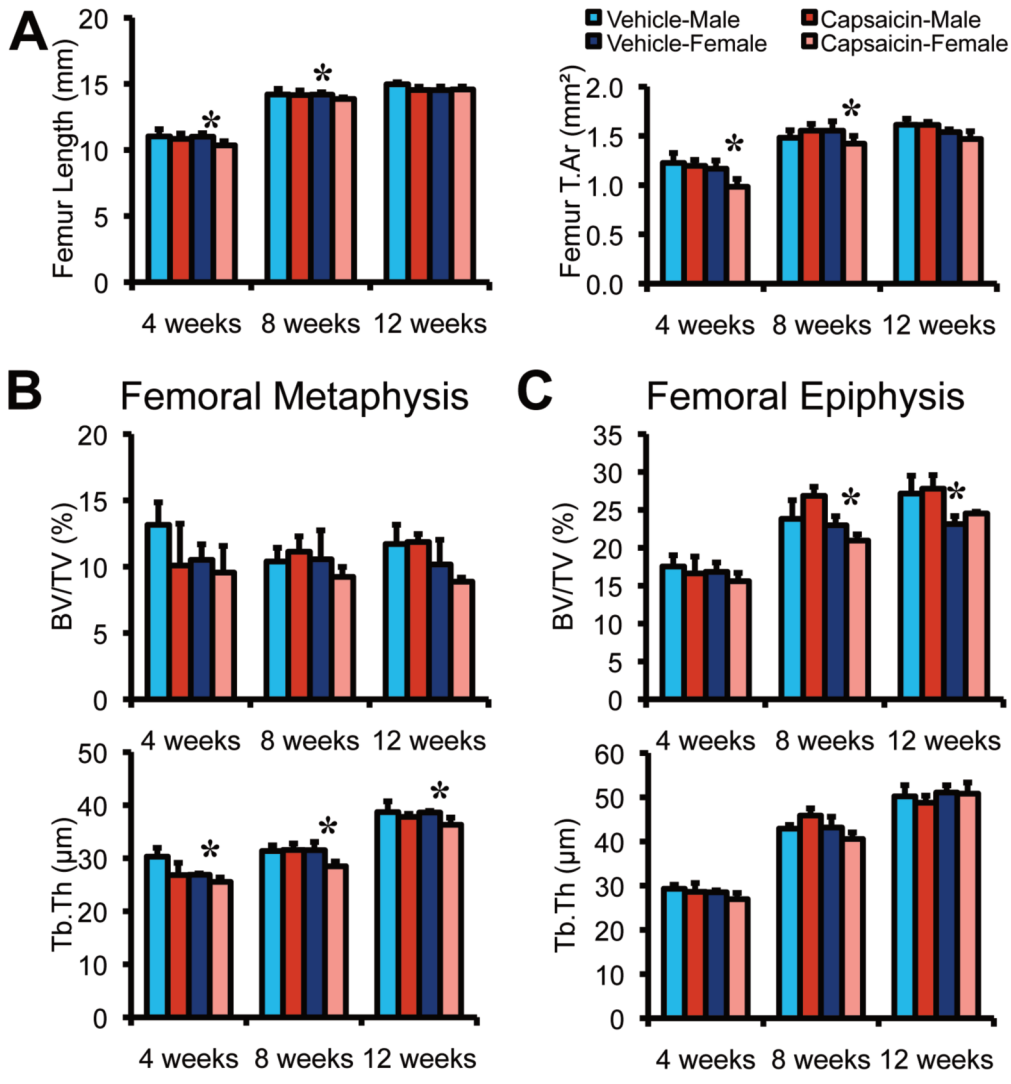

Figure 3. Micro-computed tomography of femoral cortical and trabecular bone. (**A**) Femur length and total cross-sectional area (Tt.Ar) of the femoral diaphysis were significantly affected in capsaicin-treated female mice. (**B**) Capsaicin treatment did not significantly affect trabecular bone volume fraction (BV/TV) at the femoral metaphysis but reduced trabecular thickness (Tb.Th) at this location in female mice. (**C**) Capsaicin treatment significantly affected BV/TV at the femoral epiphysis in female mice, but did not alter Tb.Th at this location. *Capsaicin vs. vehicle; $p<0.05$.

$p<0.0001$). For example, at 8 weeks of age, the average latency time of capsaicin-treated mice was 63% longer than that of vehicle-treated mice ($p=0.0002$), while at 12 weeks of age the latency time was 67% longer for capsaicin-treated mice ($p=0.0007$). This confirms that mice treated with capsaicin had decreased peripheral sensory nerve function, which persisted until at least 12 weeks of age. Age was also a main effect for latency time ($p=0.0052$); latency times for both capsaicin- and vehicle-treated mice at 12 weeks of age were significantly shorter than at 4 or 8 weeks.

Micro-computed tomography

Capsaicin treatment resulted in small but significant decreases in bone structure parameters in trabecular bone of mice relative to vehicle-treated controls (Figure 3). For example, we observed a significant main effect of capsaicin treatment on Tb.Th at the femoral metaphysis and L5 vertebral body ($p=0.0002$ and 0.0024, respectively). Female capsaicin-treated mice had 5.2-9.5% lower Tb.Th than vehicle-treated female mice at these sites at each time point ($p=0.0056$-0.049). However, we did not observe a significant effect of capsaicin treatment on BV/TV or Tb.Sp at the femoral metaphysis. At the femoral epiphysis, we observed a significant treatment*sex interaction for Tb.Th. ($p=0.026$), with female mice being more severely affected by capsaicin treatment than male mice. We also found a significant treatment*sex*age interaction for BV/TV at the femoral epiphysis. For example, female capsaicin-treated mice had 8.7% lower BV/TV at the femoral epi-

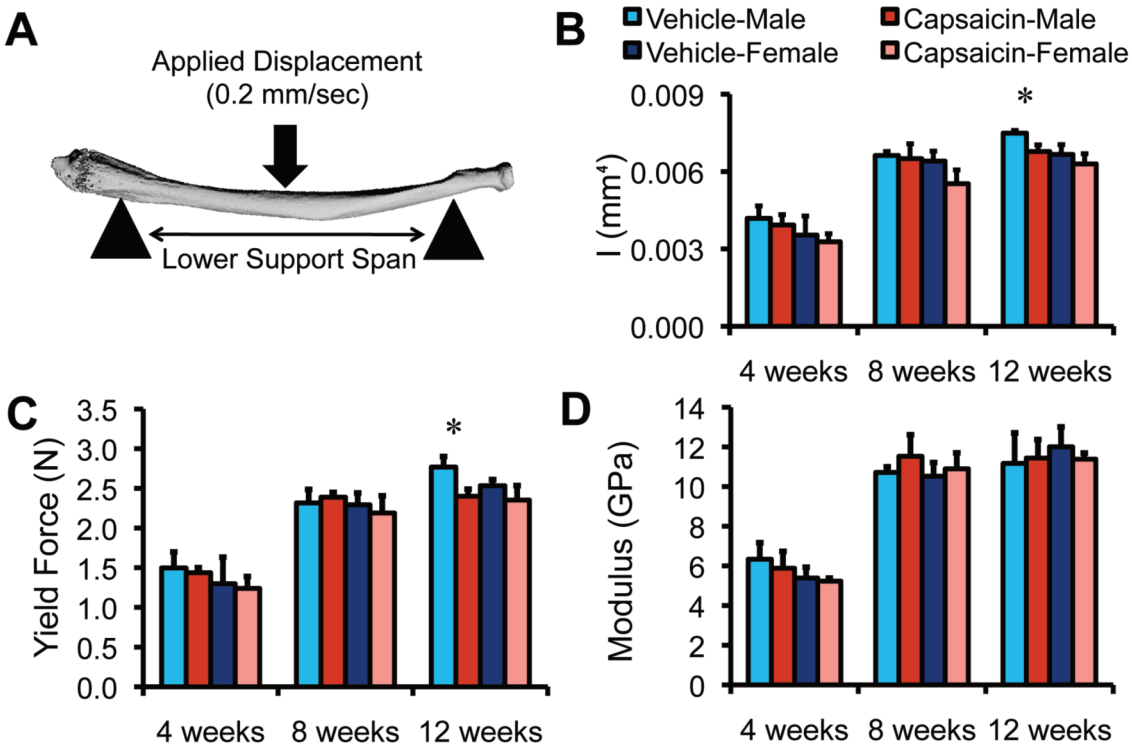

Figure 4. Mechanical properties of radii determined using three-point bending. A micro-computed tomography reconstruction of a representative radius (**A**) showing the mechanical testing setup. At 12 weeks of age, the moment of inertia (I) (**B**) and yield force (**C**) were significantly lower in capsaicin-treated male mice. However, modulus of elasticity (**D**) was not significantly different between treated and untreated mice. Age was a main effect for I, yield force and modulus. *Capsaicin vs. vehicle; $p<0.05$.

physis than vehicle-treated female mice at 8 weeks (p=0.015), whereas male mice had similar BV/TV at this time point.

We also observed significant effects of capsaicin treatment on cortical bone structure, with significant main effects of capsaicin treatment on femur length, M.Ar, and Tt.Ar (p=0.0094, 0.026, and 0.026, respectively). For example, femurs from female mice treated with capsaicin were 6.0% and 2.3% shorter than femurs from female vehicle-treated mice at 4 and 8 weeks, respectively (p=0.034, 0.0097). At 4 weeks, femurs from female capsaicin-treated mice had 15% smaller M.Ar and 16% smaller Tt.Ar compared with vehicle-treated mice (p=0.042, 0.031). Capsaicin treatment also affected cortical bone of the tibia. There were significant treatment*sex interactions for tibia M.Ar and Tt.Ar (p=0.025, 0.0032). At 4 weeks, the tibias from female capsaicin-treated mice had 16% smaller M.Ar and 15% smaller Tt.Ar compared with vehicle-treated mice (p=0.022, 0.029). We did not observe any significant effects of capsaicin treatment on bone mineral density of either trabecular or cortical bone. As expected, sex and age had significant effects for several measured bone structure parameters.

Three-point bending

Capsaicin treatment significantly decreased the mechanical properties of radii tested with three-point bending. For example, we observed significant main effects of capsaicin treatment on yield force and moment of inertia (p=0.047, 0.0041). At 12 weeks, radii from male treated mice yielded at 13.3% lower force compared with vehicle-treated male mice (p=0.022). Radii of male mice treated with capsaicin had 9.5% lower moment of inertia than vehicle-treated male mice at 12 weeks (p=0.028). However, calculations of yield stress and modulus of elasticity revealed no significant differences between capsaicin- and vehicle-treated mice (Figure 4). Age was a main effect for all of the mechanical properties measured, while sex was a main effect for yield force and moment of inertia.

Dynamic histomorphometry

Capsaicin treatment significantly altered bone formation parameters in the tibiae of treated mice (Figure 5). We observed significant treatment*sex*age interactions for MAR and BFR at the endosteal surface (p=0.023, 0.020) and for MAR and MS/BS at the periosteal surface (p=0.035, 0.042). For example, at 4 weeks, female capsaicin-treated mice had 39% higher MAR than female vehicle-treated mice at the endosteal surface of the tibia. At 12 weeks, female mice treated with capsaicin had 23.4% lower MS/BS (p=0.012) and 22.4% lower BFR (p=0.061) at the periosteal surface than female vehicle-treated mice. Age was a significant main effect for MAR, MS/BS and BFR at the endosteal and periosteal surfaces.

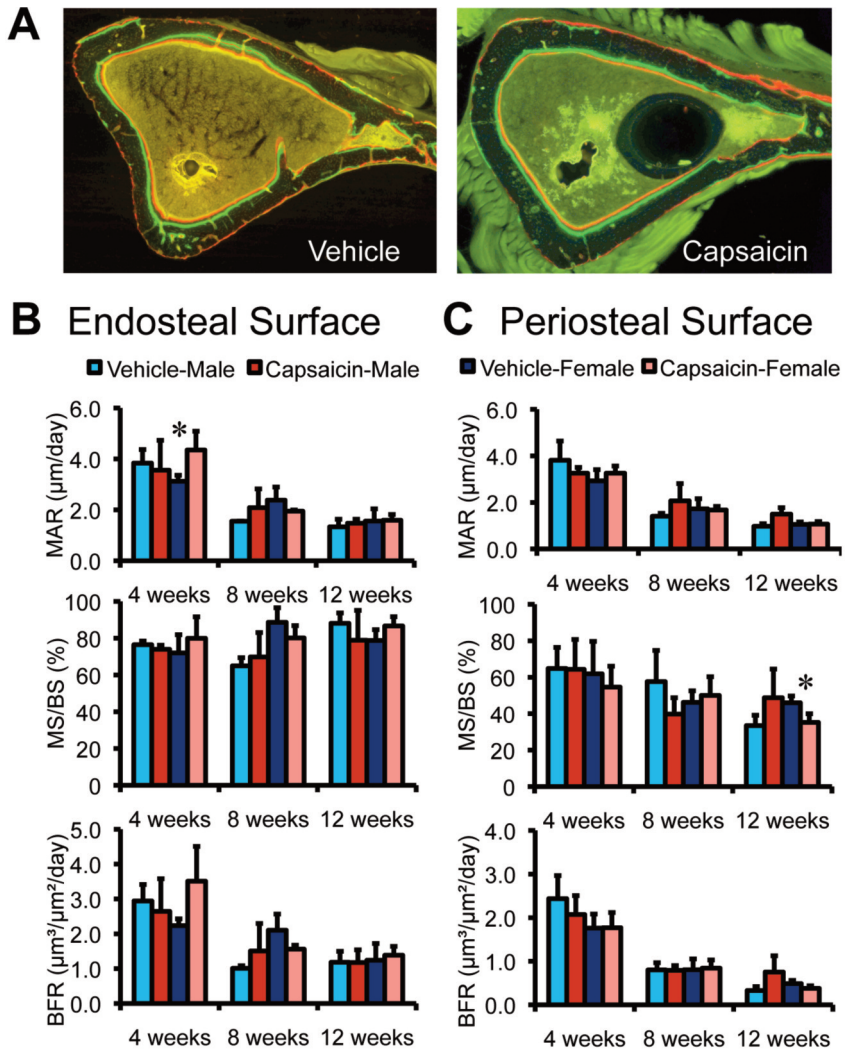

Figure 5. Dynamic histomorphometry was used to identify changes in bone formation rates in capsaicin- and vehicle-treated mice. Fluorescent images (**A**) show cortical bone from the tibias of 8 week old female vehicle- and capsaicin-treated mice. Mineral apposition rate (MAR), percent mineralizing surface (MS/BS), and bone formation rate (BFR/BS) were quantified for the endosteal (**B**) and periosteal surfaces (C). Age was a significant main effect for MAR, MS/BS and BFR at the endosteal and periosteal surfaces. *Capsaicin vs. vehicle; $p<0.05$.

Serum biomarkers

We did not detect any significant main effects of capsaicin treatment on serum concentrations of CTX-I or P1NP (Figure 6), although male capsaicin-treated mice at 8 weeks of age had 37% lower CTX-I concentrations than vehicle-treated male mice of the same age ($p=0.046$). We also observed a significant effect of sex on concentrations of CTX-I ($p=0.043$), with female mice exhibiting lower concentrations of CTX-I than male mice. P1NP serum concentrations did not vary significantly by treatment, sex, or age.

Discussion

In this study, we investigated the role of peripheral sensory nerves in bone metabolism during development in mice. We found that neonatal capsaicin treatment in mice led to modest and significant decreases in bone structure parameters, but this effect was inconsistent for mechanical properties and bone turnover rate. Capsaicin treatment had the greatest impact on trabecular bone, with treated mice exhibiting lower trabecular thickness at the femoral metaphysis and L5 vertebral body. However, contrary to our initial hypothesis, mice treated with capsaicin did not exhibit reduced mechanical properties or resistance to fracture. Yield stress and elastic modulus were similar between treated and untreated mice, suggesting that gross geometrical changes in the radii caused the lower yield force of capsaicin-treated mice. Also in opposition to our hypothesis, capsaicin treatment did not lead to substantial reductions in bone turnover rate, measured by dynamic histomorphometry and serum concentrations of CTX-I and P1NP. Altogether,

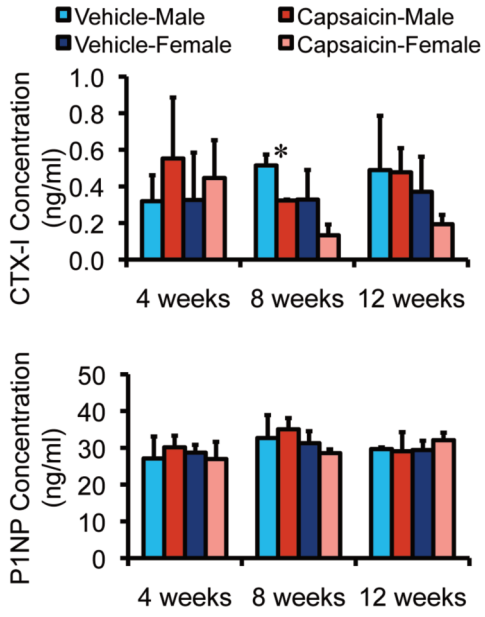

Figure 6. Capsaicin treatment did not significantly affect serum concentrations of CTX-I or P1NP, which were measured using ELISAs. Sex was a main effect for serum concentrations of CTX-I, while P1NP concentrations did not vary significantly by sex or age. *Capsaicin vs. vehicle; $p<0.05$.

these data indicate that decreased activity of peripheral sensory nerves has a small effect on the trabecular and cortical bone of mice, but that these changes do not result in a meaningful reduction in mechanical properties of whole bones.

In this study we observed only modest differences in bone parameters in capsaicin-treated mice, despite a considerable and sustained decrease in sensory nerve activity. Physiological adaptations during development may allow mice to compensate for the loss of peripheral nerve function, leading to similar development between treated and untreated mice at 12 weeks of age. It is possible that while bone structure and basal metabolic rates are conserved in capsaicin-treated mice as adults, adaptation of bone in response to mechanical loading or injury may be altered, as observed in other mouse models. For example, in a study of adult female mice lacking estrogen receptor-α, the ulnae were only 4% shorter yet demonstrated a three-fold lower osteogenic response to mechanical loading than the ulnae of wild-type littermates[38]. This is further supported by a previous study using neonatal capsaicin treatment in rats, in which capsaicin treatment did not alter normal bone growth and maintenance, but decreased the local bone remodeling response following molar extraction[22]. Future studies using this model will investigate the bone adaptation of capsaicin-treated mice to conditions such as increased mechanical loading or injury.

The effect of neonatal capsaicin treatment on bone properties had a differential effect on female mice versus male mice, although the power of this study was not sufficient to fully determine sex-based differences. At 4 and 8 weeks, female capsaicin-treated mice demonstrated the largest differences in bone structure, with shorter femurs with smaller cross-sectional area and trabecular thickness. Male capsaicin-treated mice had significantly lower trabecular thickness at the L5 vertebral body for the first time at 12 weeks of age, and lower moment of inertia and yield force of the radii compared to vehicle-treated mice at this time point. These potential sex-based differences may be related to hormonal fluctuations, as mice reach sexual maturity at 8 weeks of age.

The mouse model used in this study overcomes critical limitations of previous models investigating decreased peripheral nerve function in bone. Capsaicin treatment isolates the effects of decreased sensory nerve function without requiring surgical procedures or impairing motor function. Other studies utilizing capsaicin treatment in adult rats found that capsaicin-sensitive neurons contribute to the maintenance of trabecular bone[39,40]. However, capsaicin directly interacts with bone cells[41,42], making it difficult to separate the primary effect on bone cells from the secondary effect of decreased peripheral nerve function, as both osteoclasts and osteoblasts express receptors for capsaicin[43,44]. Treating mice as neonates instead of at maturity allows time for recovery of normal bone metabolism, and therefore isolates the effects of sensory nerve inactivation without the complication of direct action on bone cells inherent in adult treatment.

In this study we were able to detect small but significant differences in trabecular and cortical bone structure, but were unable to detect differences in bone mineral density or bone mechanical properties. This suggests that peripheral nerve inactivation may influence bone quantity, but not bone quality. If this is the case, differences in bone formation or resorption would be expected. However, imprecise methods for detecting bone turnover rates may have limited our observation of changes in capsaicin-treated mice. We were able to detect small changes in bone structure because of the high precision of micro-computed tomography. However, we were unable to detect small differences using lower resolution methods such as dynamic histomorphometry and quantification of serum biomarkers. Both of these techniques were further limited by scope: our histomorphometric analysis was limited to cortical bone, and biomarker concentrations were measured from the serum of developing mice. Similarly, three-point bending of radii may not have had adequate sensitivity to fully capture changes in bone mechanical properties.

This study is limited because it did not directly investigate the effects of capsaicin treatment on sensory neurons in bone. While we verified decreased peripheral sensory nerve function using response to a thermal stimulus, we did not perform a direct quantification in bone, such as counting neurons remaining after treatment or quantification of neuropeptides in bone. It is well established that capsaicin treatment does not affect motor neurons, however it is possible that the reduction in peripheral sensory nerve function could alter spontaneous motor activity in mice. Quantification of activity levels in vehicle- and capsaicin-treated mice could further establish that differ-

ences in bone structure are due to decreased sensory nerve function rather than decreased mechanical loading of bone. This study also did not investigate the response of bone to differing levels of sensory nerve inactivation. A more thorough disruption of peripheral sensory nerve function could have a more dramatic effect on bone metabolism than was observed in this study. Further, in this study we used neonatal capsaicin treatment as a surrogate for age-related degeneration of peripheral nerves, but did not directly make comparisons with aged animals. It is possible that aged mice demonstrate a different pattern of neural degeneration than mice treated with capsaicin as neonates. However, we were able to study the isolated effects of decreased peripheral sensory nerve function in mice up to skeletal maturity.

This study further supports a role for peripheral sensory nerves in bone metabolism. Using neonatal capsaicin treatment, we established a mouse model of decreased peripheral sensory nerve function and observed resulting changes in bone structure. We observed only small changes in bone structure with sensory nerve inactivation, with no notable changes in bone metabolism or bone quality. Therefore age-related changes in sensory innervation may not be clinically meaningful with respect to bone strength under normal loading conditions. It is possible that capsaicin-sensitive neurons may become important for bone under stress conditions such as increased mechanical loading or injury. Future studies will investigate this potential role of peripheral sensory nerves in bone adaptation.

Acknowledgements

The authors would like to acknowledge the meaningful contributions of Alexander Kelemen, Helen Raybould, Earl Carstens, Clare Yellowley, David Fyhrie, and Susan Stover. Research reported in this publication was supported by the Department of Defense – Congressionally Directed Medical Research Programs, under Award Number PR110178.

References

1. National Osteoporosis Foundation, Disease statistics "fast facts". Retrieved June 7, 2011, from National Osteoporosis Foundation Web site: http://www.nof.org/node/40.
2. Hampson G, Fogelman I. Clinical role of bisphosphonate therapy. Int J Womens Health 2012;4:455-69.
3. Russell RG. Bisphosphonates: the first 40 years. Bone 2011;49:2-19.
4. Sibai T, Morgan EF, Einhorn TA. Anabolic agents and bone quality. Clin Orthop Relat Res 2011;469:2215-24.
5. Ceballos D, Cuadras J, Verdu E, Navarro X. Morphometric and ultrastructural changes with ageing in mouse peripheral nerve. J Anat 1999;195:563-76.
6. Jacobs JM, Love S. Qualitative and quantitative morphology of human sural nerve at different ages. Brain 1985;108(Pt 4):897-924.
7. Kanda T, Tsukagoshi H, Oda M, Miyamoto K, Tanabe H. Morphological changes in unmyelinated nerve fibers in the sural nerve with age. Brain 1991;114:585-99.
8. O'Sullivan DJ, Swallow M. The fibre size and content of the radial and sural nerves. J Neurol Neurosurg Psychiatry 1968;31:464-70.
9. Swallow M. Fibre size and content of the anterior tibial nerve of the foot. J Neurol Neurosurg Psychiatry 1966; 29:205-13.
10. Dyck PJ, Karnes J, O'Brien PC, Zimmermann IR. Detection thresholds of cutaneous sensation in humans. In: Dyck PJ, Thomas PK, Lambert EH, Bunge P, eds. Peripheral Neuropathy. Philadelphia: WB Saunders; 1984:1103-38.
11. Akopian A, Demulder A, Ouriaghli F, Corazza F, Fondu P, Bergmann P. Effects of CGRP on human osteoclast-like cell formation: a possible connection with the bone loss in neurological disorders? Peptides 2000;21:559-64.
12. Bernard GW, Shih C. The Osteogenic Stimulating Effect of Neuroactive Calcitonin Gene-Related Peptide. Peptides 1990;11:625-32.
13. Cornish J, Callon KE, Bava U, Kamona SA, Cooper GJ, Reid IR. Effects of calcitonin, amylin, and calcitonin gene-related peptide on osteoclast development. Bone 2001;29:162-8.
14. D'Souza SM, MacIntyre I, Girgis SI, Mundy GR. Human synthetic calcitonin gene-related peptide inhibits bone resorption *in vitro*. Endocrinology 1986;119:58-61.
15. Granholm S, Lerner UH. The members of the calcitonin gene family of peptides, including recently discovered intermedin and CRSP, inhibit both osteoclast activity and formation. J Bone Miner Res 2006;21:S164-S.
16. Mori T, Ogata T, Okumura H, Shibata T, Nakamura Y, Kataoka K. Substance P regulates the function of rabbit cultured osteoclasts; increase of intracellular free calcium concentrations and enhancement of bone resorption. Biochem Biophys Res Commun 1999;262:418-22.
17. Owan I, Ibaraki K. The role of calcitonin gene-related peptide (CGRP) in macrophages: the presence of functional receptors and effects on proliferation and differentiation into osteoclast-like cells. Bone Miner 1994; 24:151-64.
18. Spencer GJ, Hitchcock IS, Genever PG. Emerging neuroskeletal signalling pathways: a review. FEBS Lett 2004; 559:6-12.
19. Tamura T, Miyaura C, Owan I, Suda T. Mechanism of Action of Amylin in Bone. J Cell Physiol 1992;153:6-14.
20. Wang L, Zhao R, Shi X, et al. Substance P stimulates bone marrow stromal cell osteogenic activity, osteoclast differentiation, and resorption activity *in vitro*. Bone 2009; 45:309-20.
21. Yamamoto I, Kitamura N, Aoki J, et al. Human Calcitonin Gene-Related Peptide Possesses Weak Inhibitory Potency of Bone-Resorption Invitro. Calcif Tissue Int 1986; 38:339-41.
22. Hill EL, Turner R, Elde R. Effects of neonatal sympathectomy and capsaicin treatment on bone remodeling in rats. Neuroscience 1991;44:747-55.
23. Kingery WS, Offley SC, Guo TZ, Davies MF, Clark JD,

Jacobs CR. A substance P receptor (NK1) antagonist enhances the widespread osteoporotic effects of sciatic nerve section. Bone 2003;33:927-36.
24. O'Connor BL, Palmoski MJ, Brandt KD. Neurogenic acceleration of degenerative joint lesions. J Bone Joint Surg Am 1985;67:562-72.
25. Zeng QQ, Jee WS, Bigornia AE, et al. Time responses of cancellous and cortical bones to sciatic neurectomy in growing female rats. Bone 1996;19:13-21.
26. Rix M, Andreassen H, Eskildsen P. Impact of peripheral neuropathy on bone density in patients with type 1 diabetes. Diabetes Care 1999;22:827-31.
27. Caterina MJ, Julius D. The vanilloid receptor: a molecular gateway to the pain pathway. Annu Rev Neurosci 2001;24:487-517.
28. Caterina MJ, Schumacher MA, Tominaga M, Rosen TA, Levine JD, Julius D. The capsaicin receptor: a heat-activated ion channel in the pain pathway. Nature 1997; 389:816-24.
29. Nagy JI, Iversen LL, Goedert M, Chapman D, Hunt SP. Dose-dependent effects of capsaicin on primary sensory neurons in the neonatal rat. J Neurosci 1983;3:399-406.
30. Jimenez-Andrade JM, Bloom AP, Mantyh WG, et al. Capsaicin-sensitive sensory nerve fibers contribute to the generation and maintenance of skeletal fracture pain. Neuroscience 2009;162:1244-54.
31. Mihara K, Kuratani K, Matsui T, Nakamura M, Yokota K. Vital role of the itch-scratch response in development of spontaneous dermatitis in NC/Nga mice. Br J Dermatol 2004;151:335-45.
32. Nakano T, Andoh T, Sasaki A, Nojima H, Kuraishi Y. Different roles of capsaicin-sensitive and H1 histamine receptor-expressing sensory neurones in itch of mosquito allergy in mice. Acta Derm Venereol 2008;88:449-54.
33. Jancso G, Kiraly E, Jancso-Gabor A. Pharmacologically induced selective degeneration of chemosensitive primary sensory neurones. Nature 1977;270:741-3.
34. Karl T, Pabst R, von Horsten S. Behavioral phenotyping of mice in pharmacological and toxicological research. Exp Toxicol Pathol 2003;55:69-83.
35. Doube M, Klosowski MM, Arganda-Carreras I, et al. BoneJ: Free and extensible bone image analysis in ImageJ. Bone 2010;47:1076-9.
36. Baron R, Vignery A, Neff L, Silverglate A, Santa Maria A. Processing of undecalcified bone specimens for bone histomorphometry. In: Recker R, ed. Bone histomorphometry: techniques and interpretations1983:13-9.
37. Hale LV, Galvin RJ, Risteli J, et al. PINP: a serum biomarker of bone formation in the rat. Bone 2007;40:1103-9.
38. Lee KC, Jessop H, Suswillo R, Zaman G, Lanyon LE. The adaptive response of bone to mechanical loading in female transgenic mice is deficient in the absence of oestrogen receptor-alpha and -beta. J Endocrinol 2004;182:193-201.
39. Offley SC, Guo TZ, Wei T, et al. Capsaicin-sensitive sensory neurons contribute to the maintenance of trabecular bone integrity. J Bone Miner Res 2005;20:257-67.
40. Ding Y, Arai M, Kondo H, Togari A. Effects of capsaicin-induced sensory denervation on bone metabolism in adult rats. Bone 2010;46:1591-6.
41. Kobayashi M, Watanabe K, Yokoyama S, et al. Capsaicin, a TRPV1 Ligand, Suppresses Bone Resorption by Inhibiting the Prostaglandin E Production of Osteoblasts, and Attenuates the Inflammatory Bone Loss Induced by Lipopolysaccharide. ISRN Pharmacol 2012;2012:439860.
42. Lieben L, Carmeliet G. The Involvement of TRP Channels in Bone Homeostasis. Front Endocrinol (Lausanne) 2012;3:99.
43. Abed E, Labelle D, Martineau C, Loghin A, Moreau R. Expression of transient receptor potential (TRP) channels in human and murine osteoblast-like cells. Mol Membr Biol 2009;26:146-58.
44. Rossi F, Siniscalco D, Luongo L, et al. The endovanilloid/endocannabinoid system in human osteoclasts: possible involvement in bone formation and resorption. Bone 2009;44:476-84.

Bone Adaptation in a Mouse Model of Reduced Sensory Nerve Function

By

MOLLIE ALEXANDRIA HEFFNER

B.S. (University of California, Davis) 2011

DISSERTATION

Submitted in partial satisfaction of the requirements for the degree of

DOCTOR OF PHILOSOPHY

In

Biomedical Engineering

in the

OFFICE OF GRADUATE STUDIES

of the

UNIVERSITY OF CALIFORNIA, DAVIS

Approved:

_____

Blaine A. Christiansen, Ph.D., Chair

_____

David P. Fyhrie, Ph.D.

_____

Damian C. Genetos, Ph.D.

Committee in Charge

2016

Mollie Alexandria Heffner
February 2016
Biomedical Engineering

Bone Adaptation in a Mouse Model of Reduced Sensory Nerve Function

Abstract

Long bones are richly innervated with a presence of fibers in the periosteum, cortical bone and bone marrow. Emerging evidence suggests that these nerves are involved in more than just pain transmission. Nerve damage not only affects bone during development, but also contributes to bone loss following injury. As bone cells express receptors for several neurotransmitters, nerves may regulate bone metabolism through local release of neuropeptides.

The objective of this research was to elucidate the contribution of peripheral sensory nerves to bone adaptation. We used a chemical model of decreased nerve function, administering the naturally occurring compound, capsaicin, to neonatal mice. With the use of different imaging modalities and mechanical testing techniques, we assessed the effects of denervation on skeletal development. We next used a model of increased mechanical loading (tibial compression) to investigate how denervation alters the bone response to an anabolic stimulus. Finally, we measured changes in bone concentrations of neuropeptides CGRP and substance P in response to increased loading (tibial compression) and decreased loading (hindlimb unloading).

Capsaicin treatment resulted in shorter femurs possessing thinner trabeculae. Denervation also altered the bone response to increased mechanical loading, with capsaicin-treated mice exhibiting greater changes in bone mass and mineral apposition rates. Neuropeptide

concentrations were also changed by the mechanical environment with an increase in CGRP following tibial compression. Our findings indicate an important role for sensory nerves in bone metabolism, and suggest a potential target for therapeutics aimed at bone diseases characterized by abnormal bone formation.

Acknowledgments

Completion of this dissertation work was only accomplished through the support of many members of the UC Davis community. First and foremost, I would like to thank Dr. Blaine Christiansen under whose guidance this research was conducted. I was a capricious graduate student and without your steadfast support I would not have made it to the end. Many thanks are also owed to Dr. Damian Genetos who taught me about the biological aspects of research and gave me a second chance at pipetting. I would like to thank Dr. David Fyhrie who as a member of my committees advised me, and as teacher got me interested in bone. Much of my technical training was gained through encouragement from Matthew Anderson – thank you. I would also like to acknowledge the outstanding people in VetMed 3A. I would like to thank Dr. Susan Stover for unfailing encouragement in lab meetings and Tanya Garcia for all the help with microCT. Thanks are also owed to Dr. Clare Yellowley for her generosity with her time and lab supplies and to Dr. Alice Wong who provided kind assistance and answers to my technical questions. I would also like to acknowledge Drs. Jinyi Qi, Laura Marcu, and Tingrui Pan for allowing me to be a teaching assistant in their classes. Finally, I cannot express enough my gratitude for the financial and moral support of my family over the last five years. You guys supported me despite my incessant whining, midnight printing and general disagreeableness without once doubting that I would make it through.

Contents

List of Figures

List of Tables

1 Introduction

1.1 Motivation

Treatments of adverse bone conditions, such as osteoporosis, often address symptoms as underlying causes remain largely unknown. Changes in peripheral nerve function provide a possible cause for conditions such as age-related bone loss. Considerable degeneration of peripheral nerve tissue and function occurs with aging [1-5], likely affecting bone metabolism in aged subjects. Identifying mechanisms of age-related bone loss would aid in the development of treatments aimed at maintaining healthy bone turnover using the natural processes of bone. Development of such treatments would have widespread applications, since osteoporosis affects an estimated 44 million Americans [6]. Changes in nerve function also occur with disease, including diabetes. Peripheral neuropathy may play an unexpected role in the reduced bone mineral density observed in patients with type 1 diabetes [7]. Determining whether nerve damage affects the response of bone to increased exercise may change treatment options. Furthermore, neurogenic inflammation causes heterotopic ossification, providing evidence of nervous system irregularities affecting bone tissue [8]. Conversely, nerves may play a larger role than anticipated in the response of bone to injury. Knowing the implications of altered nerve function would be useful in treating an injury such as fracture. In all of these instances, a better understanding of the interaction between peripheral nerves and bone would have bearing on the prescribed treatment.

1.2 Bone Innervation

Osteoblasts, osteoclasts, osteocytes and bone lining cells comprise the cellular milieu responsible for growth and maintenance of the skeleton. Osteoblasts differentiate from mesenchymal stem cells and in response to extracellular cues lay down osteoid at approximately 1 μm/day.

Multinuclear osteoclasts resorb bone at tens of μm/day and originate from hemopoietic cells in the marrow. Osteocytes play a role in stimulating remodeling in response to strain, communicating via processes extending through neighboring lacunae. In addition to becoming osteocytes, former osteoblasts may become quiescent bone lining cells. They may also influence remodeling by sensing mechanical strain and communicating with osteocytes. Traditional regulators of these bone cells include cytokines, growth factors and hormones. A combination of the bone cells may express receptors for the different factors or even express the factors themselves. Receptor expression for the cytokine interleukin 6 increases in differentiating osteoblasts and interleukin 6 accelerates differentiation in pre-osteoblasts [9]. Osteoblasts also produce this cytokine, which stimulates bone resorption by osteoclasts [10]. As osteoclasts dissolve collagen and demineralize bone, they release growth factors from the bone matrix that enhance osteoblast differentiation and function. Transforming growth factor beta, insulin-like growth factor I, and bone morphogenetic proteins liberated during resorption unify the remodeling process by activating osteoblasts. The coupling of bone resorption to bone formation helps partly explain the complex effects of estrogen – one of the major hormonal regulators of bone metabolism. Estrogen directly inhibits osteoblast apoptosis, promoting bone maintenance. Estrogen also directly affects osteoclasts, inducing apoptosis and inhibiting RANKL-induced differentiation. However, osteocytes may be the most important target of estrogen as it decreases apoptosis and inhibits bone remodeling. Estrogen treatment for deficiency reduces serum markers of bone resorption and eventually markers of bone formation [11]. As systemic factors, hormones may regulate bone metabolism in order to maintain optimum calcium concentration in the plasma. Whereas local factors may regulate bone cells to reduce microcracks, preserving bone integrity for functional loading.

However, neurons present a potential additional mechanism for controlling bone through bone cell regulation. As evidenced by skeletal pain, bone contains a dense network of sensory nerves, which might function as more than just a transducer of sensory stimuli. Correlative evidence includes the fact that more metabolically active regions of bone possesses greater innervation by neuropeptide containing fibers [12]. Clinically, a painful neuroma may be treated by cutting the nerve and inserting the proximal end into a hole drilled in the metacarpal. The bone does not heal the defect, and such a response would compress the nerve, suggesting some interaction between the bone cells and nerve [13]. In addition to bone healing, nerves may be involved in bone development. A study of thalidomide induced dysmelia showed that the degree of long bone reduction matched the segmental sensory innervation of the limb [14]. The radiographic findings suggest an involvement of the sensory nervous system in limb morphogenesis, which implies a trophic effect in addition to the classical role of sensation.

1.2.1 Nerve Growth

Most adult neurons generate from progenitor cells during early embryonic life. Proliferation of neuroectoderm cells in the neural plate leads to folds that form the neural tube. The neural tube gives rise to the brain and spinal cord. The ventral area (basal plate) of the neural tube becomes the ventral horn of the spinal cord and contains the cell bodies of somatic motor neurons. The dorsal division of the neural tube (alar plate) develops into the dorsal horn, containing the synapses of sensory neurons. Neural crest cells from lateral portions of the neural tube migrate to locations throughout the body where they form most of the peripheral nervous system. In addition to forming the neurons with cell bodies in the dorsal root ganglia, neural crest cells also produce Schwann cells and pigment cells of the skin. The ultimate position of most neurons

depends on several factors. Intracellularly, the actin and microtubule cytoskeleton of the neuron may influence destination by deciding which neurite grows the fastest. Initially, a growing neuron develops several short processes with the fastest growing of these neurites becoming the axon. Loose actin filaments may provide an outlet for microtubules and lead to the 5-10 times faster elongation of a given neurite [15]. Extracellular matrix molecules such as laminin and fibronectin also provide a framework for migrating neurons. Adhesion molecules, including calcium-dependent cadherins and calcium-independent neural cell adhesion molecules, promote binding that assists the migration of neurons to their final location. In addition, chemical cues seem to guide the tip of a growing neuron, called the growth cone, to its target. *In vitro* experiments using patterned substrates and immature hippocampal neurons revealed that the first neurite to contact a stripe of brain derived neurotrophic factor becomes the axon [16]. During neuron growth, mitochondria, membrane vesicles, proteins involved in synapse function, and other cytoplasmic components move toward the nascent axon. Few of the molecules directing this activity have been identified. Apoptosis removes some of the neurons created during fetal development, and determines the final neural network.

Similar to humans, sensory innervation of the murine skeleton occurs during embryonic development. A study of the hindlimb skeletons of mice from embryonic day 15 to postnatal day 20, revealed a functional nerve supply in areas of high osteogenic activity [17]. Calcitonin gene-related peptide (CGRP) immunoreactivity appears as early as embryonic day 16.5 in the developing mouse limb bud, in close proximity to the cartilaginous skeleton [18]. The sparsely branching CGRP staining fibers appear in the distal femoral and proximal tibial perichondrium and diaphyseal periosteum. By embryonic day 19, the single branching, nonvascular fibers

appear in the primary ossification center of these long bones, concomitant with the first signs of ossification. During this gestational period, the dorsal part of the spinal cord and the dorsal root ganglion develop and sensory innervation of the skin matures [19]. After birth, the CGRP containing fibers appear in the epiphysis and endosteum of the distal femur and proximal tibia. The increase in CGRP fibers after postnatal day 1 coincides with the bone modeling and remodeling necessary for shaping long bones. By postnatal day 6, the fibers appear in the cartilage canal and two days later in the secondary ossification centers. Substance P containing neurons follow the same developmental pattern as the CGRP positive ones [20]. The density of thick, branching fibers rich in varicosities increases near the growth plate in the tibias and femurs during development. Some appear as single fibers, others in association with blood vessels. Unlike sensory neurons containing CGRP, autonomic fibers staining for NPY do not appear in bone until postnatal day 4. The autonomic fibers first appear as single, non-vascular, branching fibers in the tibial and femoral periosteum. The NPY fibers next appear in the medullary cavity accompanying blood vessels until postnatal day 14, when the occurrence of the fibers decreases in all bone compartments. The change of neuron distribution with development may regulate local bone growth. Neurons containing CGRP in the femoral metaphysis increase in number from preterm to postnatal day 10 as the bone marrow cavity expands in rats [21]. When the animals begin using their limbs, the neuron density decreases in the metaphysis and innervation becomes denser in the femoral epiphysis. Rats acquire complete motor function in the hindlimbs by postnatal day 9 [22]. Innervation of the slow growing epiphysis may influence bone turnover as it bears body weight to protect the growth plate. Motor neurons in the anterior horn of the spinal cord containing CGRP appear by embryonic day 15 in the rat.

1.2.2 Nerve Structure

A large variety exists in the structure of adult neurons; however they share some basic features. A mature peripheral sensory nerve contains many axons and layers of connective tissue. Endoneurium surrounds each axon and perineurium surrounds each bundle of axons, called a fascicle. Epineurium binds groups of fascicles, which comprise the nerve. Within a nerve, the neuron is the basic information processing center and includes the cell body (soma), processes and axon terminals. The cell body surrounds the nucleus and Golgi complex, and may be responsible for the neuronal maintenance functions, including the creation and regulation of proteins. A neuron process may be a dendrite or an axon. Dendrites have receptors for neurotransmitter binding, often with dendritic spines to increase the receptive area. Axons originate at a tapered region of the cell body known as the axon hillock and present a large number of varicosities or boutons commonly located along thin axon branches [23]. Arrays of microtubules and microfilaments provide structural stability and a fast means of transport between the cell body and axon terminals. Kinesin quickly transports peptides and proteins synthesized at the rough endoplasmic reticulum to the axon terminals. Dynein carries factors such as nerve growth factor towards the cell body along the microtubules. The axon terminals contain the neurotransmitters and may connect with the dendrites of other neurons, muscles, organs, or receiving tissues. Each neuron may vary in diameter and may be myelinated or unmyelinated. Usually myelinated fibers conduct signals faster, dependent on the distance between the nodes of Ranvier. The thinnest axons belong to C fibers of the peripheral nervous system, which have diameters on the order of a single micrometer and conduct action potentials at 0.5 to 2.5 meters/second. C fibers are mostly sensory axons implicated in chronic pain and temperature, where conduction speed is less critical. Larger axons are all myelinated. Myelin in

the peripheral nervous system originates from Schwann cells. Collateral arterial branches from adjacent arteries provide the circulation to peripheral nerves.

A fully formed and functioning nerve transduces a sensory signal into an electrical signal within a neuron. A sensory signal may be transduced through a receptor or simply the peripheral end of a sensory axon. Mechanical deformation, temperature changes or noxious stimuli from damaged tissue causes ion channels in the membrane of neurons to open, causing the membrane voltage to change from the resting, polarized state of -40 to -90 mV. When depolarization of the neuron causes the voltage to increase beyond a threshold determined at the axon hillock, electrical activity in the form of an action potential is generated. Action potentials are fixed in amplitude and have uniform shape, so the frequency of action potential generation encodes the intensity of the stimulus. Action potential initiation begins at the Na^+ channel-dense axon initial segment and propagates orthodromically to the terminal for neurotransmitter release. The neurotransmitter may bind to a postsynaptic neuron, receptor or effector cell. The effect on the receptive end of the synapse may be excitatory or inhibitory. Neurons may also communicate with each other through electrical synapses, and gap junctions allow changes in membrane permeability in one neuron to simultaneously affect an adjoining neuron.

1.2.3 Nerve Distribution

Sensory nerves transmit information from peripheral stimuli to the spinal cord. From the spinal cord, signals are relayed to processing centers in the brain [24]. Peripheral sensory nerves contain neurons with cell bodies in the cranial nerve (trigeminal, nodose, petrosal, etc.) ganglia or dorsal root ganglia. Dorsal root ganglia cells are unipolar and have a peripheral axon that

terminates on a receptor and a central axon extending into the central nervous system through the dorsal horn of the spinal cord (Fig.1). Peripheral sensory nerves may be somatic or autonomic, with autonomic ones relaying information about the viscera. Sensory nerves in long bones and skin belong to the somatic nervous system. For example, damage to the L4 nerve root may impair sensation in the medial part of the leg. Motor neurons also belong to the somatic nervous system, with one process innervating skeletal muscle and the other originating in the ventral horn of the spinal cord. Efferent autonomic nerves compose the remainder of the peripheral nervous system and can be further divided into the sympathetic and parasympathetic systems. Sympathetic preganglionic motor neurons have cell bodies in the intermediolateral cell column, between the dorsal and ventral horns, from the first thoracic spinal segment to the third lumbar segment. The axons from these neurons exit through the ventral roots with the somatic motor neurons. Postganglionic neurons of the sympathetic system tend to be long and travel with other nerves or along blood vessels to the target organ. The sympathetic nervous system prepares the body for action, increasing heart rate and blood pressure and dilating blood vessels in muscle. Parasympathetic preganglionic neurons have cell bodies in the medulla, pons and midbrain as well as in sacral spinal segments two through four. Terminal ganglia of the parasympathetic system distribute widely throughout the body, often within the target organ. The parasympathetic nervous system causes energy conservation in the body, increasing gastrointestinal motility and secretion. Therefore, the autonomic nervous system uses neurons to connect peripheral organs to the central nervous system, regulating organ function without conscious input. However, dense sensory innervation means that intense stimuli in the viscera can also cause conscious sensations of pain.

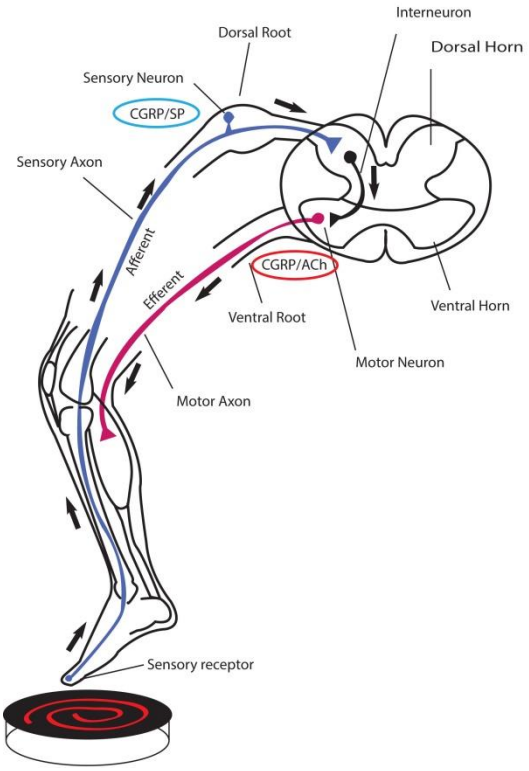

Fig. 1: Somatic sensory and motor neurons in the periphery.

Somatic sensation occurs through the transduction of stimuli at somatosensory receptors on neurons throughout the body. Neurons containing these receptors innervate skin, subcutaneous tissue, skeletal muscles, the cardiovascular system, internal organs and bones. Different types of receptors for proprioception, touch, temperature and nociception acquire information to generate the specific somatic sensation. For example, mechanoreceptors in the skin respond to bending and stretching and can provide information about touch. Pacini's corpuscle consists of onion like layers of connective tissue around a nerve terminal in subcutaneous skin that senses vibrations between 200 and 300 Hz. Compression of the connective tissue causes channels in the nerve terminal to open quickly in this rapidly adapting sensor. Free nerve endings may also act as receptors, such as for temperature detection in subcutaneous skin. Separate receptors encode information about hot and cold. For instance, the TRP channels 1-4 transduce warm

temperatures, whereas TRPM8 evokes sensations of cold. Temperature receptors may also be nociceptive, such as TRPV1, which is activated around 43°C, when tissues begin to be damaged by the stimulus. Other stimuli such as sharp objects may activate mechanical nociceptors. Nociceptive fibers consist of free nerve endings in the skin, muscle, heart, blood vessels, internal organs and bone. The axons of these fibers may be Aδ fibers which mediate sharp intense pain, or C fibers which cause dull, burning pain. Single nerve endings sensitive to combinations of painful thermal, mechanical and chemical stimuli are called polymodal nociceptors.

Murine bones receive a rich innervation of neuropeptide containing sensory fibers, especially long bones. The periosteum and perichondrium of mouse tibias and femurs contain branching neurons rich in varicosities [17]. The periosteal nerves form networks on the bone surface, with greater density at the epiphysis than midshaft of diaphyseal bones. Small branches of periosteal nerves or single fibers enter the cortical bone alongside blood vessels in Haversian and Volkmann's canals [25]. Nerves enter the medullary cavity accompanied by nutrient blood vessels and then branch into thinner fibers. In the mouse femur, the bone marrow contains the greatest number of sensory and sympathetic nerve fibers [26]. Peptidergic neurons are also found on the endosteum, from which fibers enter the cortical bone. Neonatal rats possess sensory nerves staining for substance P and CGRP in the metaphyses of long bones, cartilage canals penetrating into the epiphyses, and in the epiphyseal bone marrow [27]. The CGRP containing neurons in rat femurs near the growth plate come in contact with osteoclasts [21]. Neuropeptide containing neurons also appear in the skeleton at locations other than long bones. The calvarial bones of mice possess thinly myelinated and unmyelinated sensory fibers [28]. These CGRP

labeled fibers appear in the periosteum and marrow, but mostly in the sutures where they may influence migraines.

1.3 Neuropeptides

Neuropeptides in sensory nerves present a possible mechanism for neural regulation of bone metabolism. Neuropeptides found at presynaptic axon terminals are synthesized in the soma and transported through the Golgi complex to appear in secretory granules bound for the axon. The dense-core secretory granules have diameters between 100 and 200 nm, larger than vesicles used for traditional transmitter transport. After moving down the axon, the secretory granules are randomly dispersed in the cytoplasm of the presynaptic terminals, awaiting membrane depolarization. These peptides are identical to substances found in endocrine cells, but in the nervous system behave as neurotransmitters. Within a fraction of a millisecond of membrane depolarization, the neuropeptides are released and travel diffusely through the extracellular space. Neuropeptides may bind to receptors in a postsynaptic membrane (about 30 nm away), diffuse away or be actively taken up in a cell. Sometimes the diffusion of neurotransmitters occurs by design because release into the extracellular fluid ensures a greater target population and hence modulating effect.

The effects of neurotransmitters can vary even when they reach their targets. Neurotransmitters activate multiple types of receptors and these receptors may lead to different outcomes in the target tissue, even within the same neuron. Binding of neuropeptides to ligand-gated ion channels causes depolarization or hyperpolarization of a receptive neuron to occur within milliseconds. Binding to G protein-coupled receptors causes a response within seconds or

minutes as ion permeability changes indirectly through separate channels or messengers. The target tissue may have many types of receptors and often the presynaptic terminal releases more than one type of transmitter. In the central nervous system, neuropeptides typically co-localize with small neurotransmitters. Substance P can be found in neurons alongside acetylcholine, epinephrine, GABA, glutamate and serotonin. Low frequency stimulation of the neuron causes release of the small neurotransmitter while high frequency stimulation causes release of the neuropeptides as well. Autonomic neurons may contain as many as eight different neurotransmitters. Evidence exists that if released from free nerve endings, these transmitters may target local cells rather than a traditional postsynaptic membrane.

1.3.1 CGRP and substance P

The ubiquitous, 37-amino acid neuropeptide CGRP is produced in the thyroid, nervous system and skeleton from an alternative transcript of the calcitonin gene. A second CGRP gene encodes β-CGRP, which differs by three amino acids in humans and one amino acid in rats to the first discovered α-CGRP [29]. In the nervous system, CGRP is one of the most common peptides and α-CGRP concentration in sensory nerves outnumbers β-CGRP by a factor of three to six. Sensory neurons in the cranial and dorsal root ganglia contain CGRP and transport it to the central nervous system and peripheral tissues via secretory granules. The CGRP containing neurons of the dorsal root ganglia have small diameter unmyelinated or thinly myelinated axons, which likely convey information from sensory receptors in skin, muscle and bone. Dorsal root ganglia neurons containing CGRP may be found in the bladder and uterus. CGRP containing neurons originating in cranial ganglia innervate oral tissues [30] and the respiratory system [31]. In the stomach and intestine, CGRP containing neurons originate from both dorsal root and

cranial ganglia. Similarly, both types of sensory neurons containing CGRP are found in the liver, gall bladder and pancreas. The neuropeptide is abundant in blood vessels as well as in the myocardium [32]. In addition to a presence in sensory neurons, CGRP appears in motor neurons of the somatic nervous system, co-localized with acetylcholine for release at neuromuscular junctions to enhance muscle contraction. In bone, periosteal nerves containing CGRP appear in all four layers of the periosteum in proximity to bone lining and precursor cells. CGRP containing nerves are also found near the epiphyseal plate, in bone marrow, and around blood vessels in Volkmann's canals. Near epiphyseal trabecular bone, CGRP fibers terminate in free endings and in varicosities containing secretory vesicles near osteoblasts and osteoclasts [33].

Release of CGRP from sensory nerve terminals causes an effect mediated by a cAMP mechanism in the receptive tissue [34]. The receptor for CGRP consists of seven membrane-spanning domains similar to the G protein-coupled receptors for calcitonin, and CGRP actually binds to the calcitonin receptor with low affinity. The abundance of CGRP in the body correlates with its widespread physiologic effects. CGRP inhibits gastric juice secretion in the stomach [35] and insulin secretion in the pancreas [36]. Throughout the body, CGRP influences inflammation and vasodilation. In a rat model of experimentally induced pulpitis, researchers observed an increase in CGRP fibers in tissue surrounding severe periodontal inflammation [37]. As a potent vasodilator, CGRP relaxes contracted vessels in a dose-dependent manner including in coronary and cutaneous vascular beds [38, 39]. In the skin, CGRP also upregulates vascular endothelial growth factor (VEGF) and promotes angiogenesis [40]. The angiogenesis promoted by CGRP may indirectly influence bone formation as blood vessels are a necessary precursor to periosteal and endosteal bone growth. When investigators created a bony defect in the rat tibia, the density

of CGRP containing fibers increased near blood vessels and in accompaniment to callus formation [41]. The obligatory proximity of the neuropeptide to the bone cells exists as CGRP appears in sensory nerve endings in bone [42]. Released from sensory nerve endings, CGRP may affect bone cells since osteoblasts and osteoclasts express receptors for CGRP [43]. An *in vitro* investigation of human osteoblasts from trabecular bone demonstrated that they express CGRP, and exposure to a cAMP analog increases not only CGRP expression, but also characteristic messengers of the osteoblastic phenotype [44]. These findings suggest a potential autocrine effect of CGRP on osteoblasts. Transgenic mice expressing increased CGRP in osteoblasts demonstrate increased trabecular bone density in the distal femoral metaphyses at 12 weeks of age [45]. Mice deficient for CGRP develop osteopenia resulting from a reduced bone formation rate [46]. Similar to calcitonin, osteoclast inhibition by CGRP involves cAMP as a second messenger [47]. Administration of high doses of CGRP inhibits bone resorption and lowers serum concentrations of calcium [21]. The inhibition of bone resorption occurs through inhibited recruitment of macrophages in osteoclast-like cells and osteoclast action.

Another pervasive peptide, substance P is an undecapeptide found in sensory neurons terminating in the dorsal horn of the spinal cord. Approximately 20% of the dorsal root ganglia cells in the rat contain substance P [48]. In the periphery, substance P is found in sensory and motor nerves. The gastrointestinal tract and central nervous system also contain substance P. In bone, substance P containing nerves enter the bone marrow next to blood vessels where they separate and terminate in free endings. Substance P nerve fibers also innervate the periosteum of bone.

Substance P excites dorsal horn neurons that are also excited by noxious stimuli, including intense heat. When injected into the spinal cords of mice, substance P elicits scratching and biting behavior associated with chronic pain [49]. Osteoblast precursors, bone marrow stromal cells, express substance P receptor neurokinin-1 and exposure to the neuropeptide stimulates differentiation in a dose dependent manner [50]. Low concentrations of substance P increase alkaline phosphatase and osteocalcin expression as well as Runx2 protein levels. Differentiated mouse bone marrow stromal cells have enhanced mineralization at higher concentrations of substance P. Osteoblasts also express receptors for substance P and exposure to substance P increases osteoblast function *in vitro* [50]. Substance P facilitates RANKL induced osteoclastogenesis in bone marrow macrophages, the precursors to osteoclasts [50]. Osteoclasts also have receptors for substance P and exposure *in vitro* stimulates calcium influx and bone resorption [51]. These findings therefore suggest bone remodeling stimulation by this neuropeptide. In the distal skeleton, substance P may contribute to bone integrity. After a unilateral sciatic section in skeletally mature rats, substance P content in both tibias decreased by 50% with a rapid, attendant decrease in trabecular bone mineral density [52]. Administration of a substance P antagonist caused a further reduction in trabecular bone in the denervated limb, indicating a protective effect of the neuropeptide on bone.

Both CGRP and substance P often appear together in the small sensory neurons of the dorsal root ganglia. CGRP may facilitate substance P release in dorsal horn neurons and enhance activation, because rats with sensory neuropathy contain fewer CGRP containing sensory neurons [53]. Addition of CGRP to an intrathecal injection of substance P in rats causes caudally directed biting to extend from a few minutes to up to forty minutes, providing further evidence of an

interaction between these neuropeptides in the dorsal horn [54]. The effects of these neuropeptides in the respiratory system may differ. Both are found in the same sensory nerve endings, but the binding sites for CGRP are denser in pulmonary blood vessels and for substance P in airway smooth muscles. Substance P alone induces disruption of the blood aqueous barrier in the eye, resulting in aqueous flare, which is enhanced when given with CGRP [55]. Both neuropeptides have a similar distribution in bone, although CGRP containing fibers are more numerous.

1.3.2 NPY, glutamate and VIP

Neuropeptides other than CGRP and substance P influence bone metabolism. Neuropeptide Y plays a role in the central nervous system optimization of bone mass to body weight and in local bone metabolism as osteoblasts express this neuropeptide. Mice lacking neuropeptide Y demonstrate enhanced osteoblastic activity and increased bone mass [56]. Glutamate, a traditional excitatory neurotransmitter in the central nervous system, stimulates osteoclastic resorption *in vitro* and osteoclasts, osteoblasts and osteocytes express glutamate receptors [57]. One source of glutamate could be the peripheral nerves containing glutamate found in the bone marrow in the vicinity of bone cells [58]. Osteoblasts also produce glutamate, and it might be involved in paracrine signaling between bone cells since glutamate expression decreases in response to mechanical loading of osteocytes [59]. A 28 amino acid peptide, vasoactive intestinal peptide (VIP) is usually found in parasympathetic nerves and to a lesser extent in primary sensory neurons. VIP acts a neurotrophic factor, stimulating neuronal growth, differentiation and survival and aids in transmitter synthesis. In bone, VIP is found in sympathetic nerves. Sympathetic postganglionic neurons containing VIP appear in the periosteum and bone of

porcine ribs [60]. They also appear near the epiphysis in long bones and not often around blood vessels. Osteoblasts and osteoclasts express receptors for VIP. *In vitro,* VIP inhibits osteoclast recruitment, associated with downregulation of RANK expression in osteoclasts [61]. Osteoblast expression of RANKL decreases and expression of the RANK antagonist osteoprotegerin increases. Chemically destroying VIP nerves in rats causes an increase in mandible surface covered by osteoclasts [62]. VIP also affects osteoblast function, stimulating osteoblastic alkaline phosphate activity *in vitro,* and potentially having an anabolic effect on bone [63].

1.4 Animal Models of Decreased Nerve Function

Investigation of the interaction between nerves and bone often involves reducing nerve function and observing the resulting effects on bone. As a clinical model, experimenters may section nerves without regenerative potential to observe the effects of denervation on target tissues. For example, removing the nerve supply to long bones may initially impair bone development. Sectioning the sciatic nerve in one month old rats caused the metatarsals to be 3-5% shorter on the denervated side [64]. The tibias, which contain additional nerves, were the same length after sciatic denervation. Genetic models may also be employed to clarify the role of nerve function on bone metabolism. When mice lack semaphorin 3A, an axonal chemorepellant important to axon guidance, bone mass also changes [65]. Depletion of semaphorin 3A decreased sensory innervation of trabecular bone and led to low bone mass due to decreased bone formation in 8 week old mice. Other genetic models reduce nerve activation or neuropeptide concentration to examine the effects on bone. Mice lacking TRPV1, a channel found on sensory neurons, display a similar phenotype to wildtype mice, with similar size and bodyweight. However, a study of bone using TRPV1 knockout mice revealed a reduction in the basal levels of the osteoclast

activation biomarker TRAP in the femur [66]. Additionally, ovariectomy in the knockout mice did not cause the elevation in TRAP levels or bone loss observed in wildtype mice. Genetic ablation can also reduce neuropeptide concentration in mice. αCGRP knockout mice display osteopenia associated with low bone formation rate without changes in osteoblast number or surface [46]. The findings from the knockout model suggest a role for the peptide on osteoblast function and subsequently bone metabolism.

Different animal models have also been used to investigate the effects of reduced nerve function on bone adaptation. Sample et al. used bupivacaine to induce perineural anesthesia of the brachial plexus of rats to achieve temporary neuronal blocking [67]. The bupivacaine was administered five minutes prior to ulnar compression, and paralysis of the limb was resolved within two hours of the increased loading. Such a model eliminates the complication of load bearing changes resulting from compression. Furthermore, temporarily blocking neuronal signaling was sufficient to reduce labeled bone area by 81% in the compressed ulna within ten days. Later research by these investigators examined the mechanism of neuronal influence on bone by altering CGRP concentration in fatigue loaded rats [68]. The group directly altered the neuropeptide concentration by using a subcutaneously implanted osmotic pump that continuously released saline, CGRP or a CGRP antagonist. Rats administered the CGRP antagonist had a significantly greater density of resorption spaces in the ulnas loaded to fatigue, compared to loaded ulnas in rats administered saline or CGRP. Neuropeptide concentration may also be altered in animal models using casting. Immobilization of rat hindlimbs achieved through casting, elevates substance P and CGRP concentrations in the sciatic nerve [69]. When combined with tibia fracture, casting also elevates these neuropeptide concentrations, which contribute to

inflammation and pain. The combination of altered neuropeptide levels and an event known to stimulate remodeling provide an opportunity for investigating nerve and bone interactions.

However, different protocols aimed at changing nerve function often result in differing effects in the complex *in vivo* environment. Capsaicin treatment provides a useful animal model for isolating the effects of decreased peripheral sensory nerve function. Capsaicin activates the transient receptor potential cation channel subfamily V member 1 (TRPV1), which is expressed by unmyelinated and small diameter myelinated sensory neurons, but not motor neurons, large diameter sensory neurons, or sympathetic neurons [70, 71]. Therefore, treatment does not disrupt muscle activity or subsequent mechanical loading of bone. Subcutaneous injection of capsaicin in neonatal animals destroys unmyelinated and small-diameter myelinated sensory neurons for the lifetime of the animal [72]. Treating neonatal mice with capsaicin thus provides a consistent model of decreased peripheral nerve function that allows consideration of different environments and treatment options. Such a model permits us to study bone adaptation in cases of decreased nerve function.

1.5 Capsaicin

Capsaicin (8-methyl-N-vanillyl-6-nonenamide, Fig. 2) is produced in the fruits of *Capsicum* chili peppers. It provides the pungency of chilies, a characteristic that discourages consumption by inefficient seed dispersers [73]. While the piquancy deters many vertebrate predators, humans have been consuming capsaicin for thousands of years [74]. By the early 19^{th} century, researchers had isolated capsaicin and in 1930, completely synthesized it. Nelson and Dawson confirmed that a vanillyl group and hydrocarbon tail constitute the capsaicin molecule [75].

Variations in the hydrocarbon tail account for the remaining four naturally occurring compounds that comprise the capsaicinoids. Capsaicin is the most potent of this group of vanillyl fatty acid amides [76].

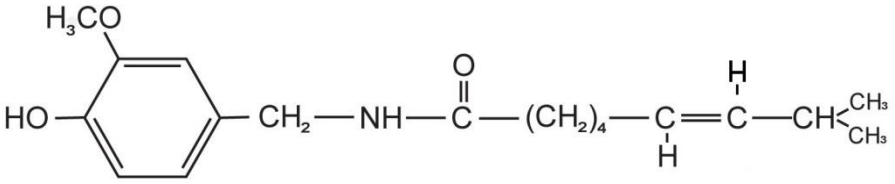

Fig. 2: Capsaicin (above) has molecular formula $C_{18}H_{27}NO_3$ and a molecular weight of 305.4 g/mol.

The properties of capsaicin render it useful not only as a food flavoring and preservative but as an analgesic agent. A study involving topical application of 0.025% capsaicin cream revealed a pain reduction of 57% in the knees of rheumatoid arthritis patients [77]. Similarly, a higher dose (0.075%) cream was able to reduce pain in osteoarthritic hands [78]. Interestingly, while capsaicin may not alleviate painful diabetic neuropathy [79], it may relieve the symptoms of type 1 diabetes. Eliminating pancreatic TRPV1+ sensory neurons using capsaicin normalized insulin sensitivity and insulitis in mice [80]. Furthermore, an in vitro study found that capsaicin can induce apoptosis in gastric cancer cells [81]. While these studies suggest numerous and diverse potential benefits of capsaicin administration, few have investigated the implications for bone.

1.5.1 Mechanism of action

Capsaicin acts as a neuropeptide releasing agent, both conveying sensory information and affecting local cell function. It works by binding to the receptor TRPV1, a six-transmembrane spanning protein with cytoplasmic amino and carboxy termini (Fig. 3). Most TRPV1 receptors can be found on the terminals and unmyelinated axons of peripheral neurons such as polymodal

nociceptors [82]. Inflammatory mediators such as prostaglandins enhance translation and transport of TRPV1 to the terminals of the neurons in a process called sensitization. Binding of capsaicin causes expansion of the pore region between transmembrane segments 5 and 6, allowing calcium ions to enter the neuron and initiate depolarization. The excited neuron releases neuropeptides (substance P and CGRP) from its peripheral terminals and centrally to relay a message of pain to the brain. Additionally, a study of CGRP demonstrated non-synaptic release of neuropeptides through vesicular exocytosis along unmyelinated axons [83]. Peripherally released neuropeptides can stimulate gastrointestinal and salivary secretions, contract smooth muscle, and increase microvascular permeability in an inflammatory cascade [84]. Over-stimulation depletes neuropeptide concentrations and desensitizes the neuron, abrogating the sense of pain. The neuron remains insensitive to external stimuli while capsaicin is bound to TRPV1 because of the durable refractory state [85].

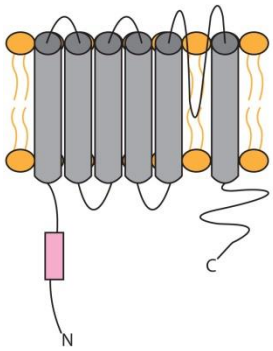

Fig. 3: TRPV1 is a six-transmembrane spanning protein activated by capsaicin.

The effects of capsaicin depend on the route and timing of administration. Topical application generates a burning sensation as capsaicin binds to TRPV1, a receptor also activated by noxious thermal stimuli, acid, and certain chemicals. The feeling of heat subsides as substance P stores in the neuron diminish. While bound with capsaicin, the neuron will be incapable of transmitting pain caused by conditions such as arthritis. The bond between capsaicin and TRPV1 is

temporary, and over-the-counter creams recommend multiple applications daily. Systemic administration of capsaicin impairs the sensitivity of specific neurons, eliminating neurogenic inflammation in response to sensory irritants. Younger animals demonstrate a greater and irreversible decline in sensory function following capsaicin administration, with a larger effect in 2 day old than 20 day old animals [86]. Subcutaneous injection of capsaicin in neonatal rats damages sensory neurons, resulting in permanent insensitivity. Disruption of the fine structure of the neurons can be observed as early as 30 minutes after capsaicin treatment in neonates. By 4 hours, phagocytosing glial cells can be seen ingesting the degenerated axons of unmyelinated neurons [87]. Capsaicin treatment of mice on days 2 and 5 of life, reduces the unmyelinated axons of the sural nerve by half [88]. Reductions in neuropeptide concentration, including substance P and CGRP, accompany the capsaicin induced degeneration of sensory neurons. Neonatal injection of capsaicin in rats causes a persistent reduction of substance P in the dorsal root ganglia until at least 4 months after treatment [89]. The decrease in unmyelinated neurons and neuropeptide content following systemic capsaicin administration in animals also depends on the administered dose. Neonatal capsaicin injection at 50 mg/kg (a widely used dose) reduces the number of unmyelinated neurons in the L3 dorsal roots by 90%, with a similar decline in substance P concentration [72].

The influx of calcium likely contributes to the neurotoxic action of systemically administered capsaicin. Cell damage results when high-dose capsaicin administration causes more Ca^{2+} to accrue in the neuron than can be disposed of. Studies of neurons in culture have shown that excessive Ca^{2+} accumulation leads to degeneration similar to that seen in rats treated with capsaicin as neonates [90]. The calcium activates degradative enzymes and proteases which

disrupt the cytoskeletal organization and axoplasmic flow. Administration in neonatal animals also inhibits axoplasmic transport of nerve growth factor in sensory nerves. Another mechanism by which capsaicin administration may lead to sensory neuron degeneration involves the entry of Na^+ and Cl^- into the cell. The net gain of NaCl causes an uptake of water and fiber swelling followed by osmotic lysis. Both pathways occur physiologically, leading to more rapid damage of the neurons.

1.5.2 Capsaicin-sensitive neurons

Capsaicin binds to TRPV1, a receptor found on sensory neurons in the peripheral and central nervous systems. Capsaicin-sensitive neurons are generally sensory neurons with unmyelinated axons (C-fibers) and cell bodies in the dorsal root and trigeminal ganglia [91]. However, a group of sensory neurons with thin myelinated axons (Aδ) are also sensitive to capsaicin. All of these neurons express TRPV1, one of a family of six vanilloid receptors. The distribution of TRPV1 has been examined using resiniferatoxin, a compound that mimics the agonist action of capsaicin. Radiolabeled resiniferatoxin revealed the presence of TRPV1 in the dorsal horn of the spinal cord, where small nociceptive neurons of the dorsal root ganglia terminate. The peripheral ends of these sensory axons exist throughout the body, with a presence in the skin and skeleton. Using neonatal treatment in rats, researchers found that capsaicin reduces the density and length of $CGRP^+$ nerve fibers in the mid-diaphysis femoral periosteum [92]. The periosteum of the tibia also possesses a network of substance P and CGRP containing fibers, which run longitudinally and are densest at the epiphysis. Capsaicin treatment greatly reduces innervation of the periosteum by these substance P and CGRP containing fibers [62]. Besides in the periosteum, rats possess $CGRP^+$ nerve fibers near the femoral growth plates, with a greater density of fibers

in the epiphysis than metaphysis [21]. Capsaicin-sensitive neurons may also be found traversing cortical bone. Nerve fibers staining positive for substance P and CGRP were found in Volkmann's canals in the dorsal epiphyseal region of rat tibias and femurs, where they associate with blood vessels [42]. Bone marrow also contains neurons expressing these neuropeptides, with a demonstrated decrease in arthritic rats [93]. A study of (^{3}H)resiniferatoxin showed that in addition to its presence in the periphery, TRPV1 has a widespread distribution in the mouse (C57Bl6) brain, with a possible role in pain processing [94]. Comparison with TRPV1 knockout mice confirmed the presence of this receptor in the olfactory nuclei, cerebral cortex, thalamus, hypothalamus, and cerebellar cortex. The TRPV1 expressing neurons in the central nervous system may also contribute to body temperature regulation as elevated temperatures have been reported in capsaicin-desensitized mice [95].

Capsaicin-sensitive neurons also exist in other physiological systems, and TRPV1 can be found in non-neuronal cells. Sensory nerves in the heart express TRPV1 and in addition to transmitting cardiac changes to the brain, can release substance P and CGRP [96]. Release of these neuropeptides in response to capsaicin may enhance cardiac blood flow [97]. Furthermore, substance P and CGRP release in the respiratory system following TRPV1 activation causes bronchoconstriction and airway hyperactivity [98]. In the urinary system, TRPV1 may regulate normal bladder function. In a study of TRPV knockout mice, researchers found that mice lacking the receptor had increased bladder volume and more frequent low-volume urinations [99]. Capsaicin-sensitive neurons in the gastrointestinal tract transmit gastric pain to the brain in an afferent manner while releasing substance P and CGRP in an efferent fashion. Activation of these neurons by capsaicin has a protective effect as mucus and HCO_3^- secretions increase [100].

Additionally, capsaicin-sensitive neurons play an important part in minor systems. Capsaicin ingestion registers as spicy because gustatory neurons express TRPV1 receptors. When activated by capsaicin, increases in cochlear blood flow may alter hearing [101]. Studies of human hair have shown that exposure to capsaicin inhibits hair shaft elongation and induces apoptosis [102]. Non-neuronal cells expressing TRPV1 include mast cells, glial cells, bronchial epithelial cells and keratinocytes [103]. Furthermore, osteoblasts and osteoclasts express TRPV1, and the receptor promotes differentiation of these cell types [104]. Expression of TRPV1 in non-neuronal cells has also been implicated in inflammation, infection and immunity [105].

1.6 Effects of Sensory Nerves on Bone Metabolism

Investigation of nerve involvement in bone metabolism motivated the development of the mouse model used in this research. *In vitro* studies have demonstrated a link between neuropeptides and bone cell function [106], and previous animal studies indicate that peripheral nerves have an effect on bone metabolism *in vivo* [59]. However, the role of sensory nerves in bone growth and adaptation remains unknown. To explicate sensory nerve involvement in bone metabolism, we used capsaicin treatment to impair sensory nerve function. First, we used this model in an attempt to clarify the effects of sensory innervation on bone development. We then explored the relative importance of capsaicin-sensitive neurons to adaptation of bone to increased mechanical demands. While others have examined the effects of reduced nerve function on bone response, the results have been conflicting. We proposed that any observed effects would be the result of sensory regulation of bone cells through expression of neuropeptides. Neuropeptides provide both a sensing aspect and effector mechanism for sensing mechanical changes in bone and responding with an appropriate metabolic cascade. Therefore, we measured bone concentrations

of neuropeptides after exposure to altered mechanical environments. The following work adds to the growing body of knowledge about neural regulation of bone.

2 Specific Aims and Hypotheses

We sought to establish the role of peripheral sensory nerves in bone metabolism *in vivo* using capsaicin-treated mice as models of decreased sensory nerve function. We tested three hypotheses to examine the role of decreased peripheral sensory nerve function in bone metabolism and bone mechanotransduction.

2.1 Bone Development

2.1.1 Hypothesis 1

Capsaicin treatment decreases the resting rate of bone turnover in developing mice, resulting in observable changes in bone quantity and bone quality.

2.1.2 Specific Aims

Compare capsaicin-treated and vehicle-treated mice at intermittent stages of skeletal development (4, 8, and 12 weeks of age). Determine the effects of neonatal capsaicin treatment on bone structure and metabolism compared to vehicle-treated mice using microCT, three-point bending, dynamic histomorphometry and assays of serum biomarkers.

2.2 Increased Mechanical Loading

2.2.1 Hypothesis 2

Capsaicin-treated mice will have reduced bone adaptation responses to mechanical loading compared to vehicle-treated mice.

2.2.2 Specific Aims

Subject capsaicin-treated (12 weeks of age) and vehicle-treated (12 weeks of age) mice to increased mechanical loading via tibial compression. Determine the bone adaptation response of capsaicin-treated and vehicle-treated mice using microCT and bone dynamic histomorphometry.

2.3 Neuropeptide Concentration

2.3.1 Hypothesis 3

Neuropeptide concentrations in bone will change in response to altered loading conditions.

2.3.2 Specific Aims

Subject mice (12 weeks of age) to either increased mechanical loading via tibial compression or hindlimb unloading via tail suspension. Determine the concentrations of CGRP and substance P in the tibias in response to the altered loading environment using ELISAs.

3 Bone Development

3.1 Introduction

Osteoporosis is characterized by decreased bone mass and increased risk of fracture [6]. Common treatments for osteoporosis manipulate bone turnover primarily by inhibiting osteoclastic bone resorption [107, 108] but can also target osteoblastic bone formation [109]. However, the mechanisms underlying age-related bone loss remain elusive. Degeneration of peripheral nerves may be a contributing factor for age-related bone loss, as substantial changes in peripheral nerve structure and function occur with aging [1-5]. The reductions in axon number and fiber size in aged subjects are associated with decreased peripheral nerve function, with cutaneous thermal and tactile thresholds significantly increased [110]. Further, there is now a well-established link between peripheral nerve function and bone metabolism *in vitro* [50, 106, 111-119]. In addition, denervation has been shown to cause bone loss *in vivo* [52, 120-122], and peripheral neuropathy has been identified as an independent predictor of low bone mass in the affected limb of diabetic subjects [7]. Despite strong evidence of a link between the function of peripheral nerves and bone metabolism, the potential role of decreased peripheral nerve function in age-related bone loss has not been investigated.

Capsaicin treatment is a useful method for isolating the effects of decreased peripheral sensory nerve function in animal models. Capsaicin treatment activates the TrpV1 receptor, which is expressed by unmyelinated and small diameter myelinated sensory neurons, but not by motor neurons, large diameter sensory neurons or sympathetic neurons [70, 71]. In this way, capsaicin treatment is able to isolate the effects of peripheral sensory neurons without disrupting normal mechanical loading, which is a confounding consequence of complete denervation. Subcutaneous injection of capsaicin in neonatal animals destroys unmyelinated and small-

diameter myelinated sensory neurons for the lifetime of the animal [72]. Neonatal capsaicin treatment is a well-established model that has been used previously to investigate pain in rats [92] and itch in mice [123, 124]. We are aware of only one study that used neonatal capsaicin treatment for a study of bone metabolism in rats. This study found that neonatal capsaicin treatment in rats did not appear to alter normal bone growth and maintenance, but that decreased sensory nerve function may decrease local bone remodeling following molar extraction. However, this study did not investigate developmental changes resulting from capsaicin treatment. Importantly, this previous study also did not quantify trabecular bone structure, and did not investigate bone mechanical properties. We are unaware of any studies that have used neonatal capsaicin treatment to investigate bone metabolism in mice.

In this study, we used neonatal capsaicin treatment in mice to investigate the effects of decreased peripheral sensory nerve function on skeletal development and bone metabolism in mice, and to establish a mouse model of decreased peripheral sensory nerve function *in vivo* for future studies in bone. Using vehicle- and capsaicin-treated mice at multiple stages of development (4, 8, and 12 weeks of age) we assessed bone structure using micro-computed tomography, mechanical properties and fracture resistance using three-point bending, and bone turnover rate using dynamic histomorphometry and serum biomarkers. We hypothesized that decreased peripheral nerve function in capsaicin-treated mice would result in decreased bone structure, decreased resistance to fracture, and decreased bone turnover rate.

3.2 Methods

Neonatal capsaicin treatment

A total of 42 male and female C57BL/6 neonatal mice were used in this study, from 7 timed pregnant females (Harlan Laboratories, Indianapolis, IN). Neonatal capsaicin treatment was performed as previously described [87]. Briefly, neonatal mice were given subcutaneous injections of capsaicin (50 mg/kg) or vehicle (10% ethanol, 10% Tween 80 in isotonic saline) on day 2 and 5 after birth (n = 21 vehicle, 21 capsaicin). Following capsaicin or vehicle treatment, neonatal mice were returned to normal cage activity until weaning (28 days). Mice were sacrificed 4, 8, or 12 weeks after birth, with a total of 7 vehicle- and 7 capsaicin-treated mice per time point (2-5 mice per age/sex/treatment group). We selected these time points to observe developmental changes from weaning until skeletal maturity, and to account for any possible recovery from sensory nerve inactivation by adulthood. Mice were weighed 1-2 times per week from birth until sacrifice.

Hot-plate analgesia testing

Capsaicin- and vehicle-treated mice were subjected to hot-plate analgesia testing at 4, 8, and 12 weeks of age to determine response time to a constant thermal stimulus of 55 °C as previously described [125]. Mice were placed on a hot-plate (LE 7406, Coulborn Instruments, Whitehall, PA) and removed after indication of discomfort, determined as twitching or licking of a hind limb or jumping, or after a maximum of 30 seconds, and the latency time of the response was recorded. Each mouse was tested twice at each time point, and the latency times were averaged for each mouse/time point.

Micro-computed tomography analysis of bone structure

Right tibias, right femurs, and L5 vertebrae were removed post mortem and preserved in 70% ethanol. Bones were scanned using micro-computed tomography (SCANCO, µCT 35, Bassersdorf, Switzerland); images were acquired at 6 µm nominal voxel size (energy=55 kVp, intensity=114 µA, integration time = 900 ms). Trabecular bone was analyzed at the metaphysis and epiphysis of the distal femur and at the L5 vertebral body using manually drawn contours inside the cortical shell on two-dimensional slices. The metaphysis was defined by a 900 µm thick volume of interest beginning below the middle break of the growth plate. Trabecular bone volume per total volume (BV/TV), trabecular number, trabecular thickness (Tb.Th), trabecular separation (Tb.Sp), and bone mineral density (BMR) were determined using the manufacturer's 3-D analysis tools. Cortical bone was analyzed at the mid-diaphysis of the tibia and femur, using a 240 µm thick volume of interest centered at the measured midpoint of each bone. Bone area (B.Ar), medullary area (M.Ar), total cross-sectional area (Tt.Ar), cortical thickness (Ct.Th), and bone mineral density (BMR) were determined using the manufacturer's 3-D analysis tools.

Three-point bending

Bilateral radii were removed post mortem and preserved in 70% ethanol. Bones were scanned using micro-computed tomography as described above, with a volume of interest that included the entire bone. Average bending moment of inertia for the central 1.0 mm (100 slices) was determined using BoneJ analysis of the microCT images [126]. Following µCT scanning, radii were rehydrated for 25 minutes in phosphate buffered saline (PBS), and then mechanically tested in three-point bending to determine cortical bone material properties. The lower supports had a span of 5.02 mm for 4 week samples, and a span of 7.45 mm for 8 and 12 week samples (Fig.

4A), and the center loading platen was driven at 0.2 mm/sec until failure. Resulting force and displacement data were analyzed to determine stiffness and yield force. Modulus of elasticity and yield stress were determined using Euler-Bernoulli beam theory.

Dynamic histomorphometry

Mice received injections of calcein green (10 mg/kg; Sigma-Aldrich, St. Louis, MO) and Alizarin-3-methlimino-diacetic acid (30 mg/kg; Sigma-Aldrich, St. Louis, MO) 10 days and 3 days prior to sacrifice, respectively. After scanning with μCT, the right tibias were embedded in Technovit (Kulzer, Wehrheim, Germany) using standard techniques for undecalcified bone [127]. Two sections were cut from each bone on a bandsaw (Model 310, Exakt Technologies, Norderstedt, Germany) in the transverse plane at 40% of the length from the proximal end. Sections were ground to an approximate thickness of 40 μm. Two color fluorescent images were obtained at 10x magnification (Nikon Eclipse TE2000-E, Tokyo, Japan). Dynamic histomorphometric analysis was performed using commercial software (Bioquant, Nashville, TN) and the results were averaged for the replicate slides from each bone. Mineral apposition rate (MAR), percent mineralizing surface (MS/BS), and bone formation rate (BFR/BS) were quantified for the endosteal and periosteal surfaces.

Serum biomarkers

Blood was collected from capsaicin- and vehicle-treated mice immediately prior to sacrifice for quantification of systemic biomarkers of bone metabolism. Mice were anesthetized with isoflurane and approximately 100-200 μL of blood was collected retro-orbitally. Samples were allowed to clot for 2-4 hours in an ice bath and then centrifuged at 1000 g for 5 minutes. The

supernatants were collected and frozen rapidly to -80 °C until analyzed. Serum was analyzed in duplicate to determine the concentrations of carboxy-terminal collagen crosslinks I (CTX-I) and procollagen type 1 amino-terminal propeptide (P1NP) using commercial mouse-specific ELISAs (Cusabio, Wuhan, China) per the manufacturer's instructions. CTX-I is a common biomarker for bone resorption, while P1NP is a biomarker for bone formation [128].

Statistics

Hot-plate, μCT, three-point bending, histomorphometry and biomarker data were analyzed using three-way ANOVA stratified by age, sex, and treatment (JMP, SAS Institute Inc., Cary, NC). Between-group differences were analyzed using an unpaired Student's t-test of capsaicin- vs. vehicle-treated mice at each time point. Data are reported as mean ± SD. Significance was defined as $p<0.05$.

3.3 Results

Mouse body weights

Neonatal capsaicin treatment did not have a statistically significant effect on body weights of male mice; there was no difference in body weight between capsaicin- and vehicle-treated male mice for any time point from weaning through 12 weeks (Fig. 4). However, capsaicin treatment significantly affected body weights of female mice at early time points. Female mice treated with capsaicin had 8-13% lower body weights than vehicle-treated female mice from weaning until 47 days of age (Fig. 1; $p < 0.05$ for both time points). There were no significant differences in body weights for capsaicin- and vehicle-treated female mice from 8 to 12 weeks of age.

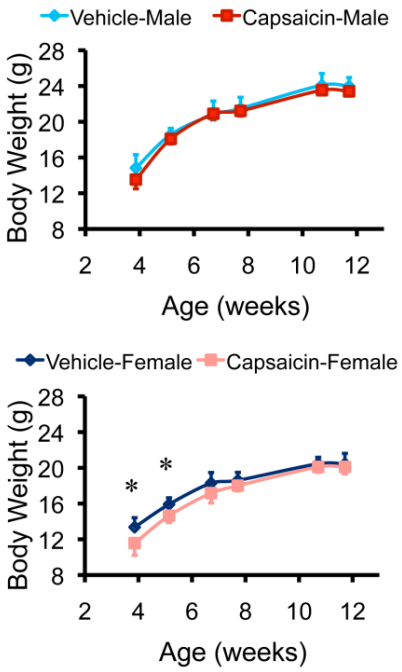

Fig. 4: Body weights of treated and untreated mice were recorded from weaning until 12 weeks of age. Female mice treated with capsaicin had lower body weight than vehicle-treated female mice from weaning until day 47. Body weights of male mice were unaffected at all time points. * Capsaicin vs. vehicle; $p < 0.05$.

Hot-plate analgesia testing

Mice treated with capsaicin had significantly longer latency times when exposed to the constant thermal stimulus than vehicle-treated mice at all time points examined (Fig. 5; $p < 0.0001$). For example, at 8 weeks of age, the average latency time of capsaicin-treated mice was 63% longer than that of vehicle-treated mice ($p = 0.0002$), while at 12 weeks of age the latency time was 67% longer for capsaicin-treated mice ($p = 0.0007$). This confirms that mice treated with capsaicin had decreased peripheral sensory nerve function, which persisted until at least 12 weeks of age. Age was also a main effect for latency time ($p = 0.0052$); latency times for both capsaicin- and vehicle-treated mice at 12 weeks of age were significantly shorter than at 4 or 8 weeks.

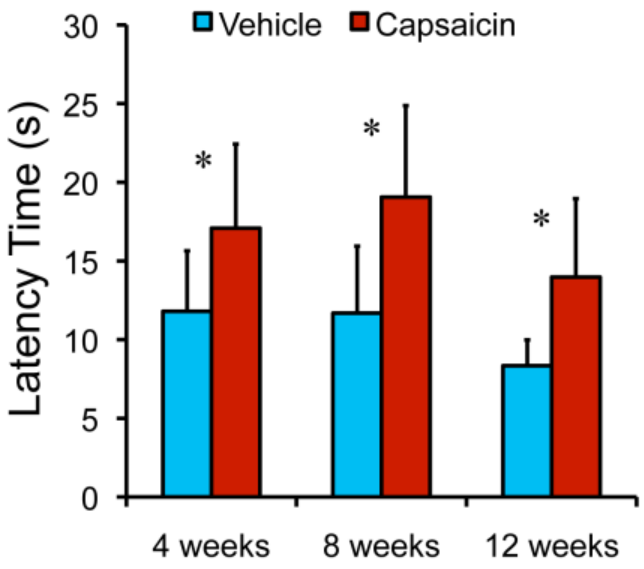

Fig. 5: Hot-plate analgesia testing of treated and untreated mice was performed to verify decreased peripheral sensory nerve function. Treatment and age were main effects for latency time ($p < 0.0001$, $p = 0.0052$). Capsaicin-treated mice had significantly longer latency times than vehicle-treated mice at all time points when exposed to a constant 55° C thermal stimulus. * Capsaicin vs. vehicle; $p < 0.05$.

Micro-computed tomography

Capsaicin treatment resulted in small but significant decreases in bone structure parameters in trabecular bone of mice relative to vehicle-treated controls (Fig. 6). For example, we observed a significant main effect of capsaicin treatment on Tb.Th at the femoral metaphysis and L5 vertebral body ($p = 0.0002$ and 0.0024, respectively). Female capsaicin-treated mice had 5.2-9.5% lower Tb.Th than vehicle-treated female mice at these sites at each time point ($p = 0.0056$-0.049). However, we did not observe a significant effect of capsaicin treatment on BV/TV or Tb.Sp at the femoral metaphysis. At the femoral epiphysis, we observed a significant treatment*sex interaction for Tb.Th. ($p = 0.026$), with female mice being more severely affected by capsaicin treatment than male mice. We also found a significant treatment*sex*age interaction for BV/TV at the femoral epiphysis. For example, female capsaicin-treated mice had

8.7% lower BV/TV at the femoral epiphysis than vehicle-treated female mice at 8 weeks (p = 0.015), whereas male mice had similar BV/TV at this time point.

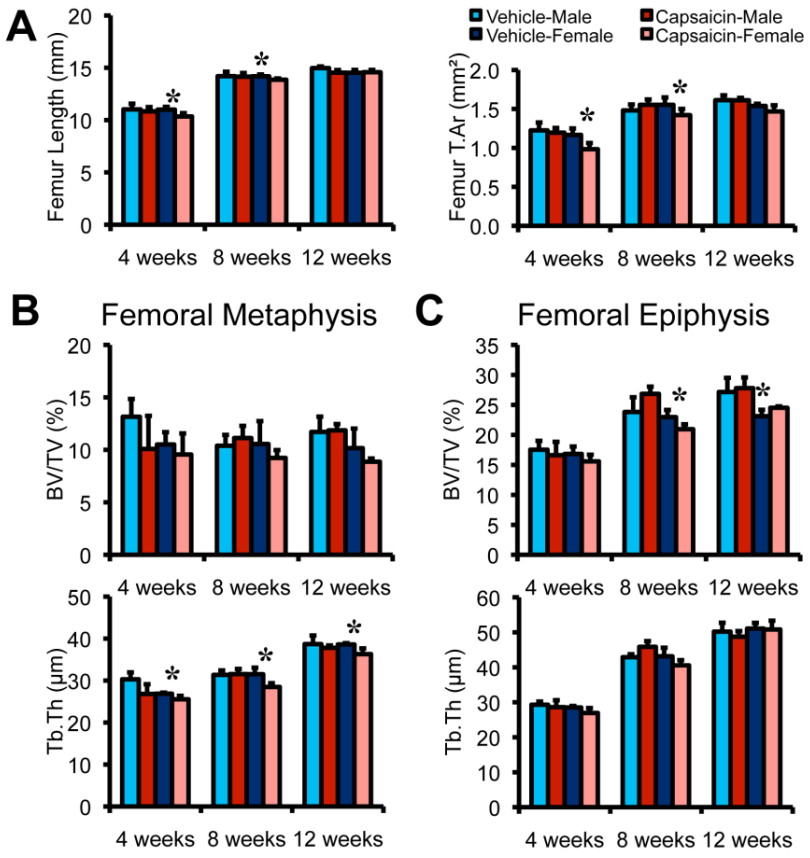

Fig. 6: Micro-computed tomography of femoral cortical and trabecular bone. (A) Femur length and total cross-sectional area (Tt.Ar) of the femoral diaphysis were significantly affected in capsaicin-treated female mice. (B) Capsaicin treatment did not significantly affect trabecular bone volume fraction (BV/TV) at the femoral metaphysis but reduced trabecular thickness (Tb.Th) at this location in female mice. (C) Capsaicin treatment significantly affected BV/TV at the femoral epiphysis in female mice, but did not alter Tb.Th at this location. * Capsaicin vs. vehicle; $p < 0.05$.

We also observed significant effects of capsaicin treatment on cortical bone structure, with significant main effects of capsaicin treatment on femur length, M.Ar, and Tt.Ar (p = 0.0094, 0.026, and 0.026, respectively). For example, femurs from female mice treated with capsaicin were 6.0% and 2.3% shorter than femurs from female vehicle-treated mice at 4 and 8 weeks, respectively (p = 0.034, 0.0097). At 4 weeks, femurs from female capsaicin-treated mice had

15% smaller M.Ar and 16% smaller Tt.Ar compared with vehicle-treated mice ($p = 0.042$, 0.031). Capsaicin treatment also affected cortical bone of the tibia. There were significant treatment*sex interactions for tibia M.Ar and Tt.Ar ($p = 0.025$, 0.0032). At 4 weeks, the tibias from female capsaicin-treated mice had 16% smaller M.Ar and 15% smaller Tt.Ar compared with vehicle-treated mice ($p = 0.022$, 0.029). We did not observe any significant effects of capsaicin treatment on bone mineral density of either trabecular or cortical bone. As expected, sex and age had significant effects for several measured bone structure parameters.

Three-Point bending

Capsaicin treatment significantly decreased the mechanical properties of radii tested with three-point bending. For example, we observed significant main effects of capsaicin treatment on yield force and moment of inertia ($p = 0.047$, 0.0041). At 12 weeks, radii from male treated mice yielded at 13.3% lower force compared with vehicle-treated male mice ($p = 0.022$). Radii of male mice treated with capsaicin had 9.5% lower moment of inertia than vehicle-treated male mice at 12 weeks ($p = 0.028$). However, calculations of yield stress and modulus of elasticity revealed no significant differences between capsaicin- and vehicle-treated mice (Fig. 7). Age was a main effect for all of the mechanical properties measured, while sex was a main effect for yield force and moment of inertia.

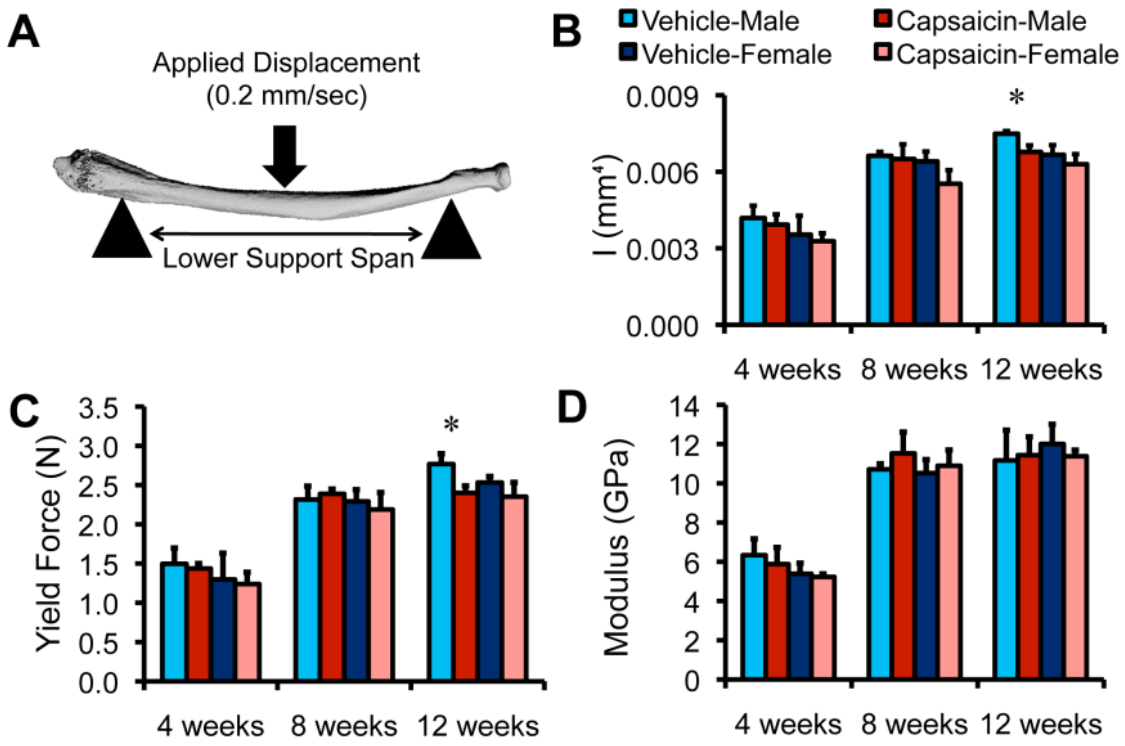

Fig. 7: Mechanical properties of radii determined using three-point bending. A micro-computed tomography reconstruction of a representative radius (A) showing the mechanical testing setup. At 12 weeks of age, the moment of inertia (I) (B) and yield force (C) were significantly lower in capsaicin-treated male mice. However, modulus of elasticity (D) was not significantly different between treated and untreated mice. Age was a main effect for I, yield force and modulus. * Capsaicin vs. vehicle; $p < 0.05$.

Dynamic histomorphometry

Capsaicin treatment significantly altered bone formation parameters in the tibiae of treated mice (Fig. 8). We observed significant treatment*sex*age interactions for MAR and BFR at the endosteal surface ($p = 0.023, 0.020$) and for MAR and MS/BS at the periosteal surface ($p = 0.035, 0.042$). For example, at 4 weeks, female capsaicin-treated mice had 39% higher MAR than female vehicle-treated mice at the endosteal surface of the tibia. At 12 weeks, female mice treated with capsaicin had 23.4% lower MS/BS ($p = 0.012$) and 22.4% lower BFR ($p = 0.061$) at

the periosteal surface than female vehicle-treated mice. Age was a significant main effect for MAR, MS/BS and BFR at the endosteal and periosteal surfaces.

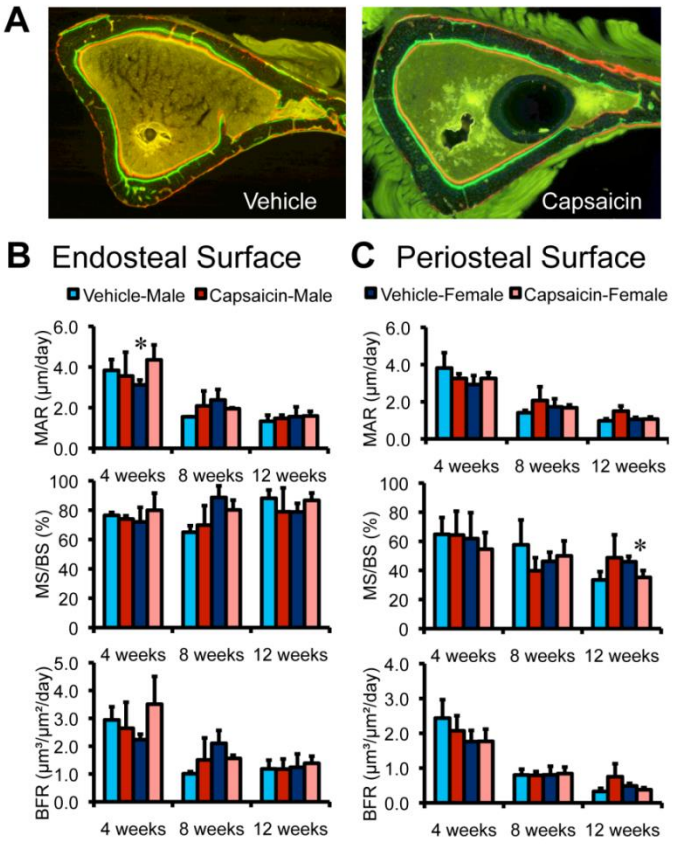

Fig. 8: Dynamic histomorphometry was used to identify changes in bone formation rates in capsaicin- and vehicle-treated mice. Fluorescent images (A) show cortical bone from the tibias of 8 week old female vehicle- and capsaicin-treated mice. Mineral apposition rate (MAR), percent mineralizing surface (MS/BS), and bone formation rate (BFR/BS) were quantified for the endosteal (B) and periosteal surfaces (C). Age was a significant main effect for MAR, MS/BS and BFR at the endosteal and periosteal surfaces. * Capsaicin vs. vehicle; $p < 0.05$.

Serum biomarkers

We did not detect any significant main effects of capsaicin treatment on serum concentrations of CTX-I or P1NP (Fig. 9), although male capsaicin-treated mice at 8 weeks of age had 37% lower CTX-I concentrations than vehicle-treated male mice of the same age ($p = 0.046$). We also observed a significant effect of sex on concentrations of CTX-I ($p = 0.043$), with female mice

exhibiting lower concentrations of CTX-I than male mice. P1NP serum concentrations did not vary significantly by treatment, sex, or age.

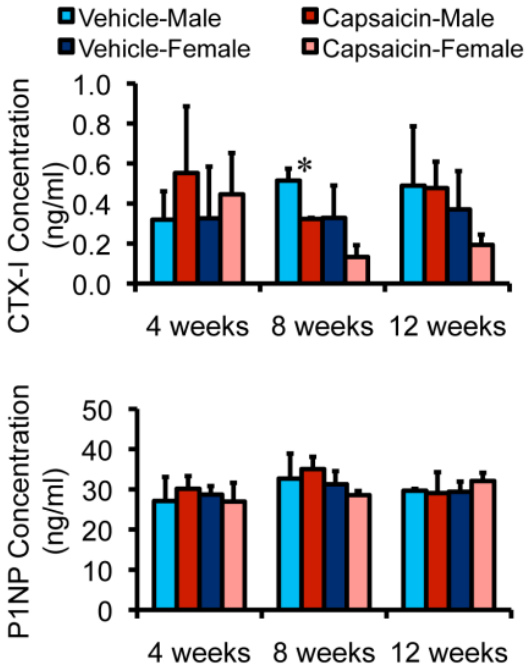

Fig. 9: Serum concentrations of CTX-I or P1NP were not significantly affected by capsaicin treatment, as measured using ELISAs. Sex was a main effect for serum concentrations of CTX-I, while P1NP concentrations did not vary significantly by sex or age. * Capsaicin vs. vehicle; $p < 0.05$.

3.4 Discussion

In this study, we investigated the role of peripheral sensory nerves in bone metabolism during development in mice. We found that neonatal capsaicin treatment in mice led to modest and significant decreases in bone structure parameters, but this effect was inconsistent for mechanical properties and bone turnover rate. Capsaicin treatment had the greatest impact on trabecular bone, with treated mice exhibiting lower trabecular thickness at the femoral metaphysis and L5 vertebral body. However, contrary to our initial hypothesis, mice treated with capsaicin did not exhibit reduced mechanical properties or resistance to fracture. Yield stress and elastic modulus

were similar between treated and untreated mice, suggesting that gross geometrical changes in the radii caused the lower yield force of capsaicin-treated mice. Also in opposition to our hypothesis, capsaicin treatment did not lead to substantial reductions in bone turnover rate, measured by dynamic histomorphometry and serum concentrations of CTX-I and P1NP. Altogether, these data indicate that decreased activity of peripheral sensory nerves has a small effect on the trabecular and cortical bone of mice, but that these changes do not result in a meaningful reduction in mechanical properties of whole bones.

In this study we observed only modest differences in bone parameters in capsaicin-treated mice, despite a considerable and sustained decrease in sensory nerve activity. Physiological adaptations during development may allow mice to compensate for the loss of peripheral nerve function, leading to similar development between treated and untreated mice at 12 weeks of age. It is possible that while bone structure and basal metabolic rates are conserved in capsaicin-treated mice as adults, adaptation of bone in response to mechanical loading or injury may be altered, as observed in other mouse models. For example, in a study of adult female mice lacking estrogen receptor–α, the ulnae were only 4% shorter yet demonstrated a three-fold lower osteogenic response to mechanical loading than the ulnae of wild-type littermates [129]. This is further supported by a previous study using neonatal capsaicin treatment in rats, in which capsaicin treatment did not alter normal bone growth and maintenance, but decreased the local bone remodeling response following molar extraction [120]. Future studies using this model will investigate the bone adaptation of capsaicin-treated mice to conditions such as increased mechanical loading or injury.

The effect of neonatal capsaicin treatment on bone properties had a differential effect on female mice versus male mice, although the power of this study was not sufficient to fully determine sex-based differences. At 4 and 8 weeks, female capsaicin-treated mice demonstrated the largest differences in bone structure, with shorter femurs with smaller cross-sectional area and trabecular thickness. Male capsaicin-treated mice had significantly lower trabecular thickness at the L5 vertebral body for the first time at 12 weeks of age, and lower moment of inertia and yield force of the radii compared to vehicle-treated mice at this time point. These potential sex-based differences may be related to hormonal fluctuations, as mice reach sexual maturity at 8 weeks of age.

The mouse model used in this study overcomes critical limitations of previous models investigating decreased peripheral nerve function in bone. Capsaicin treatment isolates the effects of decreased sensory nerve function without requiring surgical procedures or impairing motor function. Other studies utilizing capsaicin treatment in adult rats found that capsaicin-sensitive neurons contribute to the maintenance of trabecular bone [130]. However, capsaicin directly interacts with bone cells [131, 132], making it difficult to separate the primary effect on bone cells from the secondary effect of decreased peripheral nerve function, as both osteoclasts and osteoblasts express receptors for capsaicin [133, 134]. Treating mice as neonates instead of at maturity allows time for recovery of normal bone metabolism, and therefore isolates the effects of sensory nerve inactivation without the complication of direct action on bone cells inherent in adult treatment.

In this study we were able to detect small but significant differences in trabecular and cortical bone structure, but were unable to detect differences in bone mineral density or bone mechanical properties. This suggests that peripheral nerve inactivation may influence bone quantity, but not bone quality. If this is the case, differences in bone formation or resorption would be expected. However, imprecise methods for detecting bone turnover rates may have limited our observation of changes in capsaicin-treated mice. We were able to detect small changes in bone structure because of the high precision of micro-computed tomography. However, we were unable to detect small differences using lower resolution methods such as dynamic histomorphometry and quantification of serum biomarkers. Both of these techniques were further limited by scope: our histomorphometric analysis was limited to cortical bone, and biomarker concentrations were measured from the serum of developing mice. Similarly, three-point bending of radii may not have had adequate sensitivity to fully capture changes in bone mechanical properties.

This study is limited because it did not directly investigate the effects of capsaicin treatment on sensory neurons in bone. While we verified decreased peripheral sensory nerve function using response to a thermal stimulus, we did not perform a direct quantification in bone, such as counting neurons remaining after treatment or quantification of neuropeptides in bone. It is well established that capsaicin treatment does not affect motor neurons, however it is possible that the reduction in peripheral sensory nerve function could alter spontaneous motor activity in mice. Quantification of activity levels in vehicle- and capsaicin-treated mice could further establish that differences in bone structure are due to decreased sensory nerve function rather than decreased mechanical loading of bone. This study also did not investigate the response of bone to differing levels of sensory nerve inactivation. A more thorough disruption of peripheral sensory

nerve function could have a more dramatic effect on bone metabolism than was observed in this study. Further, in this study we used neonatal capsaicin treatment as a surrogate for age-related degeneration of peripheral nerves, but did not directly make comparisons with aged animals. It is possible that aged mice demonstrate a different pattern of neural degeneration than mice treated with capsaicin as neonates. However, we were able to study the isolated effects of decreased peripheral sensory nerve function in mice up to skeletal maturity.

This study further supports a role for peripheral sensory nerves in bone metabolism. Using neonatal capsaicin treatment, we established a mouse model of decreased peripheral sensory nerve function and observed resulting changes in bone structure. We observed only small changes in bone structure with sensory nerve inactivation, with no notable changes in bone metabolism or bone quality. Therefore age-related changes in sensory innervation may not be clinically meaningful with respect to bone strength under normal loading conditions. It is possible that capsaicin-sensitive neurons may become important for bone under stress conditions such as increased mechanical loading or injury. Future studies will investigate this potential role of peripheral sensory nerves in bone adaptation.

4 Increased Mechanical Loading

4.1 Introduction

Over half of Americans 50 years and older have osteoporosis or low bone mass [135]. With age, there is an imbalance in bone turnover, with bone resorption exceeding formation, resulting in a net loss of bone. The underlying causes of this imbalance in bone remodeling are not fully understood. Innervation of bone provides a potential mechanism for influencing bone metabolism. Micrographs of bone reveal a dense neural network [26, 58] leading to speculation of a role for nerves beyond that of sensation. Many in vitro studies have shown that bone cells have receptors for neuropeptides and that differing concentrations of neuropeptides affect bone cell function [25, 59, 106, 136]. Furthermore, studies of knockout mice have shown that alterations to nerves affect the quantity of bone [56, 65]. These studies suggest that sensory nerves could influence bone metabolism through neuropeptide action on bone cells.

The interaction between nerves and bone can be studied using capsaicin, a natural, irritant compound. Treatment of neonatal mice with capsaicin destroys unmyelinated and small diameter myelinated sensory neurons [72, 88]. This mouse model has been extensively used for studies of itch [123, 124] and pain [92], and may also be useful for investigating the role of peripheral sensory nerves in bone metabolism and bone adaptation. In a previous study, we found that reduction in thermal sensitivity persisted until at least 12 weeks of age in capsaicin-treated mice [137]. However, by 12 weeks of age, capsaicin-treated mice had comparable bone mass to vehicle-treated mice with the exception of reduced trabecular thickness at the distal femoral metaphysis. The small changes observed in bone during development suggest that capsaicin-sensitive neurons may not have a considerable role in bone metabolism under normal loading conditions. However, it is possible that decreased peripheral sensory nerve function may be

important during bone adaptation. In a study with capsaicin-treated rats, investigators found that normal tibial growth was not impaired, but remodeling induced by maxillary molar removal differed between capsaicin-treated and control rats [120]. Similarly, rats with temporary neuronal blocking had a diminished bone adaptation response to ulnar compression [67].

In order to investigate the role of sensory nerves in bone adaptation, we subjected mice treated with capsaicin as neonates to two weeks of tibial compression. Capsaicin- and vehicle-treated mice received tibial compression at loading magnitudes of either 3 N or 7 N. Bone adaptation was quantified using μCT and dynamic histomorphometry analysis of the mouse tibias. We hypothesized that the reduced sensory nerve function in capsaicin-treated mice would impair bone adaptation to mechanical loading.

4.2 Methods

Neonatal capsaicin treatment

A total of 35 female C57BL/6 neonatal mice were used in this study, from 13 timed pregnant females (Harlan Laboratories, Indianapolis, IN). Neonatal capsaicin treatment was performed as previously described [87]. Briefly, neonatal mice were given subcutaneous injections of capsaicin (50 mg/kg) or vehicle (10% ethanol, 10% Tween 80 in isotonic saline) on day 2 and 5 after birth (n = 18 vehicle, 17 capsaicin). Previous studies have shown that this treatment protocol decreases peripheral sensory nerve function for the lifetime of the animal, but motor function is not affected [90]. Following capsaicin or vehicle treatment, neonatal mice were returned to normal cage activity until weaning (28 days). Mice were subjected to tibial

compression starting at 12 weeks of age with magnitudes of either 3 N or 7 N, with a total of 7-10 mice/treatment group/compressive force.

Mechanical loading protocol

The tibial compression loading protocol was similar to that used by others in studies of bone adaptation [138, 139]. The tibial compression system consisted of two custom-built loading platens, positioned vertically within an electromagnetic materials testing machine (Bose ElectroForce 3200, Eden Prairie, MN, USA). The bottom platen held the flexed knee and the top platen positioned the foot. A slight preload (<0.5N) maintained the position of the limb. Mice were anesthetized with isoflurane inhalation while the right lower leg of each mouse was subjected to cyclic axial compressive loading for 1200 cycles per day for a total of 10 days (M-F) over two weeks. For 18 of the mice, the top platen was driven at 5.5 mm/sec until a target compressive load of 3 N was reached. The remaining 17 mice were loaded at 8.5 mm/sec to a target compressive load of 7 N. Both loading rates resulted in an applied load frequency of approximately 4 cycles/second. Left tibias were used as internal controls. Mice were weighed on days 1, 5 and 10 of loading. Mice were sacrificed the third day after completion of two weeks of tibial compression.

Tibial bone strain measurement

A preliminary study was performed to quantify tibial strain in capsaicin- (n = 3) and vehicle-treated mice (n = 4) during axial compression. Immediately after sacrifice, a single element strain gauge (UFLK-1-11-1L, Tokyo Sokki Kenkyujo Co., Ltd., Japan) was bonded to the anteromedial surface of the tibia in alignment with the long axis of the bone. The center of the gauge was

located approximately 5 mm distal to the tibial plateau (Fig. 11A). This location is commonly used for measuring bone strain during tibial compression in mice [139-141] since positioning of the strain gauge is limited by tibia size and morphology. The strain gauge was wired to amplification circuitry and the data acquired in LabView. The lower leg of each mouse was compressed in intervals of 1 N from 1 N to 7 N at a loading rate of 5.5 mm/sec.

Hot-plate analgesia testing

Capsaicin- and vehicle-treated mice were subjected to hot-plate analgesia testing at 12 weeks of age before the start of tibial compression to determine response time to a constant thermal stimulus of 55 °C as previously described [125]. Mice were placed on a hot-plate (LE 7406, Coulborn Instruments, Whitehall, PA) and removed after indication of discomfort, determined as twitching or licking of a hind limb or jumping, or after a maximum of 30 seconds, and the latency time of the response was recorded. Each mouse was tested twice and the latency times were averaged for each mouse.

Micro-computed tomography analysis of bone structure

Bilateral tibias were removed post mortem and preserved in 70% ethanol. Bones were scanned using micro-computed tomography (SCANCO, µCT 35, Brüttisellen, Switzerland); images were acquired at 6 µm nominal voxel size (energy=55 kVp, intensity=114 µA, integration time = 900 ms). Trabecular bone was analyzed at the metaphysis of the tibias using manually drawn contours inside the cortical shell on two-dimensional slices. The metaphysis was defined by a 900 µm thick volume of interest beginning below the middle break of the growth plate. Trabecular bone volume per total volume (BV/TV), trabecular thickness (Tb.Th), and trabecular

number (Tb.N) were determined using the manufacturer's 3-D analysis tools. Cortical bone was analyzed at 10, 20, 30, 40 and 50% of the tibia lengths (a region encompassing peak compressive strain [142] and known cortical bone response [143]; Fig. 10), using 600 μm thick volumes of interest centered at the measured locations. Total cross-sectional area (Tt.Ar), bone area (B.Ar), medullary area (M.Ar), cortical thickness (Ct.Th), and bone mineral content (BMC) were determined using the manufacturer's 3-D analysis tools.

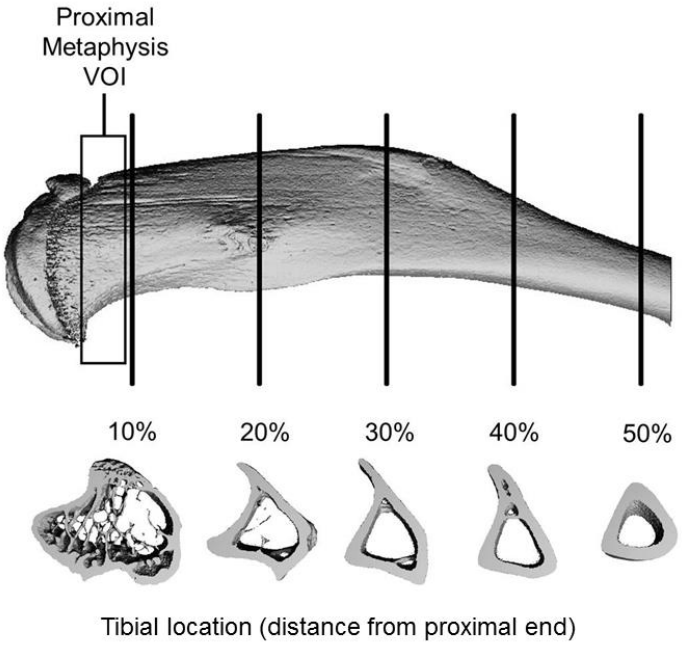

Fig. 10: MicroCT analysis of trabecular bone was performed at the proximal tibial metaphysis. Cortical bone analysis was performed using μCT and dynamic histomorphometry at 5 locations along the length of the tibias.

Dynamic histomorphometry

Mice received injections of calcein green (10 mg/kg; Sigma-Aldrich, St. Louis, MO) and Alizarin-3-methlimino-diacetic acid (30 mg/kg; Sigma-Aldrich, St. Louis, MO) 10 days and 3 days prior to sacrifice, respectively. After scanning with μCT, tibias were embedded in Technovit (Kulzer, Wehrheim, Germany) using standard techniques for undecalcified bone [127]. Sections were cut from each bone on a bandsaw (Model 310, Exakt Technologies,

Norderstedt, Germany) in the transverse plane at 10, 20, 30, 40 and 50% of the tibia length (Fig. 10). Sections were ground to an approximate thickness of 100 μm. Fluorescent images were obtained at 10x magnification (Nikon Eclipse TE2000-E, Tokyo, Japan). Dynamic histomorphometric analysis was performed using commercial software (Bioquant, Nashville, TN). Mineral apposition rate (MAR), percent mineralizing surface (MS/BS), and bone formation rate (BFR/BS) were quantified for the endosteal and periosteal surfaces of cortical bone.

Statistics

Hot-plate data were analyzed using ANOVA stratified by compressive force and treatment (JMP, SAS Institute Inc., Cary, NC). Between-group differences were analyzed using a Tukey HSD post hoc test. To account for the repeated measures nature of the study, μCT and histomorphometry data were analyzed separately using mixed effects models with factors for treatment (capsaicin or vehicle), leg (contralateral or loaded), volume of interest (10-50% of tibia length) and interactions. Between-group differences were analyzed using post hoc tests when the factor was significant and the model had an adjusted R squared greater than 0.9. Significance was defined as $p<0.05$.

4.3 Results

Animal body mass

Tibial compression was well tolerated by all animals. Both capsaicin- and vehicle-treated mice had similar body weight on loading day 1, and changes in body weight were similar between treatment groups. Average weight loss between loading days 1 and 10 was 5.6% of body weight for each compressive force.

Tibial bone strain measurement

Bone strain measured on the anteromedial surface of the tibia was not different for capsaicin- and vehicle-treated mice for compressive forces of 1-7 N (Fig. 11B). Therefore, all mice were loaded to the same target force of 3 N or 7 N for the investigation of bone adaptation.

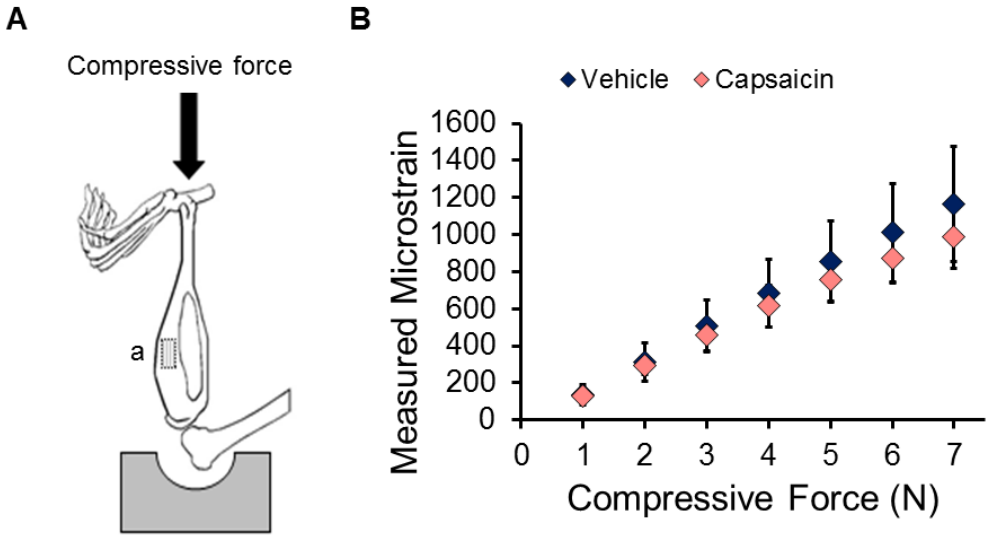

Fig. 11: Maximum bone strain during tibial compression was measured at the anteromedial surface of tibias. (A) A diagrammatic representation shows the approximate location of the strain gauge (a). (B) Maximum bone strain measured during tibial compression at compressive magnitudes from 1-7 N. There was not a significant difference in measured strain between capsaicin- and vehicle-treated mice at any of the compressive forces tested.

Hot-plate analgesia testing

At 12 weeks of age, capsaicin-treated mice took 55% longer to respond to the thermal stimulus than vehicle-treated mice, consistent with reduced peripheral sensory nerve function resulting from neonatal capsaicin treatment. Mice treated with capsaicin had comparable latency times before 3 N or 7 N tibial compression (Fig. 12). Similarly, there was not a significant difference between the latency times of vehicle-treated mice subjected to the different compressive forces.

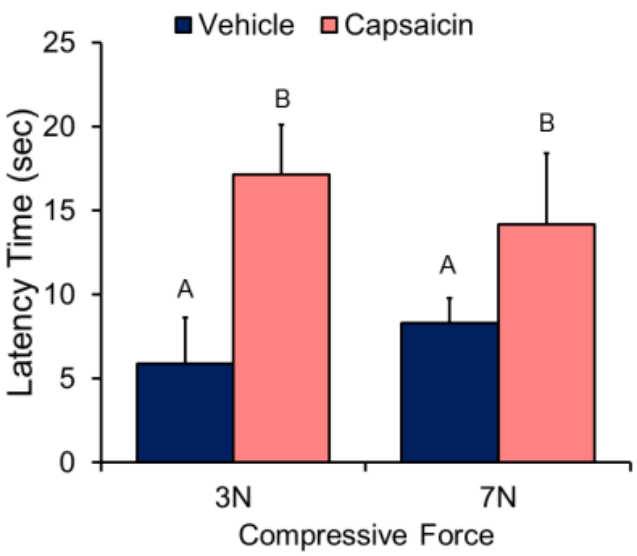

Fig. 12: Hot-plate analgesia testing of vehicle- and capsaicin-treated mice was performed at 12 weeks of age to verify decreased peripheral sensory nerve function prior to tibial compression. Capsaicin-treated mice exhibited significantly longer latency times than vehicle-treated mice in both compressive force groups when exposed to a constant 55° C thermal stimulus, indicating decreased thermal sensitivity. Groups not connected by the same letter are significantly different ($p < 0.05$).

Micro-computed tomography

MicroCT analysis revealed that mechanical loading did not affect trabecular bone volume fraction (BV/TV) of the tibial metaphysis, although the microstructure of trabecular bone was slightly altered. For example, loaded and contralateral tibias displayed a similar BV/TV at each compressive force (Table 1). However, loaded tibias had greater trabecular thickness and reduced trabecular number relative to contralateral tibias, although these trends were not statistically significant.

Table 1: Trabecular bone parameters assessed at the tibial metaphysis using microCT

Treatment Group	BV/TV		Tb.Th		Tb.N	
	Control	Loaded	Control	Loaded	Control	Loaded
3N compressive force						
Vehicle	0.107±0.013	0.110±0.011	0.0440±0.0016	0.0451±0.0022	4.28±0.244	4.25±0.164
Capsaicin	0.105±0.007	0.108±0.003	0.0421±0.0017	0.0422±0.0020	4.35±0.163	4.40±0.135
7N compressive force						
Vehicle	0.119±0.011	0.112±0.014	0.0449±0.0028	0.0503±0.0029	4.20±0.242	3.89±0.223
Capsaicin	0.127±0.008	0.129±0.017	0.0430±0.0014	0.0471±0.0031	4.51±0.280	4.30±0.351

Data reported as mean±SD.

Tibial compression significantly affected cortical bone of loaded tibias, with adaptation dependent on compressive force and location along the tibia (Fig. 13, Table 2). Compression at 7 N generated a larger cortical bone response than 3 N compression. For example, at 10% of the tibia length, Tt.Ar increased 16% at 7 N compared to 3.3% at the lower compressive force. In addition, BMC increased only 1.5% in tibias loaded at 3 N, while the increase was six times higher in tibias loaded at 7 N. Location along the tibia also significantly affected the adaptive response of cortical bone. The largest changes were observed at 10% of the tibia length, whereas bone at 30% often displayed insignificant changes. The increase in Tt.Ar at 10% was accompanied by a 14% increase in M.Ar at the 7 N force. At 20%, the increase in M.Ar was reduced to 8.2%. Changes in Ct.Th also varied by location, with loaded tibias becoming thinner at 10% and thicker at 50% of their length. Often, capsaicin- and vehicle-treated mice displayed similar trends in adaptation to increased loading. However, tibias of capsaicin-treated mice demonstrated greater changes at some locations. For example, at 20%, capsaicin-treated mice had an 8.8% increase in Tt.Ar, while vehicle-treated mice showed no significant change.

Furthermore, the increase in BMC at 10% was almost two fold higher for capsaicin-treated mice compared to vehicle-treated mice.

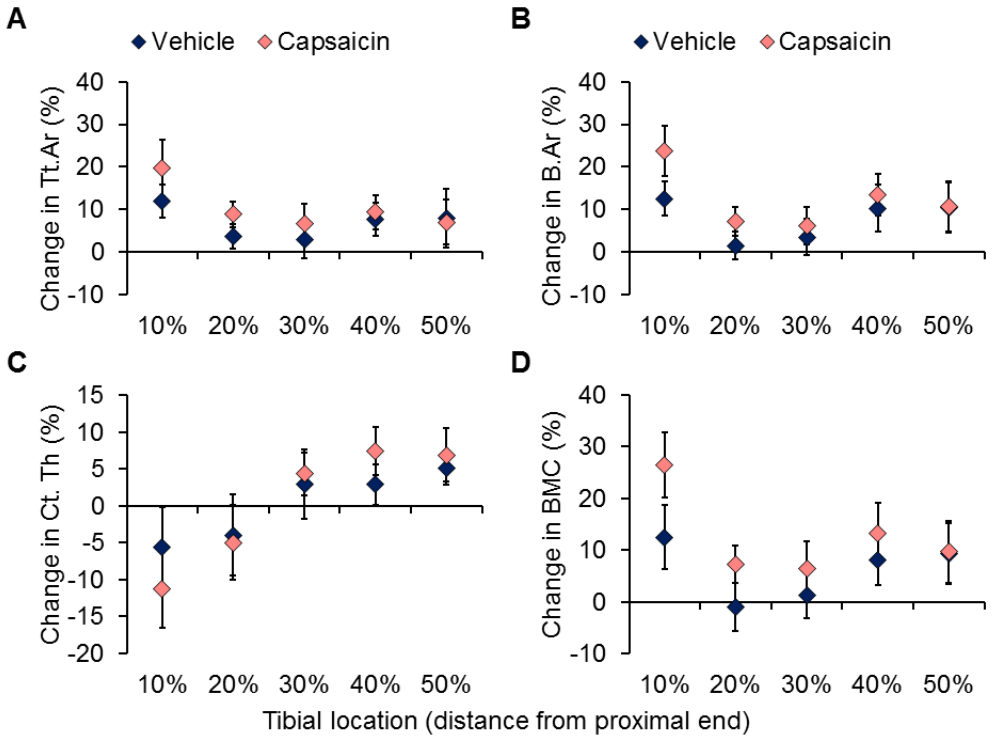

Fig. 13: Micro-computed tomography identified changes in cortical bone along the length of the tibias after two weeks of 7 N tibial compression. Diamonds represent the average change of loaded compared to control tibias with error bars indicating standard deviation. (A) Total cross-sectional area (Tt.Ar) was significantly increased in loaded tibias at all locations except 30%. (B) Changes in bone area (B.Ar) mirrored changes in Tt.Ar. (C) Cortical thickness (Ct.Th) decreased at more proximal locations along the tibia. (D) Bone mineral content (BMC) was significantly altered by tibial compression and varied by location on the tibia.

Table 2: Cortical bone parameters assessed along control and loaded tibias using microCT

Tibial Location	Treatment Group	Total area[a,b,c] (mm²)		Medullary area[a] (mm²)		Bone mineral content[a,b] (mgHA)	
		Control	Loaded	Control	Loaded	Control	Loaded
3N compressive force							
10%	Vehicle	2.82±0.18	2.97±0.28	1.91±0.17	2.02±0.24	0.60±0.03	0.63±0.04
	Capsaicin	2.65±0.15	2.67±0.16	1.79±0.13	1.80±0.11	0.60±0.04	0.57±0.05
20%	Vehicle	1.67±0.14	1.70±0.11	0.84±0.12	0.85±0.02	0.53±0.02	0.55±0.03
	Capsaicin	1.57±0.06	1.56±0.05	0.78±0.05	0.77±0.04	0.50±0.02	0.51±0.02
30%	Vehicle	1.40±0.09	1.39±0.06	0.66±0.06	0.65±0.05	0.49±0.03	0.49±0.02
	Capsaicin	1.31±0.04	1.30±0.05	0.61±0.02	0.61±0.03	0.46±0.02	0.46±0.02
40%	Vehicle	1.22±0.08	1.22±0.06	0.54±0.04	0.54±0.03	0.45±0.03	0.46±0.02
	Capsaicin	1.15±0.06	1.15±0.05	0.51±0.03	0.50±0.02	0.43±0.02	0.43±0.02
50%	Vehicle	0.94±0.05	0.92±0.06	0.37±0.03	0.36±0.04	0.40±0.02	0.39±0.02
	Capsaicin	0.89±0.06	0.87±0.04	0.35±0.03	0.34±0.03	0.37±0.02	0.37±0.02
7N compressive force							
10%	Vehicle	3.04±0.10	3.41±0.14*	2.03±0.09	2.27±0.12	0.65±0.03	0.73±0.04*
	Capsaicin	2.79±0.18	3.33±0.12*	1.85±0.13	2.17±0.10	0.60±0.04	0.75±0.04**
20%	Vehicle	1.81±0.07	1.87±0.08	0.90±0.07	0.96±0.06	0.58±0.03	0.57±0.02
	Capsaicin	1.67±0.06	1.82±0.06*	0.81±0.04	0.90±0.06	0.54±0.03	0.58±0.02
30%	Vehicle	1.52±0.04	1.57±0.06	0.72±0.04	0.74±0.04	0.53±0.02	0.54±0.02
	Capsaicin	1.42±0.09	1.51±0.05	0.64±0.05	0.68±0.04	0.51±0.03	0.54±0.01
40%	Vehicle	1.30±0.04	1.40±0.05	0.58±0.03	0.61±0.03	0.49±0.02	0.53±0.03*
	Capsaicin	1.22±0.06	1.33±0.06	0.52±0.03	0.54±0.03	0.47±0.03	0.53±0.03*
50%	Vehicle	1.00±0.03	1.08±0.06	0.39±0.02	0.41±0.03	0.43±0.01	0.47±0.03*
	Capsaicin	0.95±0.06	1.01±0.05	0.36±0.03	0.37±0.03	0.41±0.02	0.45±0.02

Data reported as mean±SD.
[a]: significant leg*VOI interaction, 7N compressive force
[b]: significant treatment*leg*VOI interaction, 7N compressive force
[c]: significant leg*VOI interaction, 3N compressive force
*: significant difference between control and loaded, $p<0.05$
**:significant difference between capsaicin and vehicle response, $p<0.05$

Dynamic histomorphometry

Dynamic histomorphometric analysis revealed that 7 N tibial compression altered bone formation parameters on the endosteal and periosteal surfaces of loaded tibias (Table 3). In general, bone formation increased on the periosteal surface of the tibias and decreased on the endosteal surface at locations closest to the proximal metaphysis. There was a significant effect of treatment on the response of MAR to increased loading, with capsaicin-treated mice displaying a larger response compared to vehicle-treated mice at many tibial locations (Fig. 14). For example, at 20% of the tibia length, the loaded tibias of capsaicin-treated mice had an average decrease in MAR of 37% compared to a 24% decrease in MAR in vehicle-treated mice. While MAR was lower in loaded tibias compared to controls at 10, 20 and 30% of the tibia length on the endosteal surface, MAR was increased at all measured locations on the periosteal surface. At 20%, capsaicin-treated mice again demonstrated a larger response to increased loading with an approximately 2.5 times larger increase in MAR than vehicle-treated mice on the periosteal surface. There was a significant effect of loading on MS/BS that varied with location along the tibia. However, treatment was not a factor in the response of MS/BS on the periosteal surface. Loading also caused a significant increase in BFR at all locations on the periosteal surface, with a significantly greater response in capsaicin-treated mice at 20% of the tibia length. Tibial compression at 3 N caused a significant decrease in MAR on the endosteal surface at 10 and 20%, but the effect did not differ between treatment groups. Furthermore, the lower magnitude compression did not significantly affect MS/BS or BFR on either surface of the loaded tibias.

Table 3: Bone formation parameters for 7 N compression assessed using dynamic histomorphometry

Tibial Location	Treatment Group	MAR[a,b] (μm/day)		MS/BS[a,b] (%)		BFR[a,b] (μm³/μm²/day)	
		Control	Loaded	Control	Loaded	Control	Loaded
Endosteal Surface							
10%	Vehicle	2.05±0.03	1.62±0.01*	62±1	53±5*	1.28±0.03	0.85±0.08*
	Capsaicin	1.96±0.04	1.71±0.02**	65±2	50±3*	1.27±0.05	0.85±0.05*
20%	Vehicle	1.30±0.01	0.98±0.03*	51±3	30±3*	0.66±0.03	0.30±0.03*
	Capsaicin	1.59±0.05	0.99±0.03**	49±5	26±3*	0.77±0.07	0.25±0.03*
30%	Vehicle	1.11±0.01	0.97±0.02*	53±8	40±2*	0.59±0.09	0.39±0.03*
	Capsaicin	1.25±0.02	0.85±0.03**	51±4	36±2*	0.64±0.05	0.31±0.03*
40%	Vehicle	1.07±0.02	1.07±0.02	49±6	39±1*	0.53±0.07	0.41±0.02*
	Capsaicin	0.79±0.03	0.98±0.03*	38±2	33±4	0.30±0.02	0.33±0.04
50%	Vehicle	1.01±0.03	1.11±0.02*	36±6	37±4	0.37±0.06	0.41±0.04
	Capsaicin	0.66±0.02	0.90±0.09**	26±2	37±6*	0.17±0.01	0.33±0.08*

		MAR[a,b] (μm/day)		MS/BS[a] (%)		BFR[a,b] (μm³/μm²/day)	
		Control	Loaded	Control	Loaded	Control	Loaded
Periosteal Surface							
10%	Vehicle	0.91±0.01	1.82±0.02*	10±1	29±3	0.09±0.01	0.52±0.05*
	Capsaicin	1.02±0.02	2.09±0.03*	12±0	33±2	0.13±0.01	0.70±0.05**
20%	Vehicle	1.53±0.02	1.95±0.02*	19±2	43±4	0.29±0.03	0.85±0.08*
	Capsaicin	1.06±0.02	1.77±0.02**	15±1	47±3	0.16±0.01	0.82±0.05**
30%	Vehicle	0.75±0.03	1.11±0.02*	10±1	41±2	0.07±0.01	0.46±0.02*
	Capsaicin	0.82±0.03	1.29±0.03*	10±1	44±7	0.09±0.01	0.56±0.09*
40%	Vehicle	0.87±0.02	1.49±0.02*	11±1	52±5	0.10±0.01	0.77±0.08*
	Capsaicin	0.82±0.04	1.39±0.10*	14±1	53±8	0.11±0.01	0.74±0.14*
50%	Vehicle	0.77±0.02	1.11±0.04*	14±4	52±5	0.11±0.03	0.58±0.07*
	Capsaicin	0.55±0.03	1.14±0.03**	17±1	60±11	0.09±0.01	0.69±0.13*

Data reported as mean±SD.
[a]: significant leg*VOI interaction, 7N compressive force
[b]: significant treatment*leg*VOI interaction, 7N compressive force
*: significant difference between control and loaded, $p<0.05$
**:significant difference between capsaicin and vehicle response, $p<0.05$

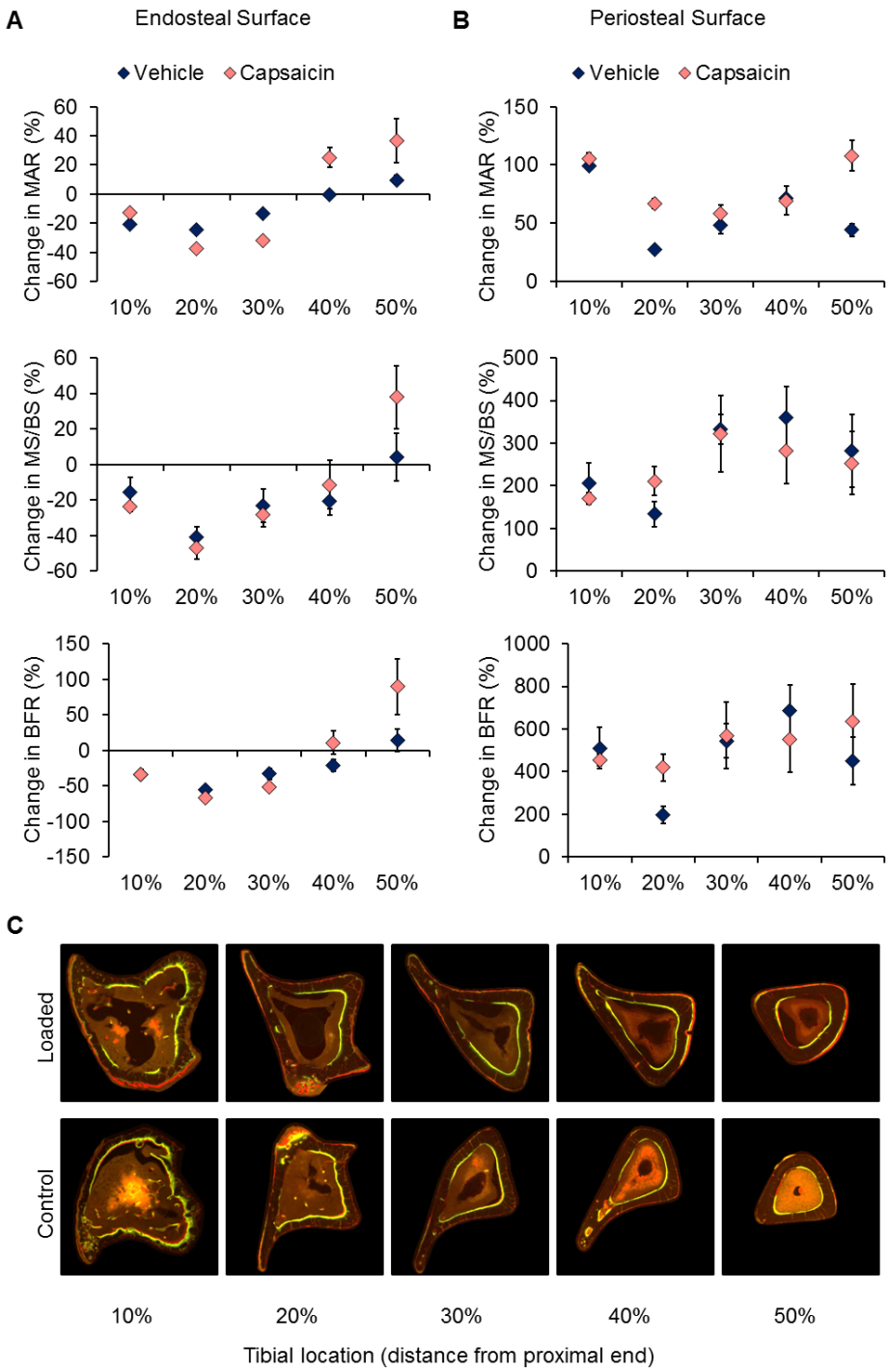

Fig. 14: Dynamic histomorphometry was used to identify changes in bone formation rate after 7 N tibial compression in capsaicin- and vehicle-treated mice. Mineral apposition rate (MAR), percent mineralizing surface (MS/BS) and bone formation rate (BFR) were quantified for the endosteal (**A**) and periosteal surfaces (**B**). Fluorescent images (**C**) show cortical bone from the control and loaded tibias of a vehicle-treated mouse.

4.4 Discussion

The purpose of this study was to investigate the role of sensory nerves in adaptation of bone to increased mechanical loading. Tibial compression, particularly at 7 N magnitude, caused an increase in cortical bone area in the loaded tibia, accompanied by changes in bone formation parameters. This adaptive response was dependent on location along the tibia, and was generally greater in capsaicin-treated mice than in vehicle-treated mice. The increased response in capsaicin-treated mice conflicts with our initial hypothesis that reduced sensory nerve function would impair the adaptation of bone to increased loading.

This study was performed at two different compressive loads, producing two different strain magnitudes on loaded tibias. Two weeks of 3 N tibial compression generated only a modest response in cortical bone assessed with μCT, and no significant changes in bone formation measured by dynamic histomorphometry. Similarly, Fritton et al. observed a 1.4% increase in whole bone mineralized tissue volume when using this compressive force, which increased to 3.4% when the loading was conducted for an additional 4 weeks [138]. Although these researchers were able to detect an increase in BMC at 10% of the tibia, we were only able to observe changes at the 7 N compressive force. Tibial compression at 7 N (approximately 28x body weight) caused a greater change in cortical bone than the lower compressive force. Interestingly, we did not observe significant changes in trabecular bone that others have reported in studies of bone adaptation [138, 139, 144]. The small magnitude of the changes in bone structure may be a result of differences in tibial compression systems. For example, we have found that higher compressive forces using our configuration may lead to knee injury and subsequent trabecular bone loss [145]. A group using a similar configuration observed a 20%

loss in BV/TV at the proximal metaphysis in tibias loaded to 8 N [144]. Another group using a different configuration for tibial compression found an increase of 44.5% in BV/TV in tibias loaded to a target compressive force of 13.5 N [143].

Location on the tibia influenced the bone adaptive response, consistent with the morphology of the mouse tibia resulting in different strain patterns along its length [141, 142]. We observed the largest changes in Tt.Ar and BMC at 10% of the tibia length, where others have reported the largest compressive magnitude [142]. The shift we observed in bone formation parameters at 30% could be a result of a shift in strain from compression to tension. Tibia surface also factored into the adaptation results, with the endosteal surface of loaded tibias displaying a decrease in BFR at 10-30% compared to control tibias. This is consistent with the observation of increased Tt.Ar and M.Ar from μCT. Tibial compression caused outward expansion of the cortex, with increased bone formation on the periosteal surface and decreased bone formation on the endosteal surface, which may help the tibia adapt to the demands of greater compression [146].

The changes we observed in cortical bone assessed with μCT are consistent with changes in bone formation parameters assessed with dynamic histomorphometry. The increase in Tt.Ar and BMC at 10% of the tibia length were attended by a large increase in MAR and BFR on the periosteal surface. A similar trend occurred at 50% of the tibia length. Although the percent changes in BFR on the periosteal surface appear large, the control values are some of the lowest of either surface. Therefore a 500% increase in BFR on the periosteal surface results in a value less than the reduced BFR on the endosteal surface. Also, the increase in BFR on the periosteal surface

and decrease on the endosteal surface could account for the modest increase in Tt.Ar at 10% of the tibia length.

Contrary to our initial hypothesis, capsaicin treatment caused greater changes in parameters such as Tt.Ar, BMC and MAR in response to increased loading. A possible explanation for this observation is that neuropeptide concentrations are antagonistic to the actions of bone cells during adaptation in vivo. In a study of ulnar compression in rats, researchers found that increases in bone area were accompanied by decreases in bone concentrations of CGRP [67]. As CGRP has an anabolic effect on osteoblasts, the reduction from baseline in response to loading appears to work against the bone forming action of osteoblasts. Similarly, another study found that hindlimb casting in rats caused elevated CGRP concentrations in the sciatic nerve [69]. The bone loss associated with immobilization may be antagonized by increased concentrations of this neuropeptide. By reducing nerve function with capsaicin treatment, we may be limiting the antagonistic role of neuropeptides in bone adaptation, allowing a greater response to loading.

This investigation of the role of sensory nerves on bone adaptation is limited by the fact that we did not directly quantify the effect of capsaicin treatment on nerve function or neuropeptide concentrations in bone. Instead, we measured a functional outcome, the response of treated mice to a thermal stimulus. Others have evaluated the chemosensitivity of the cornea to assess sensory denervation resulting from neonatal capsaicin treatment [92, 124]. A study of capsaicin treatment in adult rats showed that unmyelinated sensory axons were destroyed and neuropeptide concentrations reduced in the tibia [130]. The effect of sensory nerves on bone may be limited to a local interaction, with neuropeptide concentrations affecting bone metabolism. While

capsaicin-treated mice demonstrated reduced thermal sensitivity at the periphery, they may have developed a compensatory mechanism in bone.

5 Neuropeptide Concentration

5.1 Introduction

The initial rapid loss of bone following spinal cord injury suggests that factors other than disuse osteoporosis may be at work [59]. Indeed, electrical stimulation of muscle does not restore bone mass post trauma [147]. Similarly, unilateral sciatic nerve transection causes bone loss not only in the denervated limb, but in the contralateral limb as well – even when use remains unchanged [52]. A reduction in neuropeptide concentration accompanies the osteoporosis, and an antagonist for the neuropeptide receptor further increases bone loss. These findings indicate that peripheral nerves may be important for bone adaptation. With a presence in the periosteum and medullary canal of long bones, sensory neurons provide a potential mechanism for regulating bone cells through the action of neuropeptides.

Calcitonin gene related peptide (CGRP) and substance P are two of the main neuropeptides found in the sensory nerves innervating bone. CGRP is a 37 amino acid peptide produced from alternative splicing of the calcitonin gene. Nerves containing CGRP appear in proximity to bone lining and precursor cells in the periosteum. CGRP containing nerves are also found near the epiphyseal plate, in bone marrow, and around blood vessels in Volkmann's canals. Near epiphyseal trabecular bone, CGRP fibers terminate in free endings near osteoblasts and osteoclasts, which both express receptors for the neuropeptide [33]. Osteoblasts respond to CGRP with an increase in intracellular cAMP and corresponding changes in cell morphology and function [136]. The neuropeptide also affects osteoclasts, inhibiting their function and the recruitment of macrophages into osteoclast-like cells. In vivo, administration of high doses of CGRP inhibits bone resorption and lowers serum concentrations of calcium [21]. CGRP neurons in bone are more numerous than substance P containing ones, although the 11 amino acid peptide

plays an important role. The traditional role of substance P is transmission of pain signals in nociceptive afferents. Nerves containing substance P are found in the periosteum of long bones and in the bone marrow next to blood vessels, where they separate and terminate in free endings. Osteoblasts express the substance P receptor neurokinin-1 and exposure to substance P increases osteoblast function in vitro [50]. Osteoclasts also have receptors for substance P and exposure in vitro stimulates calcium influx and bone resorption [51]. Both CGRP and substance P often appear together in the small sensory neurons, including Aδ and C fibers. CGRP may facilitate substance P release and enhance activation [53]. Addition of CGRP to an intrathecal injection of substance P in rats, causes caudally directed biting to extend from a few minutes to up to forty minutes [54].

The presence of these neuropeptides in peripheral sensory nerves suggests that they could be important when the target tissue experiences local mechanical alterations. When investigators created a bony defect in the rat tibia, the density of CGRP containing fibers increased near blood vessels and in accompaniment to callus formation [41]. Cyclic ulnar compression caused a decrease in bone CGRP and substance P concentrations from one hour to 10 days after the single round of the increased loading [67]. In an example of unloading, both CGRP and substance P levels were increased in the sciatic nerve after 4 weeks of cast immobilization [69]. These findings provide evidence for a role of neuropeptides in the regulation of local bone cell function.

In order to investigate whether neuropeptide concentrations alter in response to the mechanical environment of their target tissue, we used two different loading protocols. A well-established

model of non-invasive loading [145], we used tibial compression to model increased mechanical loading of the limb. To simulate decreased mechanical stimulation, we subjected mice to tail suspension. For both loading protocols, we examined two different time points to determine the constancy of modified neuropeptide levels in bone. We hypothesized that both neuropeptides would be elevated after tibial compression because of their expected anabolic effect on bone and likewise diminished by hindlimb unloading.

5.2 Methods

Animals

A total of 32 female C57BL/6 mice were used in this study (Harlan Laboratories, Indianapolis, IN). Mice were allowed to acclimate to the housing facility for two weeks prior to the beginning of the experimental protocol. Mice were housed 4 to a cage and allowed food and water ad libitum. Mice were subjected to a mechanical stimulus of tibial compression or hindlimb unloading starting at 12 weeks of age for 1 or 5 days, with a total of 8 mice/stimulus/stimulus duration.

Mechanical loading protocol

The tibial compression loading protocol was similar to that used by others in studies of bone adaptation [138, 139]. The tibial compression system consisted of two custom-built loading platens, positioned vertically within an electromagnetic materials testing machine (Bose ElectroForce 3200, Eden Prairie, MN, USA). The bottom platen held the flexed knee and the top platen positioned the foot. A slight preload (<0.5N) maintained the position of the limb. Mice were anesthetized with isoflurane inhalation while the right lower leg of each mouse was subjected to cyclic axial compressive loading for 1200 cycles per day for a total of 1 day (mice

were sacrificed within an hour of the second bout of loading) or 5 days (mice were sacrificed within an hour of the fifth bout of loading). The top platen was driven at 5.5 mm/sec until a target compressive load of 5 N was reached. The loading rate resulted in an applied load frequency of approximately 4 cycles per second. Left tibias were used as controls. Mice were weighed on each day of loading and sacrificed within an hour after 1 or 5 days of tibial compression.

Hindlimb unloading protocol

To model decreased mechanical loading, mice were tail-suspended as previously described [148]. Mice were housed individually and suspended at a head-down angle of 30° so that the hindlimbs were not able to touch the cage floor. The tail was secured to a metal apparatus hung from a bar on the ceiling of the cage, permitting movement throughout the cage and rotation of 360°. Metal grid flooring was used to facilitate mouse movement. Mice were provided with Enviro-dri and/or Nestlets for environmental enrichment. Water and food were available throughout the experimental period. Mice were monitored daily for signs of distress resulting from the tail suspension protocol. Mice were suspended for either 1 day (24 hours) or 5 days (120 hours).

ELISAs of bone neuropeptides

Tibias were collected from mice immediately after sacrifice for quantification of whole bone concentrations of sensory neuropeptides. Mice were sacrificed and their tibias removed for analysis. Left tibias were transferred to vials of paraformaldehyde for later histological analysis. Right tibias were flash frozen in liquid nitrogen, and transferred to a -80 °C freezer until protein

isolation. Frozen whole bones were cut in half and homogenized in Trizol for isolation. Protein was analyzed in duplicate to determine the concentrations of calcitonin gene related peptide and substance P using commercial mouse-specific ELISAs (Cusabio, Wuhan, China) per the manufacturer's instructions. Data were normalized to total protein concentration to account for variation in extraction efficiency.

Statistics

Body weight data were analyzed using a repeated measures approach with factors for stimulus day, type of stimulus and the interaction (JMP, SAS Institute Inc., Cary, NC). Between-group differences were analyzed using a Student's t-test. ELISA data for each neuropeptide were analyzed using two-way ANOVA stratified by stimulus protocol, stimulus duration and the interaction. Between-group differences were analyzed using an appropriate post hoc test. Data are reported as mean ± SD. Significance was defined as $p<0.05$.

5.3 Results

Mouse body weights

Most mice tolerated the different mechanical loading conditions reasonably well. There was a significant effect of stimulus day ($p = 0.03$), type of stimulus ($p = 0.009$), and the interaction ($p = 0.0003$) on body weight. There was not a difference in body weight between mice assigned to the different loading protocols on the first day of the experiment (Fig. 15). Overall, there was a decrease in body weight from the first day of the loading stimulus when mice were 12 weeks of age, to the fifth day at sacrifice. The average 3% increase in body weight of mice subjected to tibial compression was overshadowed by weight loss in the hindlimb unloaded mice. Aside from

licking the junction between the suspension apparatus and their tail, mice showed no obvious signs of obvious distress during daily monitoring. However, mice lost an average of 9% of body weight from tail suspension, with one mouse losing 4.9 g during the experimental period.

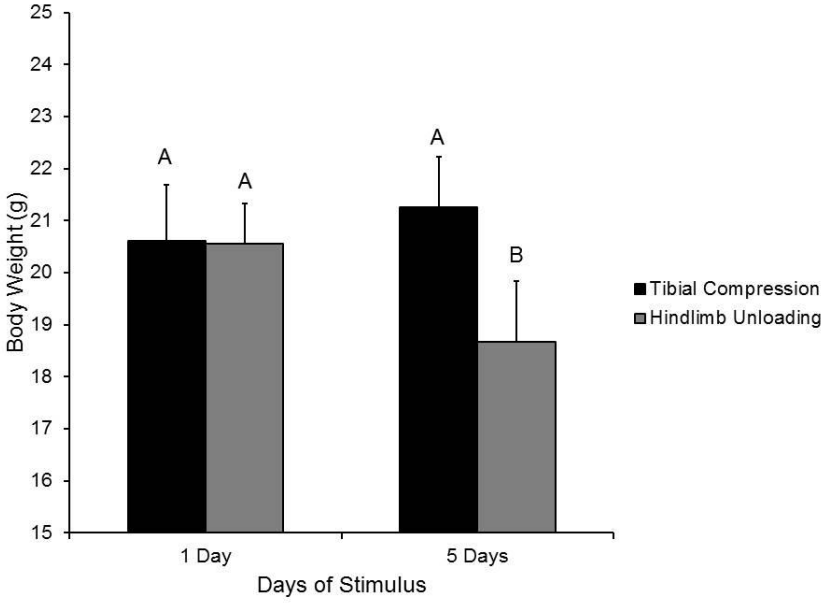

Fig. 15: Body weights of mice subjected to 5 days of either tibial compression or hindlimb unloading.

ELISAs of bone neuropeptides

Concentrations of CGRP in bone were altered by the different mechanical environments (Fig. 16). The concentration of CGRP in the tibias was significantly lower after 5 days of stimulus than after a single day ($p = 0.0005$). Including both tibial compression and hindlimb unloading, the CGRP concentration was 35% lower after 5 days than after 1 day of stimulus. The type of loading stimulus also significantly affected CGRP concentration ($p = 0.0038$). While unloaded limbs were not significantly different from control ones, tibial compression caused a significant increase in CGRP concentration. Tibial compression raised CGRP concentration 66% compared to controls. After one day of tibial compression, the average CGRP concentration was 128 pg/mg protein compared to 71.5 pg/mg protein in controls. When applied for the longer duration of 5 days, CGRP concentration did not differ significantly from control tibias.

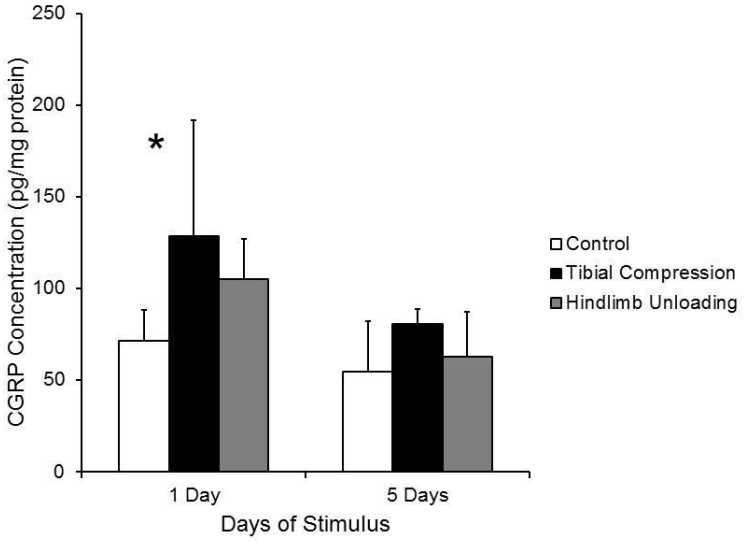

Fig. 16: CGRP concentration in the bones of mice subjected to tibial compression or hindlimb unloading to model altered mechanical conditions.

Concentrations of substance P were over 8 times lower than CGRP levels in the tibias. The effects of the altered mechanical conditions also changed trends in neuropeptide concentration. Although tibial compression increased CGRP concentration, average substance P levels decreased in response to this mechanical stimulus. The duration of altered loading did not significantly affect substance P concentration, and the different experimental groups had similar levels between stimulus days (Fig. 17). However, the type of stimulus had a significant effect on substance P bone concentration ($p = 0.047$). Irrespective of duration of stimulus, substance P concentration in hindlimb unloaded tibias was 37% higher than tibias subjected to the increased mechanical loading.

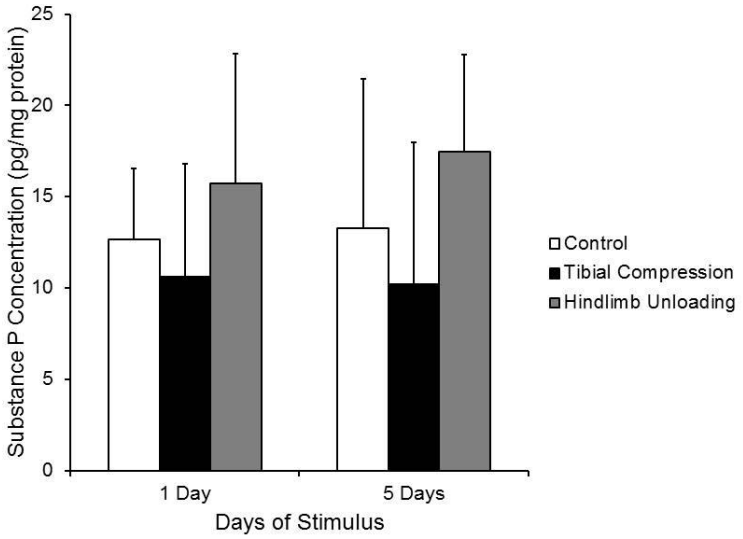

Fig. 17: Substance P concentration in the bones of mice subjected to tibial compression or hindlimb unloading to model altered mechanical conditions.

5.4 Discussion

Bones contain a dense network of sensory nerves enclosing neuropeptides known to affect bone cell function. We proposed that in addition to a role in normal bone, neuropeptides contribute to bone adaptation in altered mechanical environments. We hypothesized that bone CGRP concentration would increase in response to tibial compression, a known stimulator of bone growth. Our results were in agreement with this hypothesis, as mechanically loaded tibias demonstrated a significantly higher CGRP concentration than control ones. However, the tibias of mice subjected to tail suspension also exhibited a trend towards increased CGRP concentration, despite the unloaded environment. These findings indicate that in the complex in vivo environment, the neuropeptide may a have a different function than that suggested by the anabolic response of cultured osteoblasts. Also contrary to our hypothesis, average substance P

concentration decreased in cyclically compressed tibias and increased in unloaded bones. In all cases, the changes in neuropeptide concentration were more dramatic after a single day of applied stimulus than after 5 days. The early response might imply that neuropeptides are more important to the initial recognition of bone to an applied stimulus, and less important as the bone cells acclimate.

The results of our investigation into bone neuropeptide concentration mostly agree with previous findings from other labs. Our observed increase in bone CGRP concentration following tibial compression provides the notable exception. However, there were several differences between this work and the experiments showing a decrease in bone CGRP in response to cyclic compression. The most obvious difference was in the limb subjected to compression, with the use of an ulna rather than tibia. Also dissimilarly, we did not use an analgesic and used a lower compressive force. However, both studies found a decrease in substance P within an hour of increased loading. A possible explanation for the increase is that the osteoclastic stimulating function of substance P outweighs its anabolic function. We would expect increased loading to increase bone mass, and suppression of the resorbing effect of this neuropeptide would contribute to that end. Likewise, we would expect hindlimb unloading to decrease bone mass in the tibia and in agreement with other groups, substance P concentration was increased in the unloaded bone.

The minimal use of animals in this study presents a limitation to the interpretation of our findings. Especially with respect to substance P, bone concentrations of these neuropeptides were small. Detection of a minor change in concentration resulting from the different mechanical

stimuli would have required the use of much higher animal numbers to achieve statistical significance. For example, detecting a significant 15% difference in substance P concentration between control tibias and 1 day compressed tibias would require 162 mice. Another limitation is that while we measured bone concentration, we do not know the origin of these neuropeptides. Osteoblasts themselves express CGRP and might alter their expression as an adaptive mechanism to the new loading environment. Such action would suggest an autocrine or paracrine response rather than a neural one. A final limitation is that we did not have a separate group of mice subjected to normal cage activity to serve as a universal control. Instead we used the left tibias of the compression mice, which are likely more similar within an animal than to the tibias of the hindlimb unloaded mice. An effect of compression on the contralateral limb could also clarified by an additional control group.

Investigation of the neuropeptide concentrations in bone revealed that they change in response to altered mechanical environments. Traditionally classified as transmitters of sensory stimuli, neuropeptides may have an additional role in bone, where they have the potential to regulate the bone cell response necessary for adaptation.

6 Conclusions

Discovery of nervous system control of bone formation through adrenergic receptors on osteoblasts [149] created a resurgence of studies investigating the effect of neurons on bone metabolism. All of the factors necessary for neurons to effect bone cells are in place. First, bone contains a dense network of nerves, not only on the periosteal surface but in cortical bone and bone marrow, satisfying the requirement of proximity. Secondly, bone cells express receptors for many neurotransmitters including the sensory neuropeptides CGRP and substance P. Furthermore, in vitro studies have shown that exposure of bone cells to these neuropeptides alters the function of both osteoblasts, osteoclasts, and their precursors. Lastly, the development of knockout mice have shown that abolishing specific neuropeptides or their receptors creates an abnormal bone phenotype in vivo.

To further elucidate the role of peripheral sensory nerves on bone regulation, this dissertation work used a chemical model of denervation. We used the naturally occurring compound, capsaicin, to reduce sensory nerve function and observe resulting gross changes in bone quantity and quality. As capsaicin was administered to neonatal mice, our first study investigated the effects of denervation on bone during development. Success of reduced sensory function was verified using hot plate analgesia testing, as receptors for capsaicin are also transducers of noxious heat. As for bone effects, we found that mice treated with capsaicin had shorter femurs with thinner trabeculae, but few changes in bone quality. Our findings were consistent with observations in humans that early nerve damage can impair limb morphogenesis. However, by skeletal maturity many of the observed differences in capsaicin-treated mice were resolved, suggesting perhaps development of a compensatory mechanism. Another explanation would be

that as traditional nociceptors, these sensory neurons would be more important in altered loading conditions, when the local environment of the free nerve endings and bone cells changes.

Female mice demonstrated greater consistency in response to capsaicin treatment and in the next study of bone adaptation, male mice were excluded. We used tibial compression to model increased loading and investigated effects of denervation on consequent responses in bone structure and formation rate. Reduced sensory nerve function did not impair the adaptive response of bone to increased mechanical demands. Capsaicin-treated mice actually showed greater changes in cortical bone area at proximal tibia locations, associated with higher mineral apposition rates. However, after two weeks of tibial compression, the total area between the mice with reduced sensory function had comparable bone mass to their sensory intact counterparts. These findings suggest that capsaicin-treated mice are able to overcome developmental deficiencies and form adequate bone to address the higher mechanical demands.

We postulated that effects of neurons on bone cells are mediated through the actions of neuropeptides. To verify that neuropeptide concentrations change in response to the mechanical environment of their target tissue, we subjected mice to increased or decreased mechanical loading and measured bone concentrations of CGRP and substance P. Increased mechanical loading was once again modeled by tibial compression, and we found that it caused bone CGRP concentration to increase. The increase was consistent with an anabolic effect of CGRP on osteoblasts. Tail suspension provided a model for hindlimb unloading, and bone substance P concentrations increased in response to the altered environment. We would expect hindlimb unloading to decrease bone mass as in cases of disuse osteoporosis, and the concomitant increase

in substance P indicates the importance of the osteoclast stimulating effect of this neuropeptide. A limitation of this study was that the origins of these neuropeptides are unknown, so while important to bone adaptation, they might originate in bone cells and act in an autocrine or paracrine manner.

The findings of our research support a role for sensory neuropeptides in bone metabolism. Neurons themselves might be more important to bone development, whereas neuropeptide actions on bone cells might play a more dramatic role in bone adaptation to the mechanical environment. Future research should investigate the origins of these neuropeptides in bone and take advantage of advancements in knockout mice. The actions of neuropeptides on bone cells present a target mechanism in the treatment of bone diseases characterized by abnormal bone formation.

References

[1] Kanda, T., et al., *Morphological changes in unmyelinated nerve fibers in the sural nerve with age.* Brain, 1991. **114**: p. 585-599.

[2] Jacobs, J.M. and S. Love, *Qualitative and quantitative morphology of human sural nerve at different ages.* Brain, 1985. **108 (Pt 4)**: p. 897-924.

[3] O'Sullivan, D.J. and M. Swallow, *The fibre size and content of the radial and sural nerves.* J Neurol Neurosurg Psychiatry, 1968. **31**(5): p. 464-70.

[4] Swallow, M., *Fibre size and content of the anterior tibial nerve of the foot.* J Neurol Neurosurg Psychiatry, 1966. **29**(3): p. 205-13.

[5] Ceballos, D., et al., *Morphometric and ultrastructural changes with ageing in mouse peripheral nerve.* J Anat, 1999. **195**: p. 563-576.

[6] *National Osteoporosis Foundation, Disease statistics "fast facts". Retrieved June 7, 2011, from National Osteoporosis Foundation Web site: http://www.nof.org/node/40*.

[7] Rix, M., H. Andreassen, and P. Eskildsen, *Impact of peripheral neuropathy on bone density in patients with type 1 diabetes.* Diabetes Care, 1999. **22**(5): p. 827-31.

[8] Salisbury, E., et al., *Sensory nerve induced inflammation contributes to heterotopic ossification.* J Cell Biochem, 2011. **112**(10): p. 2748-58.

[9] Li, Y., et al., *IL-6 receptor expression and IL-6 effects change during osteoblast differentiation.* Cytokine, 2008. **43**(2): p. 165-73.

[10] Ishimi, Y., et al., *IL-6 is produced by osteoblasts and induces bone resorption.* J Immunol, 1990. **145**(10): p. 3297-303.

[11] Khosla, S., M.J. Oursler, and D.G. Monroe, *Estrogen and the skeleton.* Trends Endocrinol Metab, 2012. **23**(11): p. 576-81.

[12] Garcia-Castellano, J.M., P. Diaz-Herrera, and J.A. Morcuende, *Is bone a target-tissue for the nervous system? New advances on the understanding of their interactions.* Iowa Orthop J, 2000. **20**: p. 49-58.

[13] Dellon, A.L., *Make no bones about it (regulation and control): NGF versus TGF-beta and BMP.* Microsurgery, 2011. **31**(5): p. 337-9.

[14] McCredie, J. and H.G. Willert, *Longitudinal limb deficiencies and the sclerotomes. An analysis of 378 dysmelic malformations induced by thalidomide.* J Bone Joint Surg Br, 1999. **81**(1): p. 9-23.

[15] Barnes, A.P. and F. Polleux, *Establishment of axon-dendrite polarity in developing neurons.* Annu Rev Neurosci, 2009. **32**: p. 347-81.

[16] Shelly, M., et al., *LKB1/STRAD promotes axon initiation during neuronal polarization.* Cell, 2007. **129**(3): p. 565-77.

[17] Sisask, G., et al., *Ontogeny of sensory and autonomic nerves in the developing mouse skeleton.* Auton Neurosci, 2013. **177**(2): p. 237-43.

[18] Bidegain, M., et al., *Calcitonin gene-related peptide (CGRP) in the developing mouse limb.* Endocr Res, 1995. **21**(4): p. 743-55.

[19] Senba, E., et al., *Ontogeny of the peptidergic system in the rat spinal cord: immunohistochemical analysis.* J Comp Neurol, 1982. **208**(1): p. 54-66.

[20] Sisask, G., et al., *Ontogeny of sensory nerves in the developing skeleton.* Anat Rec, 1995. **243**(2): p. 234-40.

[21] Hara-Irie, F., N. Amizuka, and H. Ozawa, *Immunohistochemical and ultrastructural localization of CGRP-positive nerve fibers at the epiphyseal trabecules facing the growth plate of rat femurs.* Bone, 1996. **18**(1): p. 29-39.

[22] Donatelle, J.M., *Growth of the corticospinal tract and the development of placing reactions in the postnatal rat.* J Comp Neurol, 1977. **175**(2): p. 207-31.

[23] Debanne, D., et al., *Axon physiology.* Physiol Rev, 2011. **91**(2): p. 555-602.

[24] Basbaum, A.I. and H.L. Fields, *Endogenous pain control systems: brainstem spinal pathways and endorphin circuitry.* Annu Rev Neurosci, 1984. **7**: p. 309-38.

[25] Konttinen, Y., S. Imai, and A. Suda, *Neuropeptides and the puzzle of bone remodeling. State of the art.* Acta Orthop Scand, 1996. **67**(6): p. 632-9.
[26] Mach, D.B., et al., *Origins of skeletal pain: sensory and sympathetic innervation of the mouse femur.* Neuroscience, 2002. **113**(1): p. 155-66.
[27] Gajda, M., et al., *Development of sensory innervation in rat tibia: co-localization of CGRP and substance P with growth-associated protein 43 (GAP-43).* J Anat, 2005. **207**(2): p. 135-44.
[28] Kosaras, B., et al., *Sensory innervation of the calvarial bones of the mouse.* J Comp Neurol, 2009. **515**(3): p. 331-48.
[29] Ishida-Yamamoto, A. and M. Tohyama, *Calcitonin gene-related peptide in the nervous tissue.* Prog Neurobiol, 1989. **33**(5-6): p. 335-86.
[30] Mori, H., et al., *Calcitonin gene-related peptide containing sensory neurons innervating tooth pulp and buccal mucosa of the rat: an immunohistochemical analysis.* J Chem Neuroanat, 1990. **3**(3): p. 155-63.
[31] Uddman, R., A. Luts, and F. Sundler, *Occurrence and distribution of calcitonin gene-related peptide in the mammalian respiratory tract and middle ear.* Cell Tissue Res, 1985. **241**(3): p. 551-5.
[32] Wanaka, A., et al., *Distribution patterns of calcitonin gene-related peptide-containing fibers in the wall of the three different arteries: an immunohistochemical study.* Cell Mol Biol, 1987. **33**(2): p. 201-9.
[33] Imai, S., et al., *Calcitonin gene-related peptide, substance P, and tyrosine hydroxylase-immunoreactive innervation of rat bone marrows: an immunohistochemical and ultrastructural investigation on possible efferent and afferent mechanisms.* J Orthop Res, 1997. **15**(1): p. 133-40.
[34] Hirata, Y., et al., *Calcitonin gene-related peptide receptor in cultured vascular smooth muscle and endothelial cells.* Biochem Biophys Res Commun, 1988. **151**(3): p. 1113-21.
[35] Tache, Y., et al., *Calcitonin gene-related peptide: potent peripheral inhibitor of gastric acid secretion in rats and dogs.* Gastroenterology, 1984. **87**(2): p. 344-9.
[36] Pettersson, M., et al., *Calcitonin gene-related peptide: occurrence in pancreatic islets in the mouse and the rat and inhibition of insulin secretion in the mouse.* Endocrinology, 1986. **119**(2): p. 865-9.
[37] Kimberly, C.L. and M.R. Byers, *Inflammation of rat molar pulp and periodontium causes increased calcitonin gene-related peptide and axonal sprouting.* Anat Rec, 1988. **222**(3): p. 289-300.
[38] Brain, S.D., et al., *Potent vasodilator activity of calcitonin gene-related peptide in human skin.* J Invest Dermatol, 1986. **87**(4): p. 533-6.
[39] Holman, J.J., R.K. Craig, and I. Marshall, *Human alpha- and beta-CGRP and rat alpha-CGRP are coronary vasodilators in the rat.* Peptides, 1986. **7**(2): p. 231-5.
[40] Yu, X.J., et al., *Calcitonin gene-related peptide regulates the expression of vascular endothelial growth factor in human HaCaT keratinocytes by activation of ERK1/2 MAPK.* Regul Pept, 2006. **137**(3): p. 134-9.
[41] Aoki, M., K. Tamai, and K. Saotome, *Substance P- and calcitonin gene-related peptide-immunofluorescent nerves in the repair of experimental bone defects.* Int Orthop, 1994. **18**(5): p. 317-24.
[42] Bjurholm, A., et al., *Substance P- and CGRP-immunoreactive nerves in bone.* Peptides, 1988. **9**(1): p. 165-71.
[43] Bjurholm, A., et al., *Neuroendocrine regulation of cyclic AMP formation in osteoblastic cell lines (UMR-106-01, ROS 17/2.8, MC3T3-E1, and Saos-2) and primary bone cells.* J Bone Miner Res, 1992. **7**(9): p. 1011-9.
[44] Drissi, H., et al., *Expression of the CT/CGRP gene and its regulation by dibutyryl cyclic adenosine monophosphate in human osteoblastic cells.* J Bone Miner Res, 1997. **12**(11): p. 1805-14.

[45] Ballica, R., et al., *Targeted expression of calcitonin gene-related peptide to osteoblasts increases bone density in mice.* J Bone Miner Res, 1999. **14**(7): p. 1067-74.
[46] Schinke, T., et al., *Decreased bone formation and osteopenia in mice lacking alpha-calcitonin gene-related peptide.* J Bone Miner Res, 2004. **19**(12): p. 2049-56.
[47] Cornish, J., et al., *Comparison of the effects of calcitonin gene-related peptide and amylin on osteoblasts.* J Bone Miner Res, 1999. **14**(8): p. 1302-9.
[48] Lee, Y., et al., *Distribution of calcitonin gene-related peptide in the rat peripheral nervous system with reference to its coexistence with substance P.* Neuroscience, 1985. **15**(4): p. 1227-37.
[49] Piercey, M.F., et al., *Sensory and motor functions of spinal cord substance P.* Science, 1981. **214**(4527): p. 1361-3.
[50] Wang, L., et al., *Substance P stimulates bone marrow stromal cell osteogenic activity, osteoclast differentiation, and resorption activity in vitro.* Bone, 2009. **45**(2): p. 309-20.
[51] Mori, T., et al., *Substance P regulates the function of rabbit cultured osteoclast; increase of intracellular free calcium concentration and enhancement of bone resorption.* Biochem Biophys Res Commun, 1999. **262**(2): p. 418-22.
[52] Kingery, W.S., et al., *A substance P receptor (NK1) antagonist enhances the widespread osteoporotic effects of sciatic nerve section.* Bone, 2003. **33**(6): p. 927-36.
[53] Kar, S., et al., *Reduced numbers of calcitonin gene-related peptide-(CGRP-) and tachykinin-immunoreactive sensory neurones associated with greater enkephalin immunoreactivity in the dorsal horn of a mutant rat with hereditary sensory neuropathy.* Cell Tissue Res, 1989. **255**(2): p. 451-66.
[54] Wiesenfeld-Hallin, Z., et al., *Immunoreactive calcitonin gene-related peptide and substance P coexist in sensory neurons to the spinal cord and interact in spinal behavioral responses of the rat.* Neurosci Lett, 1984. **52**(1-2): p. 199-204.
[55] Wahlestedt, C., et al., *Calcitonin gene-related peptide in the eye: release by sensory nerve stimulation and effects associated with neurogenic inflammation.* Regul Pept, 1986. **16**(2): p. 107-15.
[56] Baldock, P.A., et al., *Neuropeptide Y knockout mice reveal a central role of NPY in the coordination of bone mass to body weight.* PLoS One, 2009. **4**(12): p. e8415.
[57] Chenu, C., et al., *Glutamate receptors are expressed by bone cells and are involved in bone resorption.* Bone, 1998. **22**(4): p. 295-9.
[58] Serre, C.M., et al., *Evidence for a dense and intimate innervation of the bone tissue, including glutamate-containing fibers.* Bone, 1999. **25**(6): p. 623-9.
[59] Jones, K.B., et al., *Bone and brain: a review of neural, hormonal, and musculoskeletal connections.* Iowa Orthop J, 2004. **24**: p. 123-32.
[60] Hohmann, E.L., et al., *Innervation of periosteum and bone by sympathetic vasoactive intestinal peptide-containing nerve fibers.* Science, 1986. **232**(4752): p. 868-71.
[61] Mukohyama, H., et al., *The inhibitory effects of vasoactive intestinal peptide and pituitary adenylate cyclase-activating polypeptide on osteoclast formation are associated with upregulation of osteoprotegerin and downregulation of RANKL and RANK.* Biochem Biophys Res Commun, 2000. **271**(1): p. 158-63.
[62] Hill, E.L. and R. Elde, *Distribution of Cgrp-Immunoreactive, Vip-Immunoreactive, D-Beta-H-Immunoreactive, Sp-Immunoreactive, and Npy-Immunoreactive Nerves in the Periosteum of the Rat.* Cell and Tissue Research, 1991. **264**(3): p. 469-480.
[63] Lundberg, P., et al., *Neuro-hormonal control of bone metabolism: vasoactive intestinal peptide stimulates alkaline phosphatase activity and mRNA expression in mouse calvarial osteoblasts as well as calcium accumulation mineralized bone nodules.* Regul Pept, 1999. **85**(1): p. 47-58.
[64] Garces, G.L. and M.E. Santandreu, *Longitudinal bone growth after sciatic denervation in rats.* J Bone Joint Surg Br, 1988. **70**(2): p. 315-8.
[65] Fukuda, T., et al., *Sema3A regulates bone-mass accrual through sensory innervations.* Nature, 2013. **497**(7450): p. 490-3.

[66] Rossi, F., et al., *The genetic ablation or pharmacological inhibition of TRPV1 signalling is beneficial for the restoration of quiescent osteoclast activity in ovariectomized mice.* Br J Pharmacol, 2014. **171**(10): p. 2621-30.
[67] Sample, S.J., et al., *Functional adaptation to loading of a single bone is neuronally regulated and involves multiple bones.* J Bone Miner Res, 2008. **23**(9): p. 1372-81.
[68] Sample, S.J., et al., *Role of calcitonin gene-related peptide in bone repair after cyclic fatigue loading.* PLoS One, 2011. **6**(6): p. e20386.
[69] Guo, T.Z., et al., *Immobilization contributes to exaggerated neuropeptide signaling, inflammatory changes, and nociceptive sensitization after fracture in rats.* J Pain, 2014. **15**(10): p. 1033-45.
[70] Caterina, M.J., et al., *The capsaicin receptor: a heat-activated ion channel in the pain pathway.* Nature, 1997. **389**(6653): p. 816-24.
[71] Caterina, M.J. and D. Julius, *The vanilloid receptor: a molecular gateway to the pain pathway.* Annu Rev Neurosci, 2001. **24**: p. 487-517.
[72] Nagy, J.I., et al., *Dose-dependent effects of capsaicin on primary sensory neurons in the neonatal rat.* J Neurosci, 1983. **3**(2): p. 399-406.
[73] Tewksbury, J.J. and G.P. Nabhan, *Seed dispersal. Directed deterrence by capsaicin in chilies.* Nature, 2001. **412**(6845): p. 403-4.
[74] Perry, L., et al., *Starch fossils and the domestication and dispersal of chili peppers (Capsicum spp. L.) in the Americas.* Science, 2007. **315**(5814): p. 986-8.
[75] Nelson, E.K., *The constitution of capsaicin, the pungent principle of capsicum. II.* Journal of the American Chemical Society, 1920. **42**: p. 597-599.
[76] Cordell, G.A. and O.E. Araujo, *Capsaicin: identification, nomenclature, and pharmacotherapy.* Ann Pharmacother, 1993. **27**(3): p. 330-6.
[77] Deal, C.L., et al., *Treatment of arthritis with topical capsaicin: a double-blind trial.* Clin Ther, 1991. **13**(3): p. 383-95.
[78] McCarthy, G.M. and D.J. McCarty, *Effect of topical capsaicin in the therapy of painful osteoarthritis of the hands.* J Rheumatol, 1992. **19**(4): p. 604-7.
[79] Kulkantrakorn, K., C. Lorsuwansiri, and P. Meesawatsom, *0.025% capsaicin gel for the treatment of painful diabetic neuropathy: a randomized, double-blind, crossover, placebo-controlled trial.* Pain Pract, 2013. **13**(6): p. 497-503.
[80] Razavi, R., et al., *TRPV1+ sensory neurons control beta cell stress and islet inflammation in autoimmune diabetes.* Cell, 2006. **127**(6): p. 1123-35.
[81] Chow, J., et al., *TRPV6 mediates capsaicin-induced apoptosis in gastric cancer cells--Mechanisms behind a possible new "hot" cancer treatment.* Biochim Biophys Acta, 2007. **1773**(4): p. 565-76.
[82] Gharat, L. and A. Szallasi, *Medicinal chemistry of the vanilloid (capsaicin) TRPV1 receptor: Current knowledge and future perspectives.* Drug Development Research, 2007. **68**(8): p. 477-497.
[83] Bernardini, N., et al., *Morphological evidence for functional capsaicin receptor expression and calcitonin gene-related peptide exocytosis in isolated peripheral nerve axons of the mouse.* Neuroscience, 2004. **126**(3): p. 585-90.
[84] Dray, A., *Mechanism of action of capsaicin-like molecules on sensory neurons.* Life Sci, 1992. **51**(23): p. 1759-65.
[85] Buck, S.H. and T.F. Burks, *The neuropharmacology of capsaicin: review of some recent observations.* Pharmacol Rev, 1986. **38**(3): p. 179-226.
[86] Cuello, A.C., et al., *Substance P immunoreactive neurons following neonatal administration of capsaicin.* Naunyn Schmiedebergs Arch Pharmacol, 1981. **315**(3): p. 185-94.
[87] Jancso, G., E. Kiraly, and A. Jancso-Gabor, *Pharmacologically induced selective degeneration of chemosensitive primary sensory neurones.* Nature, 1977. **270**(5639): p. 741-3.

[88] Scadding, J.W., *The permanent anatomical effects of neonatal capsaicin on somatosensory nerves.* J Anat, 1980. **131**(Pt 3): p. 471-82.
[89] Gamse, R., et al., *Differential effects of capsaicin on the content of somatostatin, substance P, and neurotensin in the nervous system of the rat.* Naunyn Schmiedebergs Arch Pharmacol, 1981. **317**(2): p. 140-8.
[90] Holzer, P., *Capsaicin: cellular targets, mechanisms of action, and selectivity for thin sensory neurons.* Pharmacol Rev, 1991. **43**(2): p. 143-201.
[91] Szallasi, A., et al., *The vanilloid receptor TRPV1: 10 years from channel cloning to antagonist proof-of-concept.* Nat Rev Drug Discov, 2007. **6**(5): p. 357-72.
[92] Jimenez-Andrade, J.M., et al., *Capsaicin-sensitive sensory nerve fibers contribute to the generation and maintenance of skeletal fracture pain.* Neuroscience, 2009. **162**(4): p. 1244-54.
[93] Hukkanen, M., et al., *Innervation of bone from healthy and arthritic rats by substance P and calcitonin gene related peptide containing sensory fibers.* J Rheumatol, 1992. **19**(8): p. 1252-9.
[94] Roberts, J.C., J.B. Davis, and C.D. Benham, *[3H]Resiniferatoxin autoradiography in the CNS of wild-type and TRPV1 null mice defines TRPV1 (VR-1) protein distribution.* Brain Res, 2004. **995**(2): p. 176-83.
[95] Szekely, M. and J. Szolcsanyi, *Endotoxin fever in capsaicin treated rats.* Acta Physiol Acad Sci Hung, 1979. **53**(4): p. 469-77.
[96] Zahner, M.R., et al., *Cardiac vanilloid receptor 1-expressing afferent nerves and their role in the cardiogenic sympathetic reflex in rats.* J Physiol, 2003. **551**(Pt 2): p. 515-23.
[97] Urban, L. and A. Dray, *Capsazepine, a novel capsaicin antagonist, selectively antagonises the effects of capsaicin in the mouse spinal cord in vitro.* Neurosci Lett, 1991. **134**(1): p. 9-11.
[98] Geppetti, P., S. Materazzi, and P. Nicoletti, *The transient receptor potential vanilloid 1: role in airway inflammation and disease.* Eur J Pharmacol, 2006. **533**(1-3): p. 207-14.
[99] Birder, L.A., et al., *Vanilloid receptor expression suggests a sensory role for urinary bladder epithelial cells.* Proc Natl Acad Sci U S A, 2001. **98**(23): p. 13396-401.
[100] Holzer, P., *Vanilloid receptor TRPV1: hot on the tongue and inflaming the colon.* Neurogastroenterol Motil, 2004. **16**(6): p. 697-9.
[101] Vass, Z., et al., *Nitric oxide mediates capsaicin-induced increase in cochlear blood flow.* Hear Res, 1996. **100**(1-2): p. 114-9.
[102] Bodo, E., et al., *A hot new twist to hair biology: involvement of vanilloid receptor-1 (VR1/TRPV1) signaling in human hair growth control.* Am J Pathol, 2005. **166**(4): p. 985-98.
[103] Premkumar, L.S. and P. Sikand, *TRPV1: a target for next generation analgesics.* Curr Neuropharmacol, 2008. **6**(2): p. 151-63.
[104] Idris, A.I., E. Landao-Bassonga, and S.H. Ralston, *The TRPV1 ion channel antagonist capsazepine inhibits osteoclast and osteoblast differentiation in vitro and ovariectomy induced bone loss in vivo.* Bone, 2010. **46**(4): p. 1089-99.
[105] Fernandes, E.S., M.A. Fernandes, and J.E. Keeble, *The functions of TRPA1 and TRPV1: moving away from sensory nerves.* Br J Pharmacol, 2012. **166**(2): p. 510-21.
[106] Spencer, G.J., I.S. Hitchcock, and P.G. Genever, *Emerging neuroskeletal signalling pathways: a review.* FEBS Lett, 2004. **559**(1-3): p. 6-12.
[107] Hampson, G. and I. Fogelman, *Clinical role of bisphosphonate therapy.* Int J Womens Health, 2012. **4**: p. 455-69.
[108] Russell, R.G., *Bisphosphonates: the first 40 years.* Bone, 2011. **49**(1): p. 2-19.
[109] Sibai, T., E.F. Morgan, and T.A. Einhorn, *Anabolic agents and bone quality.* Clin Orthop Relat Res, 2011. **469**(8): p. 2215-24.
[110] Dyck, P.J., et al., *Detection thresholds of cutaneous sensation in humans,* in *Peripheral Neuropathy,* P.J. Dyck, et al., Editors. 1984, WB Saunders: Philadelphia. p. 1103-1138.
[111] Akopian, A., et al., *Effects of CGRP on human osteoclast-like cell formation: a possible connection with the bone loss in neurological disorders?* Peptides, 2000. **21**(4): p. 559-64.

[112] Bernard, G.W. and C. Shih, *The osteogenic stimulating effect of neuroactive calcitonin gene-related peptide.* Peptides, 1990. **11**(4): p. 625-32.
[113] Cornish, J., et al., *Effects of calcitonin, amylin, and calcitonin gene-related peptide on osteoclast development.* Bone, 2001. **29**(2): p. 162-8.
[114] D'Souza, S.M., et al., *Human synthetic calcitonin gene-related peptide inhibits bone resorption in vitro.* Endocrinology, 1986. **119**(1): p. 58-61.
[115] Granholm, S. and U.H. Lerner, *The members of the calcitonin gene family of peptides, including recently discovered intermedin and CRSP, inhibit both osteoclast activity and formation.* Journal of Bone and Mineral Research, 2006. **21**: p. S164-S164.
[116] Mori, T., et al., *Substance P regulates the function of rabbit cultured osteoclasts; increase of intracellular free calcium concentrations and enhancement of bone resorption.* Biochem Biophys Res Commun, 1999. **262**: p. 418-22.
[117] Owan, I. and K. Ibaraki, *The role of calcitonin gene-related peptide (CGRP) in macrophages: the presence of functional receptors and effects on proliferation and differentiation into osteoclast-like cells.* Bone Miner, 1994. **24**(2): p. 151-64.
[118] Tamura, T., et al., *Mechanism of Action of Amylin in Bone.* Journal of Cellular Physiology, 1992. **153**(1): p. 6-14.
[119] Yamamoto, I., et al., *Human Calcitonin Gene-Related Peptide Possesses Weak Inhibitory Potency of Bone-Resorption Invitro.* Calcified Tissue International, 1986. **38**(6): p. 339-341.
[120] Hill, E.L., R. Turner, and R. Elde, *Effects of neonatal sympathectomy and capsaicin treatment on bone remodeling in rats.* Neuroscience, 1991. **44**(3): p. 747-55.
[121] O'Connor, B.L., M.J. Palmoski, and K.D. Brandt, *Neurogenic acceleration of degenerative joint lesions.* J Bone Joint Surg Am, 1985. **67**(4): p. 562-72.
[122] Zeng, Q.Q., et al., *Time responses of cancellous and cortical bones to sciatic neurectomy in growing female rats.* Bone, 1996. **19**(1): p. 13-21.
[123] Mihara, K., et al., *Vital role of the itch-scratch response in development of spontaneous dermatitis in NC/Nga mice.* Br J Dermatol, 2004. **151**(2): p. 335-45.
[124] Nakano, T., et al., *Different roles of capsaicin-sensitive and H1 histamine receptor-expressing sensory neurones in itch of mosquito allergy in mice.* Acta Derm Venereol, 2008. **88**(5): p. 449-54.
[125] Karl, T., R. Pabst, and S. von Horsten, *Behavioral phenotyping of mice in pharmacological and toxicological research.* Exp Toxicol Pathol, 2003. **55**(1): p. 69-83.
[126] Doube, M., et al., *BoneJ: Free and extensible bone image analysis in ImageJ.* Bone, 2010. **47**(6): p. 1076-9.
[127] Baron, R., et al., *Processing of undecalcified bone specimens for bone histomorphometry*, in *Bone histomorphometry: techniques and interpretations*, R. Recker, Editor. 1983. p. 13-19.
[128] Hale, L.V., et al., *PINP: a serum biomarker of bone formation in the rat.* Bone, 2007. **40**(4): p. 1103-9.
[129] Lee, K.C., et al., *The adaptive response of bone to mechanical loading in female transgenic mice is deficient in the absence of oestrogen receptor-alpha and -beta.* J Endocrinol, 2004. **182**(2): p. 193-201.
[130] Offley, S.C., et al., *Capsaicin-sensitive sensory neurons contribute to the maintenance of trabecular bone integrity.* J Bone Miner Res, 2005. **20**(2): p. 257-67.
[131] Kobayashi, M., et al., *Capsaicin, a TRPV1 Ligand, Suppresses Bone Resorption by Inhibiting the Prostaglandin E Production of Osteoblasts, and Attenuates the Inflammatory Bone Loss Induced by Lipopolysaccharide.* ISRN Pharmacol, 2012. **2012**: p. 439860.
[132] Lieben, L. and G. Carmeliet, *The Involvement of TRP Channels in Bone Homeostasis.* Front Endocrinol (Lausanne), 2012. **3**: p. 99.
[133] Abed, E., et al., *Expression of transient receptor potential (TRP) channels in human and murine osteoblast-like cells.* Mol Membr Biol, 2009. **26**(3): p. 146-58.

[134] Rossi, F., et al., *The endovanilloid/endocannabinoid system in human osteoclasts: possible involvement in bone formation and resorption.* Bone, 2009. **44**(3): p. 476-84.
[135] Wright, N.C., et al., *The recent prevalence of osteoporosis and low bone mass in the United States based on bone mineral density at the femoral neck or lumbar spine.* J Bone Miner Res, 2014. **29**(11): p. 2520-6.
[136] Elefteriou, F., *Neuronal signaling and the regulation of bone remodeling.* Cell Mol Life Sci, 2005. **62**(19-20): p. 2339-49.
[137] Heffner, M.A., et al., *Altered bone development in a mouse model of peripheral sensory nerve inactivation.* J Musculoskelet Neuronal Interact, 2014. **14**(1): p. 1-9.
[138] Fritton, J.C., et al., *Loading induces site-specific increases in mineral content assessed by microcomputed tomography of the mouse tibia.* Bone, 2005. **36**(6): p. 1030-8.
[139] De Souza, R.L., et al., *Non-invasive axial loading of mouse tibiae increases cortical bone formation and modifies trabecular organization: a new model to study cortical and cancellous compartments in a single loaded element.* Bone, 2005. **37**(6): p. 810-8.
[140] Main, R.P., M.E. Lynch, and M.C. van der Meulen, *In vivo tibial stiffness is maintained by whole bone morphology and cross-sectional geometry in growing female mice.* J Biomech, 2010. **43**(14): p. 2689-94.
[141] Willie, B.M., et al., *Diminished response to in vivo mechanical loading in trabecular and not cortical bone in adulthood of female C57Bl/6 mice coincides with a reduction in deformation to load.* Bone, 2013. **55**(2): p. 335-46.
[142] Patel, T.K., M.D. Brodt, and M.J. Silva, *Experimental and finite element analysis of strains induced by axial tibial compression in young-adult and old female C57Bl/6 mice.* J Biomech, 2014. **47**(2): p. 451-7.
[143] Sugiyama, T., J.S. Price, and L.E. Lanyon, *Functional adaptation to mechanical loading in both cortical and cancellous bone is controlled locally and is confined to the loaded bones.* Bone, 2010. **46**(2): p. 314-21.
[144] Brodt, M.D. and M.J. Silva, *Aged mice have enhanced endocortical response and normal periosteal response compared to young-adult mice following 1 week of axial tibial compression.* J Bone Miner Res, 2010.
[145] Christiansen, B.A., et al., *Musculoskeletal changes following non-invasive knee injury using a novel mouse model of post-traumatic osteoarthritis.* Osteoarthritis Cartilage, 2012. **20**(7): p. 773-82.
[146] Robling, A.G., A.B. Castillo, and C.H. Turner, *Biomechanical and molecular regulation of bone remodeling.* Annu Rev Biomed Eng, 2006. **8**: p. 455-98.
[147] Bickel, C.S., et al., *Acute molecular responses of skeletal muscle to resistance exercise in able-bodied and spinal cord-injured subjects.* J Appl Physiol (1985), 2003. **94**(6): p. 2255-62.
[148] Morey-Holton, E.R. and R.K. Globus, *Hindlimb unloading rodent model: technical aspects.* J Appl Physiol (1985), 2002. **92**(4): p. 1367-77.
[149] Takeda, S., et al., *Leptin regulates bone formation via the sympathetic nervous system.* Cell, 2002. **111**(3): p. 305-17.

Appendix

Mouse Identification

On day 2 after birth, mice treated with capsaicin had their right pinky toe clipped while vehicle-treated mice had their left one shortened. At four weeks, we administered ear punches and names (VEH# or CAP#) to distinguish between mice housed in the same cage and to monitor progress during development.

Neonatal Capsaicin Treatment

All of the capsaicin- and vehicle-treated mice used in the research were the offspring of C57BL/6 timed pregnant females (Harlan Laboratories, Indianapolis, IN). The mice were received and housed in a UC Davis facility on embryonic day 15. Neonatal mice were given subcutaneous injections of capsaicin (50 mg/kg dissolved in vehicle) or vehicle (10% ethanol, 10% Tween 80 in isotonic saline) on day 2 and 5 after birth. Mice receiving capsaicin injections were placed on a heating pad and then injected in pinched skin on the back. Following capsaicin or vehicle treatment, neonatal mice were returned to normal cage activity until weaning (4 weeks). At weaning, mice were housed 4 to a cage, with food and water freely available. Mice from the same litter were preferentially housed together.

Non-invasive Load Magnitude Effects

In order to determine the optimal force to use in our studies involving tibial compression, we conducted a pilot study using 24 female mice. The 12 week old mice were subjected to 1200 cycles of compression once a day from 1 day to 10 days at varying compressive magnitudes. We recorded ACL ruptures and changes in body weight resulting from the increased loading.

At the highest compressive force of 9 N, there was often an audible "pop" as ACLs ruptured within the first 100 cycles of loading (Table 4). The joints of all mice exposed to the 9 N force were injured on the first day and mice sacrificed, so body weight changes could not be measured. When ACLs ruptured at the highest compressive force, immediate spikes in the force-displacement graph in the Bose program confirmed injury (Fig. 18A). Occurrence of joint injuries at lower forces was less obvious (Fig. 18C). After mice were sacrificed on the 10th day of loading, we used a program known to cause injury to determine whether ACLs ruptures had occurred unobserved during the experiment. Surprisingly, several mice displayed no change in the force-displacement graph up to 16 N in magnitude, indicating previous ACL rupture.

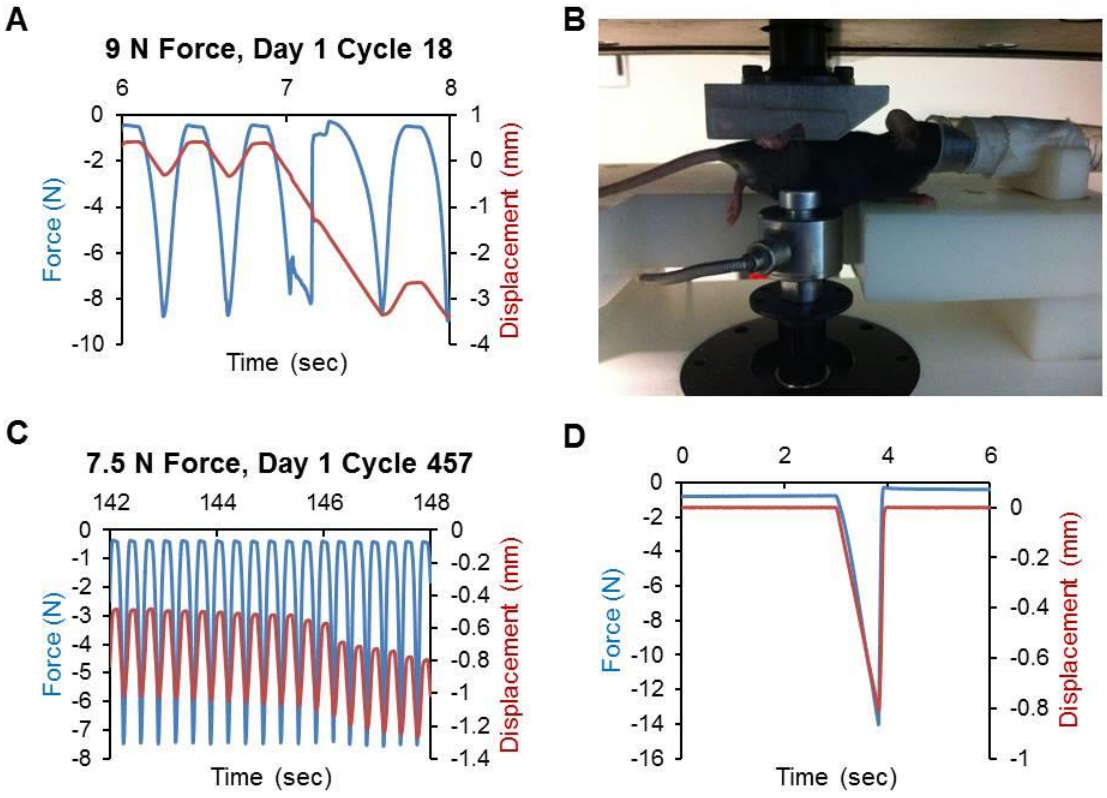

Fig. 18: Force and displacement graphs recorded during a pilot study of varying compressive magnitudes confirmed ACL rupture. Injury from 9 N force was obvious from the graphs (**A**) and from observing the mice in the compression setup (**B**). Injury at lower compressive forces was less obvious (**C**) and often a post-sacrifice test was used to determine ACL rupture (**D**).

Table 4: Effects of different tibial compressive forces on ACL rupture and body weight

	Broken ACL	Average Cycles to Break	Average Weight (g) Loading Day 1	Loading Day 10
Compressive Force				
9 N (n = 6)	6/6 = 100%	38 ± 50	20.1 ± 0.9	–
7.5 N (n = 6)	6/6 = 100%	440 ± 475	19.1 ± 0.9	19.4 ± 0.7
6 N (n = 6)	3/6 = 50%	2608 ± 2036	19.7 ± 1.5	19.8 ± 1.4
4.5 N (n = 6)	1/6 = 16.7%	10191	19.1 ± 2.0	20 ± 1.9

Lower compressive forces caused fewer joint injuries and insignificant body weight changes in the mice. The tradeoff of fewer injuries was less cortical bone formation in the tibias (Fig. 19). We decided on an intermediate compressive force of 7N, which is sufficient to stimulate cortical bone formation but not so high as to add the complexity of injury to neural response.

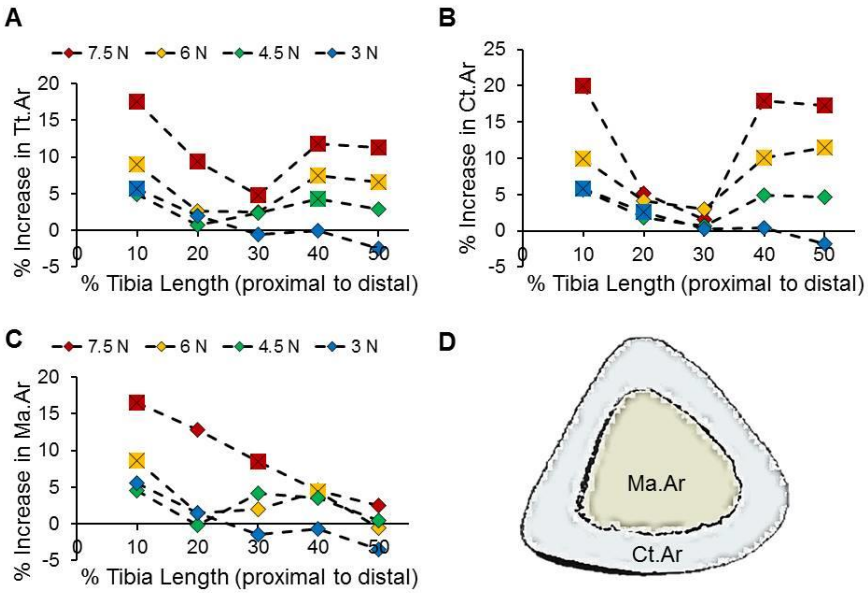

Fig. 19: Cortical bone properties changed with magnitude of the compressive force as assessed using microCT. Higher compressive forces caused the greatest increase in total bone area (**A**), cortical bone area (**B**) and medullary area (**C**). For all forces the changes were greatest at 10 and 50% of the tibia length. The diagram in (**D**) shows the location of these bone regions.

Strain Gauge Measurements

Strain gauges were used in determining whether different compressive forces were required for tibial compression of capsaicin- and vehicle-treated mice. Since bone adaptation is thought to be a function of strain on the bone tissue, we wanted the tibias of mice from each group to experience the same strain. Results from microCT analysis suggested that the tibias of capsaicin-treated mice might experience lower strain as a result of smaller bone dimensions. In a pilot study of mice, strain gauges were bonded to the tibias on the anteromedial surface immediately after sacrifice (Fig. 20). The limbs were then compressed to different magnitudes so we could ascertain strain as a function of compressive force.

Fig. 20: Strain gauges were positioned on the anteromedial surface of the tibia approximately 5 mm distal to the tibial plateau.

The strain gauge leads were attached to custom circuitry to amplify the signal (Fig. 21). A Wheatstone bridge comprised the first stage, a traditional circuit for amplifying changes in resistance. The following two stages consisted of a differential amplifier and non-inverting

amplifier to further magnify changes in resistance caused by the bending tibias. The final stage of the acquisition circuitry was a passive low pass filter to remove unwanted high frequency noise such as from 60 Hz electrical interference in the testing room. The voltage changes resulting from strain during tibial compression were recorded in a LabVIEW virtual instrument.

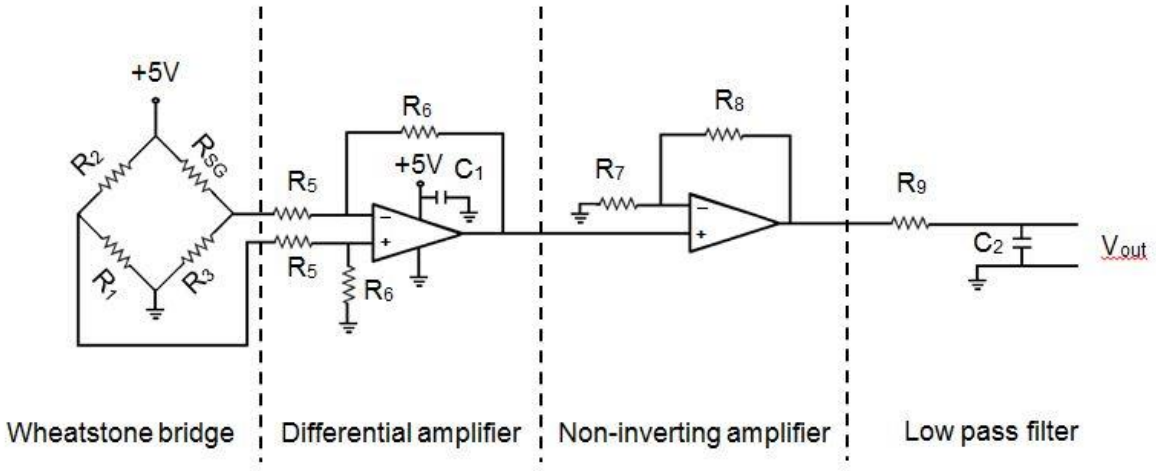

Fig. 21: Circuitry used to acquire strain data during tibial compression. In the experiment, $R_1 = R_2 = R_3 =$ 120 Ω, $R_5 = 100$ kΩ, $R_6 = 1$ MΩ, $R_7 = 12$ kΩ, $R_8 = 180$ kΩ, $R_9 = 100$ kΩ, and $C_1 = C_2 = 0.1$ µF. The cutoff frequency of the low pass filter was 15.9 Hz. The gauge factor (GF) of the strain gauge was 2.14.

Strain in the tibias resulting from changes in strain gauge resistance during tibial compression was calculated using the recorded voltage changes. The equations used to relate voltage to resistance were derived based on the acquisition circuitry (Table 5). Resistance change was then used to calculate strain based on a standard equation involving initial resistance and gauge factor.

Table 5: Gains of the different stages of acquisition circuitry for strain determination

Wheatstone bridge:	Differential amplifier:	Non-inverting amplifier:
$\Delta V = V_s\left(\frac{R_2}{R_1+R_2}-\frac{R_{SG}}{R_s+R_{SG}}\right)$	$V_{Da}=\frac{R_6}{R_5}(\Delta V)$	$V_{Na}=\left(1+\frac{R_8}{R_7}\right)V_s$
$\Delta V = 5\left(\frac{1}{2}-\frac{R_{SG}}{120+R_{SG}}\right)$	$V_{Da}=10\Delta V$	$V_{Na}=\left(1+\frac{180}{12}\right)10\Delta V$
$R_{SG}=\frac{300-120\Delta V}{2.5+\Delta V}$		$V_{Na}=160\Delta V$

$$\Delta V=\frac{V_{out}}{160}$$

$$R_{SG}=\frac{300-120\left(\frac{V_{out}}{160}\right)}{2.5+\left(\frac{V_{out}}{160}\right)}$$

$$R_{SG}=\frac{48000-120V_{out}}{400+V_{out}}$$

$$\varepsilon=\frac{\Delta R}{R_0 GF}$$

$$\varepsilon=\frac{R_{SG}-120}{(120)(2.14)}$$

$$\varepsilon=\frac{R_{SG}-120}{256.8}$$

$$tension:\ +\varepsilon\ and\ compression:\ -\varepsilon$$

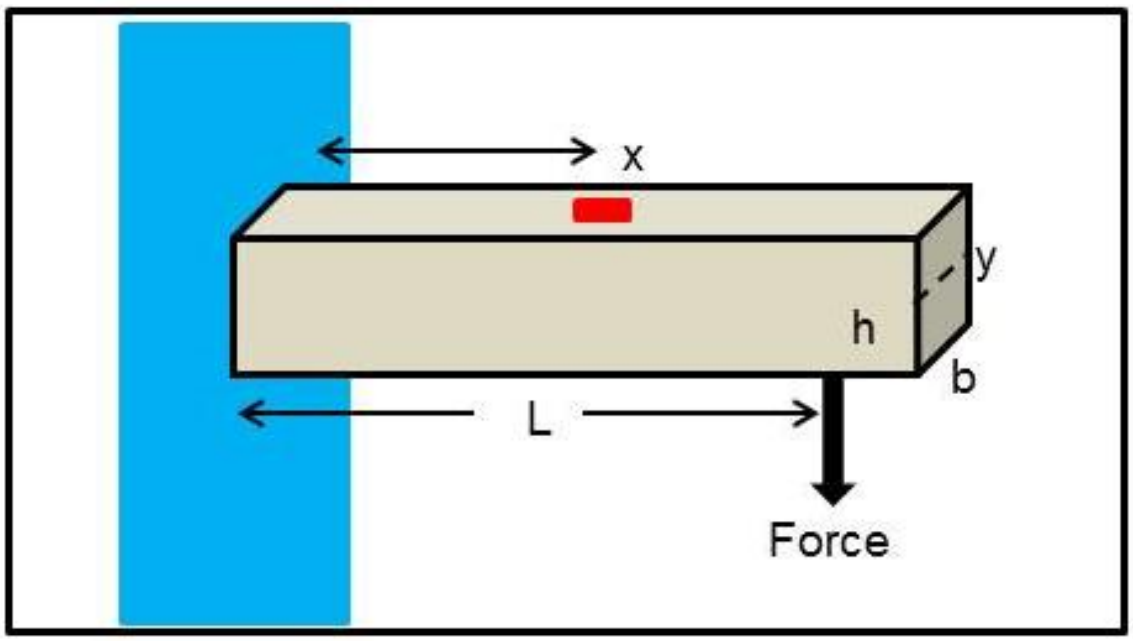

Fig. 22: The setup for calibration of strain using an aluminum alloy beam. In the experiment: L = 500 mm, x = 250 mm, h = 6.31 mm, b = 38.2 mm, and force was varied.

Before we could report the strain values in the tibias as calculated from the recorded voltage changes, we had to calibrate the setup. To do so, we used an aluminum alloy beam. The beam was secured to a laboratory table and varying magnitude loads were applied a known distance from the end of the beam. Theoretical strain was then calculated using the beam dimensions and applied force (Table 6). Next, a strain gauge was bonded to the aluminum beam (red square in Fig. 22), voltage changes recorded from applying the loads, and strain calculated using the equations for the acquisition circuitry.

Table 6: Equations used to calculate theoretical strain in an aluminum alloy

Aluminum alloy: 6061 – T6	
Bending moment, M	$M = F(L - x)$ $M = F(500\ mm - 250\ mm)$ $M = F(250\ mm)$
Distance from neutral axis, y	$y = \frac{1}{2}h$ $y = \frac{1}{2}(6.31\ mm) = 3.16\ mm$
Cross sectional moment of inertia, I_{xx}	$I_{xx} = \frac{bh^3}{12}$ $I_{xx} = \frac{(38.2\ mm)(6.31)^3}{12} = 799\ mm^4$
Stress, σ	$\sigma = \frac{My}{I_{xx}}$ $\sigma = \frac{F(3.16\ mm)}{799\ mm^4} = (0.986\ mm^4)F$
Elastic modulus, E	$E = 70000\ N \cdot mm^{-2}$
Strain, ε	$\varepsilon = \frac{(0.986\ mm^4)F}{70000\ N \cdot mm^{-2}}$

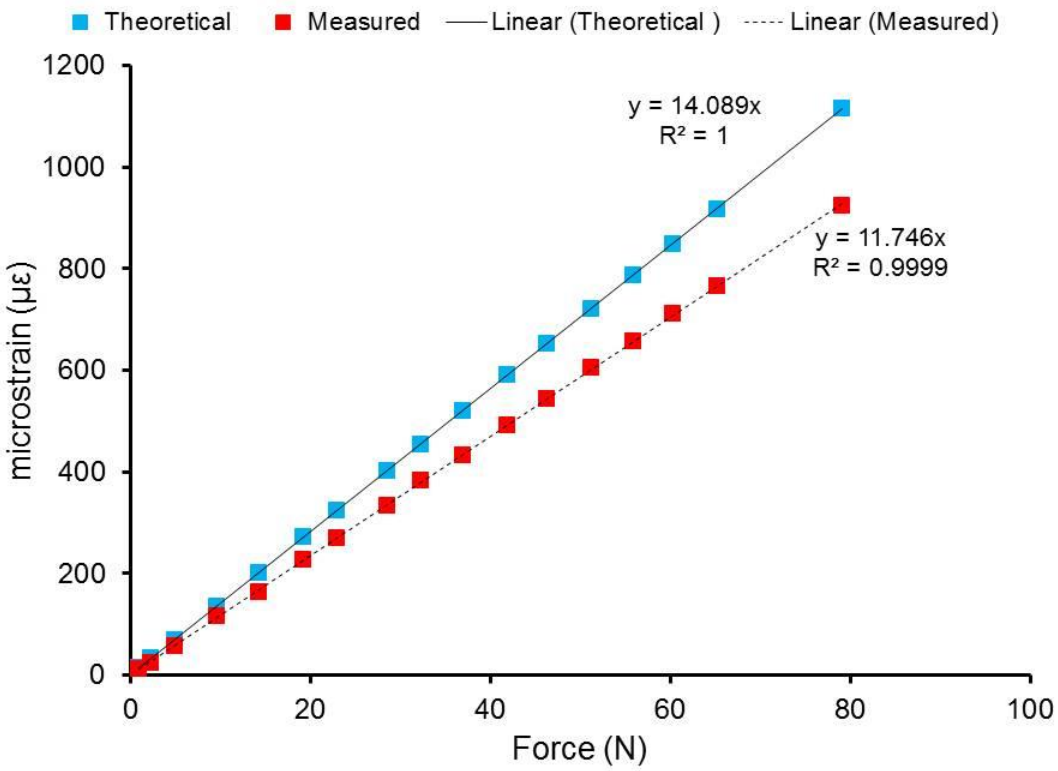

Fig. 23: Strain as a function of force applied to an aluminum beam was calculated using traditional equations and from voltage changes produced by strain gauge circuitry. The relationship between the equations was used to calibrate the strain gauge data produced by tibial compression in capsaicin- and vehicle-treated mice.

Theoretical strain measurements in the aluminum beam were compared to the strains calculated from recorded voltage changes using the acquisition circuitry. As anticipated, results from both measurement methods were linear in relation to the applied force (Fig. 23). However, theoretical strain calculations yielded higher values than measured at all forces, with a bigger difference at higher forces. Therefore, we added a correction factor to our calculation of strain from the voltage changes when reporting strain in the mouse tibias.

The correction factor was added to a custom MATLAB script which calculated strain based on the equations involving voltage change. For ease of opening and plotting the recorded voltages

and corresponding strains, a graphical user interface (GUI) was designed in MATLAB. The GUI allows the user to input the file name, subject name, and the approximate times of different applied forces so that the corresponding strains can be displayed (Fig. 24).

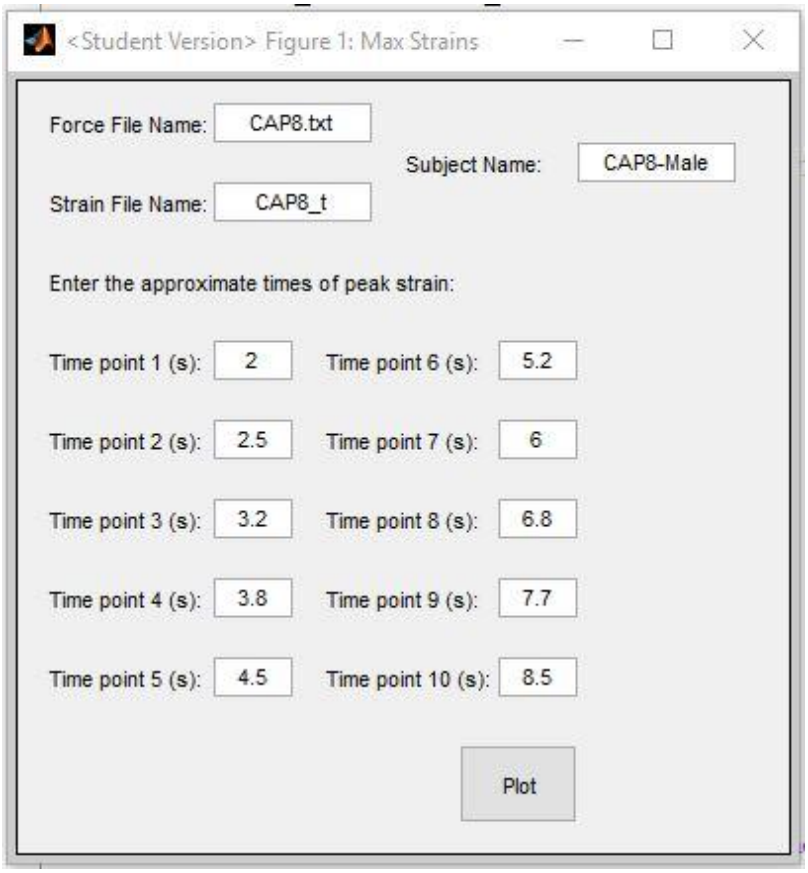

Fig. 24: The graphical user interface created in MATLAB to process data from a pilot study of tibial compression at different compressive forces.

Clicking "Plot" on the GUI generates a figure with plots of applied force, the raw voltage recording and the calculated strain in the tibia (Fig. 25).

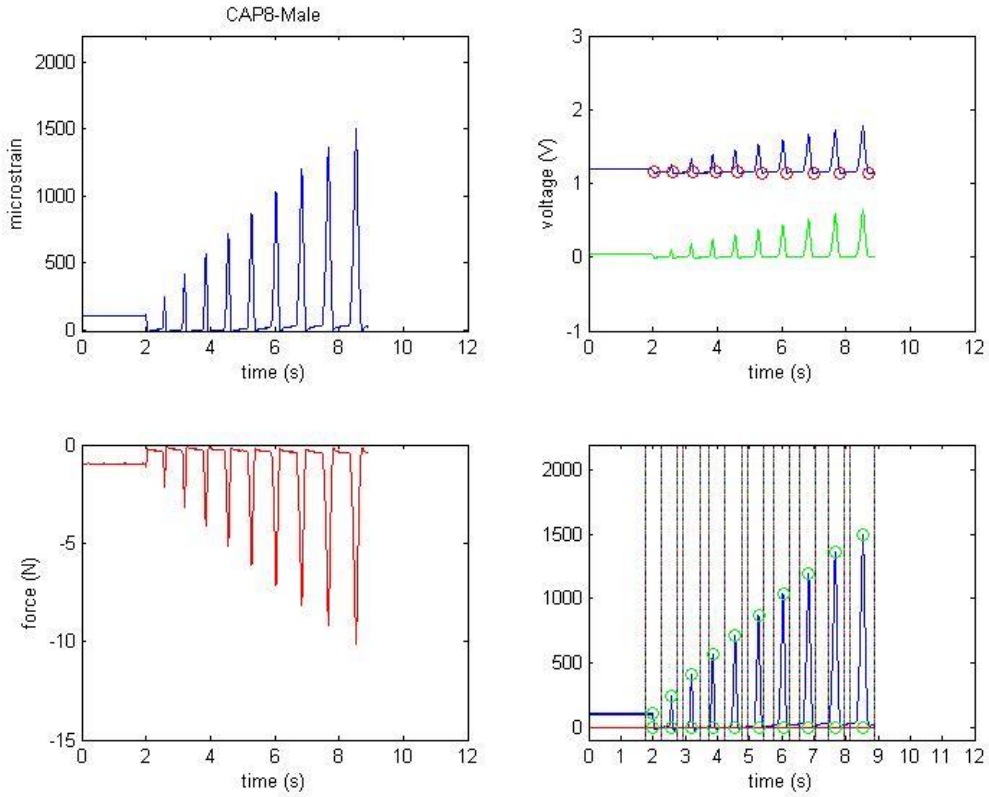

Fig. 25: Output from the MATLAB GUI includes plots of the strain in the tibia at the different applied compressive forces and the raw voltage recordings from the acquisition circuitry.

In the pilot study, we applied 10 different force magnitudes and thus recorded 10 different strains for each mouse. The GUI was designed to output the calculated strains in the MATLAB command window (Fig. 26). Strains were compared between capsaicin-treated and vehicle-treated mice and since no significant difference was observed between the two treatment groups, the same compressive force was used for each in the study involving bone adaptation to tibial compression.

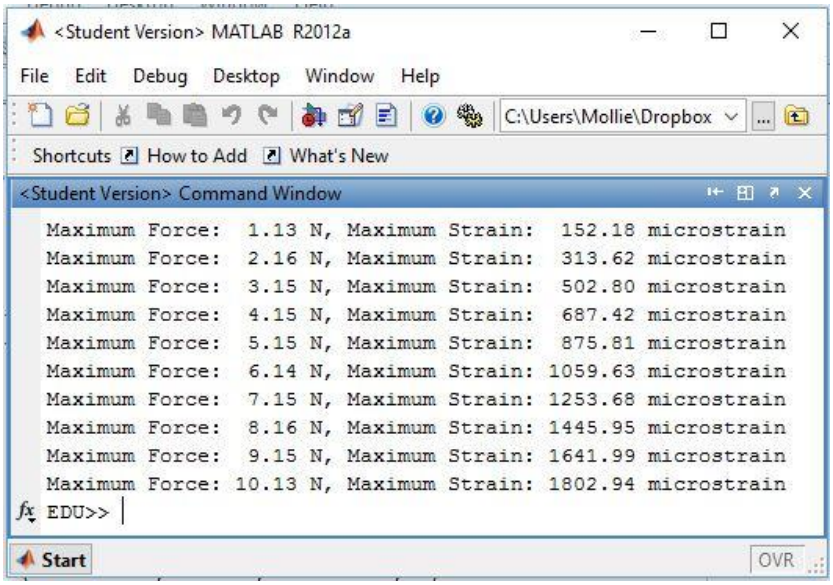

Fig. 26: Strain values calculated in MATLAB were used to determine whether the same compressive force resulted in different strains in capsaicin- and vehicle-treated mice.

Tibia Orientation in microCT Imaging

Much of the bone structure analysis in this research involved using microCT to assess changes caused by treatments such as capsaicin and tibial compression. The software accompanying the microCT unit calculates parameters such as cortical thickness based on contours manually drawn by the user. One of the parameters we are often interested in is moment of inertia (I), which gives information about how mass is distributed about the central axis of the bone. There was some concern that if the bone was tilted within the holder during imaging, the moment of inertia calculated by the software may be inaccurate. Tilt would cause the imaging plane to correspond to different heights along the bone and cross sectional calculations would then represent angled rather than horizontal sections. Such an effect would also make comparisons between bones less accurate as they could be tilted in different directions and at different angles within the holder. To assess how much the orientation of the bone in the microCT holder contributed to moment of

inertia calculations, we calculated these values in BoneJ as well, which has the ability to reorient the bones so that the vertical axis is indeed vertical.

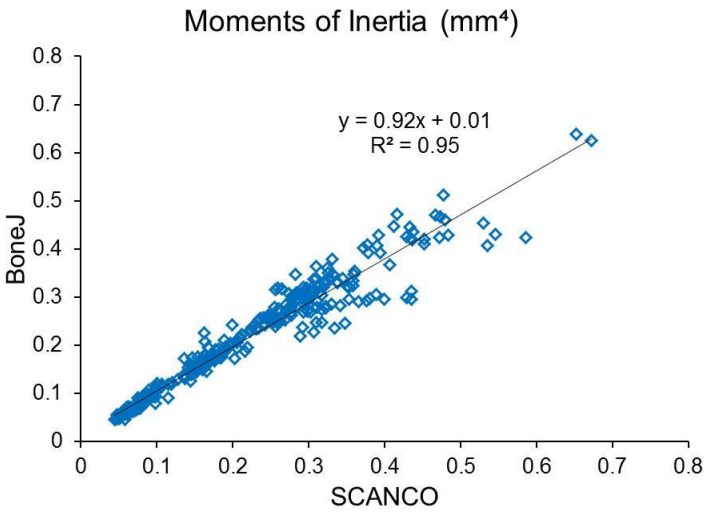

Fig. 27: Correlation of moments of inertia calculated from BoneJ and the microCT software (SCANCO). The fit was less apt at higher moments.

First, we compared the moments of inertia calculated by the microCT software (SCANCO) to those calculated by BoneJ. Overall, the correlation was tolerable, with a nearly linear fit. However at moments above 0.5 mm^4 there seemed to be some disparity, with BoneJ values being lower. To determine whether the differences could be assigned to tilt of the bones within the holder, we used the microCT images to calculate tilt (Fig. 28). We characterized tilt as the angle, θ, between the tibia and the vertical axis.

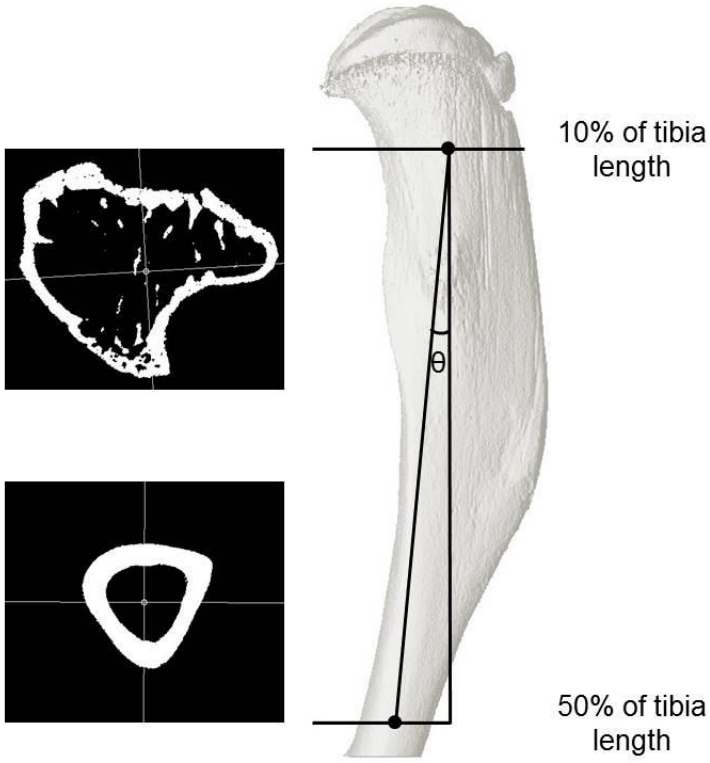

Fig. 28: Tibia angle was calculated from microCT images to see how much the bones were tilted within the holder. The angle varied between 0.60° and 12.4°.

Some of the bones were significantly tilted as assessed from the calculations of tibia angle. The tilt likely contributed to the differences we observed between the SCANCO and BoneJ calculations of moment of inertia. Larger angles tended to correspond to larger differences between the software values (Fig. 29). However, there also seemed to be an effect of location along the tibia, with more proximal locations causing larger differences in moment of inertia. A possible explanation would be that the greater density of trabecular bone at proximal locations causes any tilt to be amplified because more bone is used in the calculations.

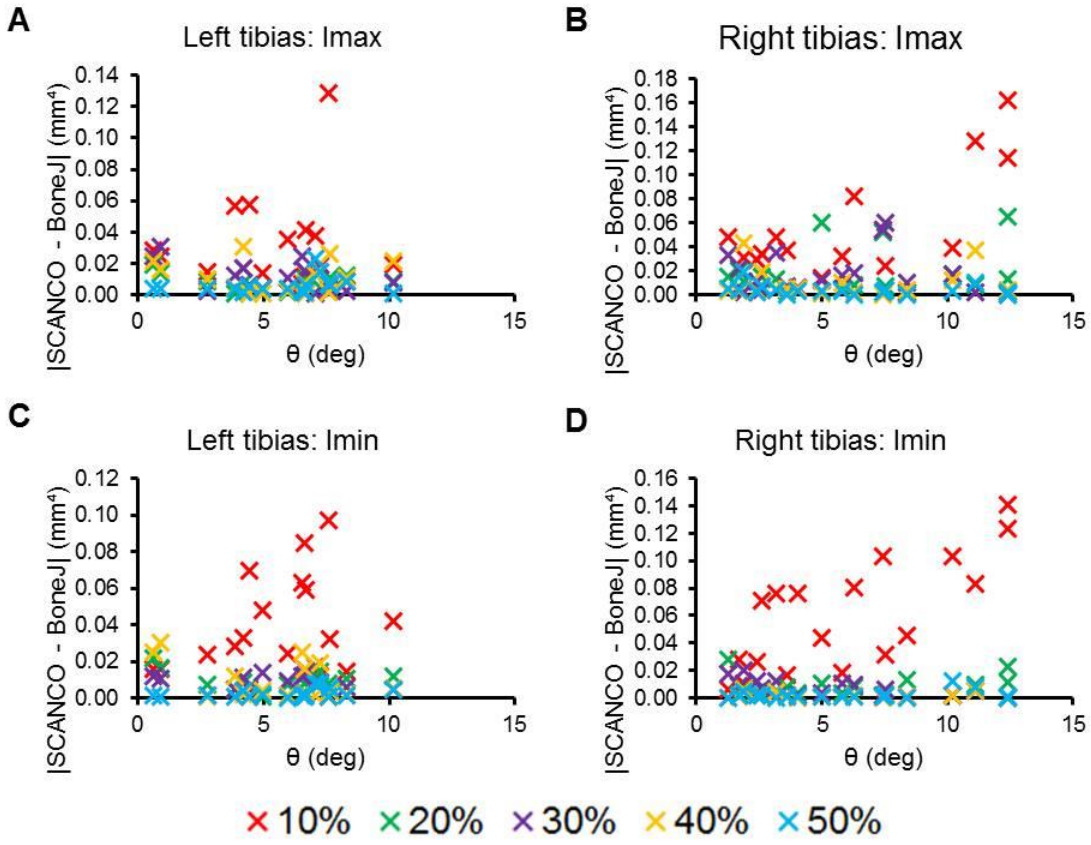

Fig. 29: Differences in SCANCO and BoneJ moments of inertia appear to be influenced by tilt of the tibia as well as location along the tibia from 10 to 50% of the length from the proximal end. We examined Imax for left (**A**) and right (**B**) tibias as well as Imin (**C, D**).

Table 7: Summary of correlation coefficients

			10%	20%	30%	40%	50%
Imax (mm^4)	Male	Left	0.96*	0.99*	0.99*	0.87*	0.93*
		Right	0.87*	0.95*	0.97*	0.97*	0.97*
	Female	Left	0.61	0.99*	0.97*	0.72*	0.71*
		Right	0.61	0.73*	0.86*	0.67	0.83*
Imin (mm^4)	Male	Left	0.88*	0.91*	0.99*	0.98*	0.96*
		Right	0.84*	0.94*	0.95*	0.99*	0.99*
	Female	Left	0.31	0.94*	0.98*	0.95*	0.87*
		Right	0.24	0.93*	0.78*	0.97*	0.66

The difference in moment of inertia values between the software programs presents an important problem because in the study of capsaicin- versus vehicle-treated mice, differences were significant using SCANCO data but not when using BoneJ data. We therefore tried to determine whether there was a systematic error in placing the tibias in the microCT holder that could be addressed in the future to limit variation (Fig. 30). Tibias from female mice had fewer significant correlations between SCANCO and BoneJ moments of inertia than male mice (Table 7). A possible explanation for this is that more of the tibias were located on the bottom of the holder (Table 8). Squishing the bones already in holder when adding new ones could cause more angling the lower they are in the holder. Another potential contributor to female differences is that right tibias were placed predominantly on the left side of the tube. Manipulating the bones in this way could inadvertently cause tiling.

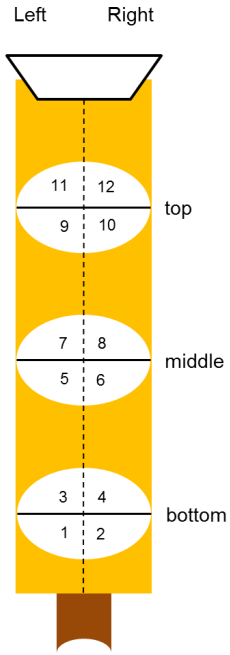

Fig. 30: MicroCT holders used to image bones can hold up to 12 tibias at a time.

Table 8: Locations of the tibias in the microCT holder

	Male		Female	
	Left tibias	Right tibias	Left tibias	Right tibias
Location	60% L, 40% R	40% L, 60% R	25% L, 75% R	75% L, 25% R
top	40%	40%	20%	20%
middle	40%	40%	20%	20%
bottom	20%	20%	40%	40%

The results from this investigation into the effects of sample handling and software analysis highlight the importance of being aware of limitations inherent to scientific techniques.